No. 1/2018

HIDRAULICA

HYDRAULICS-PNEUMATICS-TRIBOLOGY-ECOLOGY-SENSORICS-MECHATRONICS

http://hidraulica.fluidas.ro

ISSN 1453 - 7303
ISSN-L 1453 - 7303

CONTENTS

BOARD

Published by:
Hydraulics and Pneumatics Research Institute, Bucharest-Romania
Address: 14 Cuţitul de Argint, district 4, Bucharest, 040558, Romania
Phone: +40 21 336 39 91; Fax: +40 21 337 30 40; e-Mail: ihp@fluidas.ro; Web: www.ihp.ro
with support from:
National Professional Association of Hydraulics and Pneumatics in Romania - FLUIDAS
e-Mail: fluidas@fluidas.ro; Web: www.fluidas.ro

HIDRAULICA Magazine is indexed by international databases

ISSN 1453 – 7303; ISSN – L 1453 – 7303

EDITORIAL

On advisers

Ph.D.Eng. Petrin DRUMEA
MANAGING EDITOR

As a young engineer I was impressed by some people who served as advisers in a research & design unit. They were mature people, scholars, with a lot of professional experience and many technical and scientific achievements, especially in the area of practical achievements. Their main task was to quickly analyze the piece of work that someone presented to them, check if there were any visible or hidden errors and give concrete advice, even though not in the details. Their experience and professional capacity allow them to be critical, but kind, so that in the end no one felt offended and there was no strange or misleading advice.

This almost idyllic image has been shaken away from me for the first time when I was asked to endorse the appointment of a person with poor schooling and work experience in a management position in a company (back then still state-owned enterprise); we had to provide this person with 3 or 4 advisers for him to understand the affairs of a director and be able to manage the company. Finally, everyone involved in the issue realized that such an idea was bad for everyone, including the person proposed to become a director.

I admit that in my mind there was the idea that there should be two elements to enable counseling. The first element is the person under the counseling process, who should be able to receive the advice and use it in a useful manner, and the second element consists in the adviser’s ability to understand the problems and be able to supply solutions when being asked to. In the technical field, usually advisers are middle aged persons, with good professional background, who are also good educators. There are many areas where it really matters that, in addition to the theoretical knowledge of the issues, there is also enough practice in order to avoid errors that may occur in special situations, during the progress of certain activities.

Of course, the suggestion from a kind of prankish fellow for him to be provided with a young female adviser, who graduated from the "school of life" at the evening class, could be interesting; however, to my suggestion that the same person to fly the plane by which she was just about to travel to a foreign country, my colleague changed his mind and admitted that the counseling process is an act of seriousness and responsibility.

Is it that difficult for everyone in every place, even in politics and state administration, to seriously address the issue of choosing and appointing advisers? In the technical and industrial fields these people do not come forth, not even sign the final version of documents, so they should have a sense of responsibility throughout the counseling process, although formally they cannot be held guilty when delicate situations arise.

Nevertheless, I strongly believe in the usefulness of advisors in all areas, even though sometimes they exceed their attributions and neglect their tasks.

Analysis of Temperature Resistance of Pressurized Cylindrical Fuel Tanks

Assoc. Prof. PhD. Eng. **Mihai ŢĂLU**[1], Assoc. Prof. PhD. Eng. **Ștefan ŢĂLU**[2,*]

[1] University of Craiova, Faculty of Mechanics, Department of Applied Mechanics and Civil Engineering, Calea București Street, no. 107, 200512 Craiova, Dolj county, Romania. E-mail: mihai_talu@yahoo.com

[2] Technical University of Cluj-Napoca, The Directorate of Research, Development and Innovation Management (DMCDI), Constantin Daicoviciu Street, no. 15, Cluj-Napoca, 400020, Cluj county, Romania. Corresponding author* e-mail: stefan_ta@yahoo.com

Abstract: *In this study, an approach based on Finite Element Modeling (FEM) was applied to analyze the performances of three different pressurized cylindrical fuel tanks with the same lateral cover, but with various head covers geometries. A specific mechanical and thermal model based on FEM was developed. A particular analysis of temperature resistance was carried out, to define specific key performance indicators and to determine the advantageous form of tank with the minimum stress state and linear deformation.*

Keywords: *Automotive industry, corrosion, industrial engineering design, optimization methods, pressurized cylindrical fuel tank, temperature resistance*

1. Introduction

In the past decades, the fuel tanks market trend is based on key strategic business plans that promote the competitive paths in the emerging automotive field and in promoting innovative ideas to improve vehicle's performance [1-6].
The challenge for the engineers and research specialists is to formulate a sustainable strategy based on a rigorous research and analysis that promotes the development computer aided engineering process of modern fuel tanks, especially over the medium to long term, within the constraints due to the economic and financial crisis [7-12].
Cylindrical and conformable shaped storage tanks, made from aluminum alloys or various types of steel, are used in the automotive industry for safely storing fuel: compressed natural gas (CNG) or liquefied petroleum gas (LPG) [11-14].
In computer aided engineering design and construction of the fuel tanks: specific structure variables [13-15], shape design variables [16, 17], design constraints [18, 19], software tools [20-25], and design decision variables [26-28] are used to validate the optimal computational geometric models [29-36].
The homologation tests of systems and components for LPG and CNG alternative fuelling of cars according to ECE Regulation No. 67.01, ECE Regulation No. 110 and standards ISO 15500 are [37, 38]:
a) Hydrostatic pressure tests: • pressure vessel tests; • destructive tests up to a static pressure of 300 MPa; • residual strength tests; • metal as well as composite hydraulic member tests; • hydraulic hose tests.
b) Hydrodynamic pressure tests: • pulsed pressure tests; • cyclic stress tests; • cyclic stress tests of hoses.
c) Temperature and humidity tests: • tests of devices at extreme temperatures (-70 to 180 ^{0}C) and relative humidity from 10 % to 95 % up to dimensions 1000 x 1000 x 2500 mm.

2. Design methodology

In our study the test of temperature resistance, one of the special safety tests of cylindrical pressurized fuel tanks carried out at the homologation stage, was performed.
The parameterized modeling of the cylindrical pressurized fuel tank (sectioned to *½ , ¼ or $^1/_8$* of the initial model, as a consequence of the tank constructive symmetry) was done in the AutoCAD

Autodesk 2017 software [39], which was imported to SolidWorks 2017 software [40] for analysis with the: Static, Thermal and Design Study modules.
The 3D parameterized models were thermally loaded at the specified stress state to determine the maximum work temperature T_{max} and the explosion temperature T_r, at the initial and final time of exploitation of the fuel tank.
The design data used in this analysis are:

- the lateral cover with: diameter D = 250 mm and length L = 700 mm;
- the construction material of the sheet metal: steel AISI 4340;
- the maximum static hydraulic pressure: p_{max} = 30 bar;
- the working temperature between the limits: T = -30 ^{0}C to T = 60 ^{0}C;
- the exploitation period of tank: n_a = 20 years;
- the corrosion rate of the material: v_c = 0.1 mm /year.

The temperature resistance means: the maximum temperature at which the resulting stress Von Mises is equal to the admissible stress traction of material $\sigma_{rez} = \sigma_a$ and the explosion temperature is the temperature at which the Von Mises stress attain the breaking stress of the material $\sigma_{rez} = \sigma_r$.

2.1 The study at temperature resistance of the cylindrical lateral cover

The parameterized model used in calculus is a section of ¼ from the initial lateral cover of tank, taking into consideration the axial symmetry (figure 1) and the specified surfaces to which the constraints and restrictions are applied (figure 2) [8].

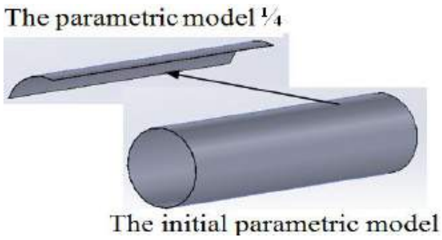

Fig. 1. The parametric model of lateral covers

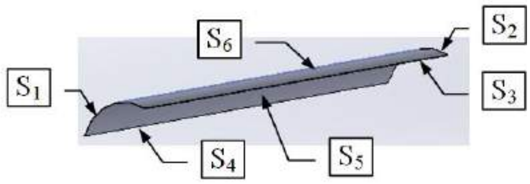

Fig. 2. The ¼ section of lateral head covers where is made the marking of the exterior surfaces

Applying the optimization procedure, a laminate sheet of AISI 4340 steel with a thickness of $s = 4^{+0.25}_{-0.6}$ mm is chosen for FEM analyses.
According to Fig. 2, to calculate the temperatures: T_{max} and T_r, the following algorithm was applied:

- the maximum pressure p_{max} = 3 N/mm^2 on inner surface S_5;
- two opposite and equal traction forces, F = 36800 N applied on surfaces: S_1 and S_2, due to the action of pressure on the inner surface of head covers;
- the high temperature on surface S_6, over T > 60 ^{0}C in order to achieve the admissible value of stress at traction equal with σ_a = 710 N/mm^2 (necessary to calculate the work maximum temperature T_{max}); and the high temperature in order to achieve the breaking stress of material with σ_r = 1100 N/mm^2 (necessary to calculate the explosion temperature T_r);
- the construction material of the lateral cover: steel AISI 4340.

The following numerical results for lateral cover were obtained:
a) for n_a = 0 years: T_{max} = 302.65 ^{0}C with the corresponding stress distribution (as shown in figure 3a); and T_r = 474.2 ^{0}C, with the corresponding stress distribution (as shown in figure 3b).
b) for n_a = 20 years: T_{max} = 182.85 ^{0}C, with the corresponding stress distribution (as shown in figure 3c); and T_r = 336.87 ^{0}C, with the corresponding stress distribution (as shown in figure 3d).

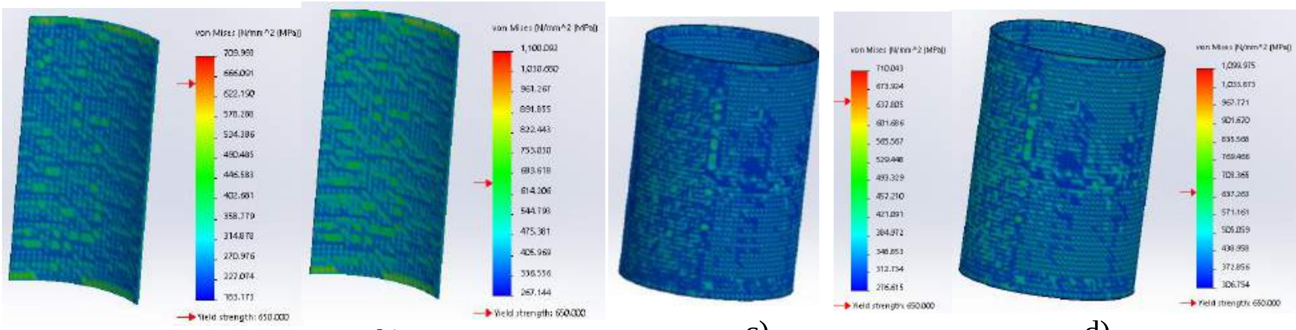

a) b) c) d)

Fig. 3. The graphs of Von Mises stress distribution at: a) the temperature T_{max} and n_a = 0 years; b) the explosion temperature T_r and n_a = 0 years; c) the temperature T_{max} and n_a = 20 years; d) the explosion temperature T_r and n_a = 20 years

2.2 The study at temperature resistance of the cylindrical pressurized tank with torospheric head covers

The parameterized model of tank (as shown in figure 4) and the sketch of torospheric head cover (as shown in figure 5) are given bellow:

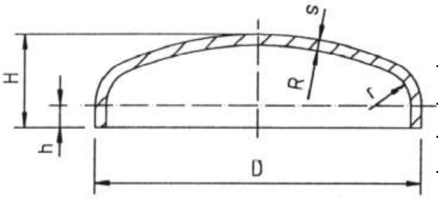

$r = 0.1 \cdot D$
$R = D$
$h \cong 3.5s$
$H = 0.2D + s + h$

Fig. 4. The parametric model of tank with torospheric head covers

Fig. 5. The sketch of torospheric head cover

After design optimization a laminate sheet of AISI 4340 steel with a thickness of $s = 5.5^{+0.25}_{-0.6}$ mm it was chosen for the manufacturing process (as shown in figure 5). Next dimensions were obtained for the head cover: R = 250 mm, r = 25 mm, h = 20 mm and H = 75.5 mm.
The following numerical results were obtained for Von Mises stress distribution at n_a = 0 years: T_{max} = 232.22 ^{0}C with the corresponding stress distribution (as shown in figures 6a and 6b); and T_r = 363.39 ^{0}C, with the corresponding stress distribution (as shown in figures 6c and 6d).
The graphs of Von Mises stress distribution were shown on the sectioned model at $^1/_8$ in figures 6a and 6c and in figures 6b and 6d for the entire model.

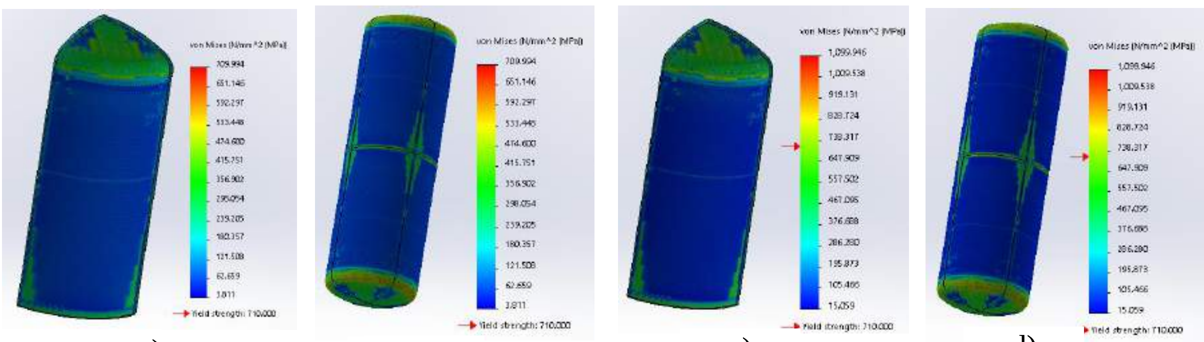

a) b) c) d)

Fig. 6. The graphs of Von Mises stress distribution for n_a = 0 years: a) and b) at the temperature T_{max}; c) and d) at the explosion temperature T_r

The following numerical results were obtained for Von Mises stress distribution at n_a = 20 years: T_{max} = 156.18 ^{0}C with the corresponding stress distribution (as shown in figures 7a and 7b); and T_r = 283.3 ^{0}C, with the corresponding stress distribution (as shown in figures 7c and 7d).

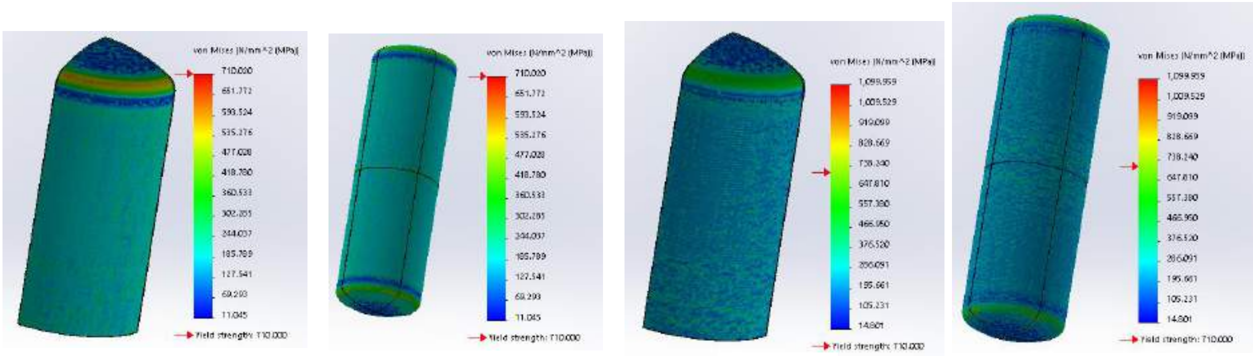

a) b) c) d)

Fig. 7. The graphs of Von Mises stress distribution for n_a = 20 years: a) and b) at the temperature T_{max}; c) and d) at the explosion temperature T_r

2.3 The study at temperature resistance of the cylindrical pressurized tank with ellipsoidal head covers

The parameterized model of tank (as shown in figure 8) and the sketch of ellipsoidal head cover (as shown in figure 9) are given bellow:

Fig. 8. The parametric model of tank with ellipsoidal head covers

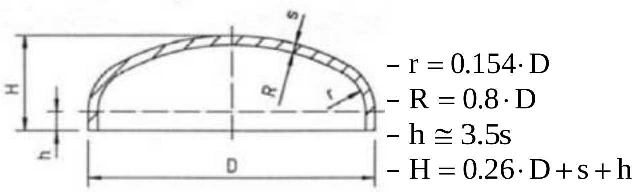

Fig. 9. The sketch of ellipsoidal head cover according the standard DIN 28013

After design optimization a laminate sheet of AISI 4340 steel with a thickness of $s = 4.5^{+0.25}_{-0.6}$ mm it was chosen for the manufacturing process (as shown in figure 9). Next dimensions were obtained for the ellipsoidal cover: R = 200 mm, r = 38.5 mm, h = 16 mm and H = 85.5 mm.
The following numerical results were obtained for Von Mises stress distribution at n_a = 0 years: T_{max} = 271.55 ^{0}C, with the corresponding stress distribution (as shown in figures 10a and 10b); and T_r = 407.15 ^{0}C, with the corresponding stress distribution (as shown in figures 10c and 10d).
The graphs of Von Mises stress distribution were shown on the sectioned model at $^1/_8$ in figures 10a and 10c and in figures 10b and 10d for the entire model.

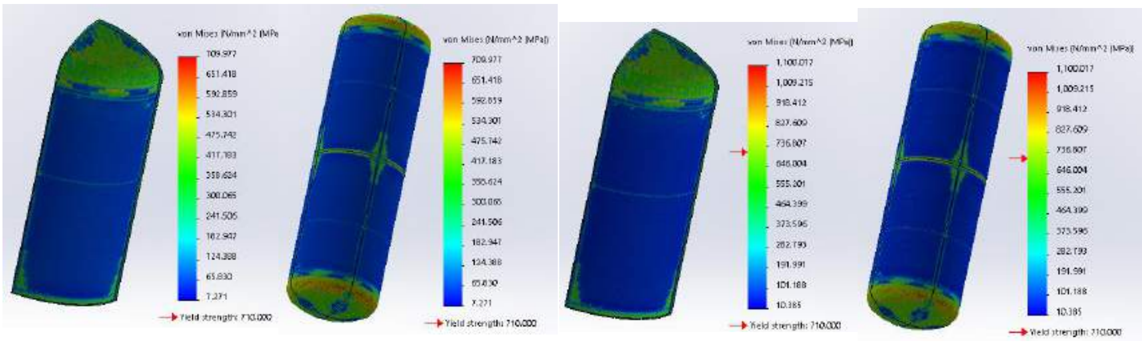

a) b) c) d)

Fig. 10. The graphs of Von Mises stress distribution for n_a = 0 years: a) and b) at the temperature T_{max}; c) and d) at the explosion temperature T_r

The following numerical results were obtained for Von Mises stress distribution at n_a = 20 years: T_{max} = 155.07 ^{0}C, with the corresponding stress distribution (as shown in figures 11a and 11b); T_r = 280.85 ^{0}C, with the corresponding stress distribution (as shown in figures 11c and 11d).

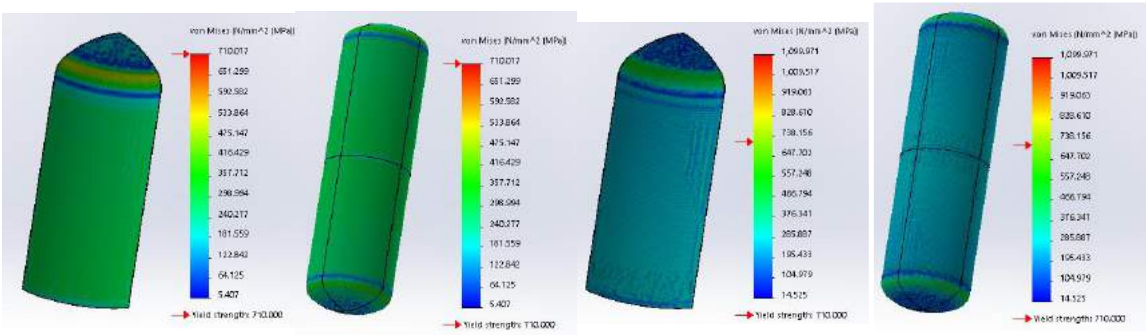

a) b) c) d)

Fig. 11. The graphs of Von Mises stress distribution for n_a = 20 years: a) and b) at the temperature T_{max}; c) and d) at the explosion temperature T_r

2.4 The study at temperature resistance of the cylindrical pressurized tank low pressure head covers

The parameterized model of tank (as shown in figure 12) and the sketch of the low pressure head cover (as shown in figure 13) are given bellow:

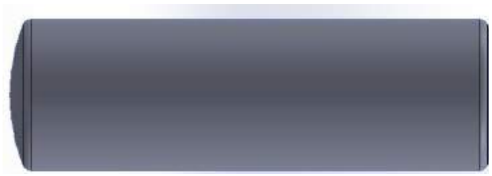

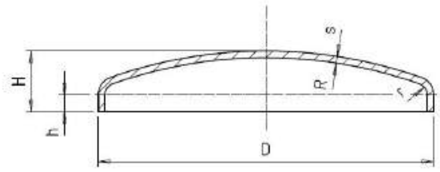

$- \ r = [15..40]\mathrm{mm}$

$- \ h = [20..25]\mathrm{mm}$

$- \ H = 0.13 \cdot D + s + h$

Fig. 12. The parametric model of tank with low pressure head covers

Fig. 13. The sketch of the low pressure head cover

After design optimization a laminate sheet of AISI 4340 steel with a thickness of s = $6.5^{+0.25}_{-0.6}$ mm it was chosen for the manufacturing process (as shown in Figure 13). Next dimensions were obtained for the low pressure head cover: h = 22 mm, r = 15 mm and H = 61 mm.
The following numerical results were obtained for Von Mises stress distribution at n_a = 0 years: T_{max} = 222.25 ^{0}C, with the corresponding stress distribution (as shown in figures 14a and 14b); and T_r = 360.94 ^{0}C, with the corresponding stress distribution (as shown in figures 14c and 14d).
The graphs of Von Mises stress distribution were shown on the sectioned model at $^1/_8$ in figures 14a and 14c and in figures 14b and 14d for the entire model.

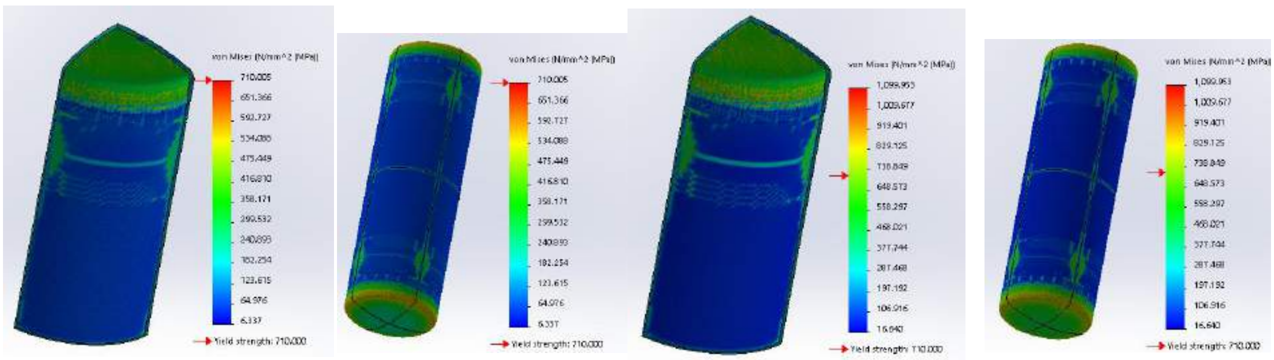

a) b) c) d)

Fig. 14. The graphs of Von Mises stress distribution for n_a = 0 years: a) and b) at the temperature T_{max}; c) and d) at the explosion temperature T_r

The following numerical results were obtained for Von Mises stress distribution at n_a = 20 years: T_{max} = 150.2 ^{0}C, with the corresponding stress distribution (as shown in figures 15a and 15b); T_r = 275.55 ^{0}C, with the corresponding stress distribution (as shown in figures 15c and 15d).

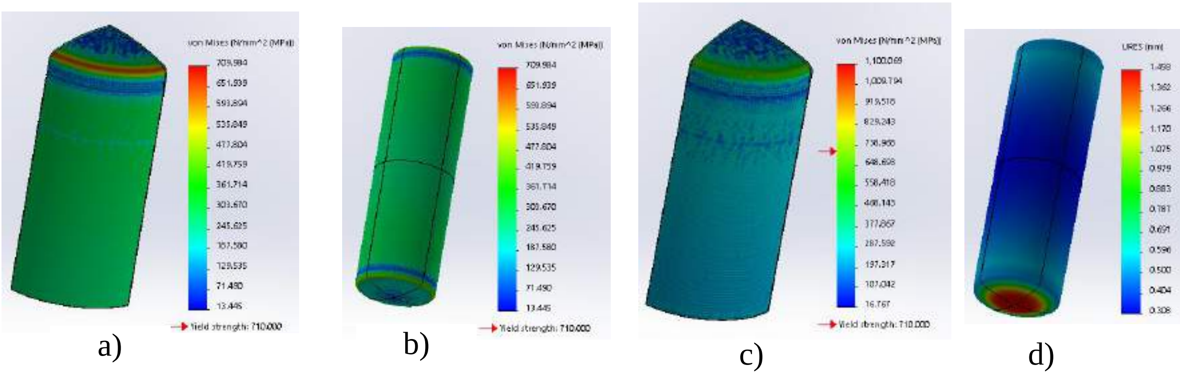

Fig. 15. The graphs of Von Mises stress distribution for n_a = 20 years: a) and b) at the temperature T_{max}; c) and d) at the explosion temperature T_r

The linear deformation corresponding to the extreme temperatures were also computed. The numerical values of state of stress and linear resultant deformation of the tanks are given in Table 1.

Table 1: The Von Mises stress and deformation of tanks at temperatures T_{max} and T_r

No.	The type of cylindrical tank	n_a [years]	T_{max} [^{0}C]	u_{max} [mm]	T_r [^{0}C]	u_r [mm]
			σ_a = 710 MPa		σ_r = 1100 MPa	
1	Tank with torosferic head covers	0	232.22	0.541	363.39	0.744
		20	156.18	0.796	283.30	0.932
2	Tank with ellipsoidal head covers	0	271.55	0.55	407.15	0.783
		20	155.07	0.782	280.85	1.005
3	Tank with low pressure head covers	0	225.25	0.713	360.94	0.912
		20	150.20	1.192	275.55	1.458

The graphical representations of $T_{max}(n_{tank})$ and $T_r(n_{tank})$ depending on the number's tank as specified in Table 1, computed for the initial and the final time of exploitation are shown in figures 16 and 17.

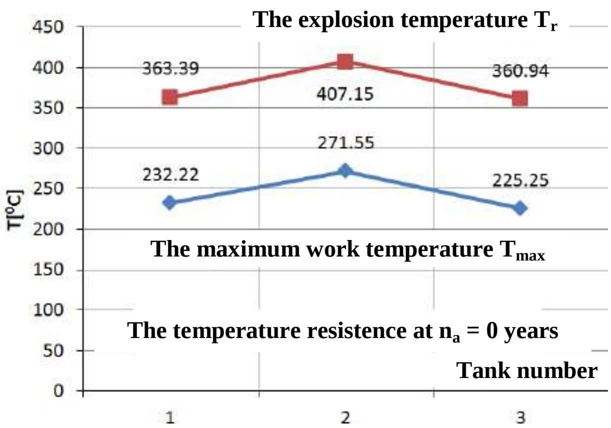

Fig. 16. The graphs of $T_r(n_{tank})$ and $T_{max}(n_{tank})$ at n_a = 0 years

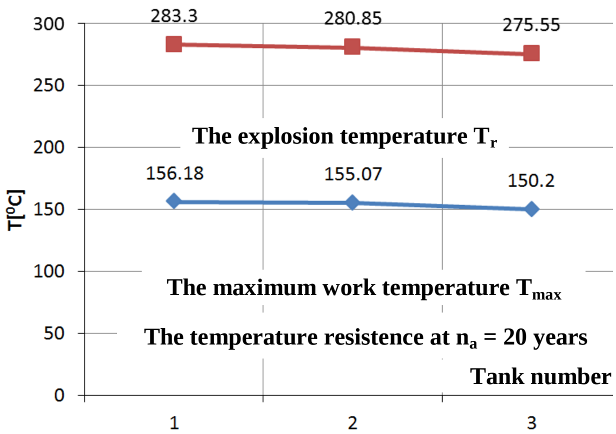

Fig. 17. The graphs of $T_r(n_{tank})$ and $T_{max}(n_{tank})$ at n_a = 20 years

The graphical representations of $T_{max}(n_{tank})$ and $T_r(n_{tank})$ depending on the number's tank as specified in Table 1, computed for the initial and the final time of exploitation (arranged on the same graph) are shown in figures 18 and 19.

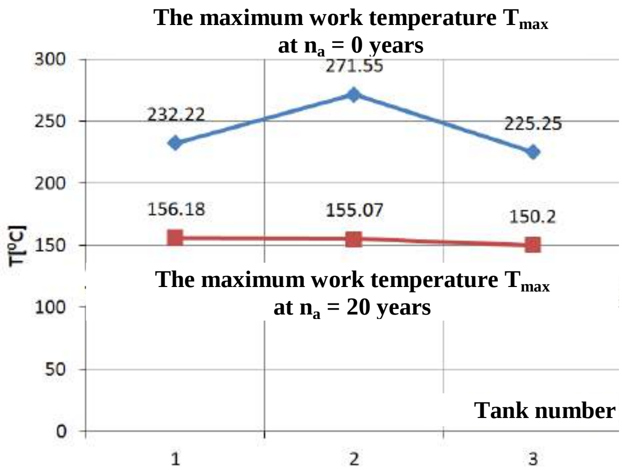

Fig. 18. The graphs of $T_{max}(n_{tank})$ at n_a = 0 and 20 years

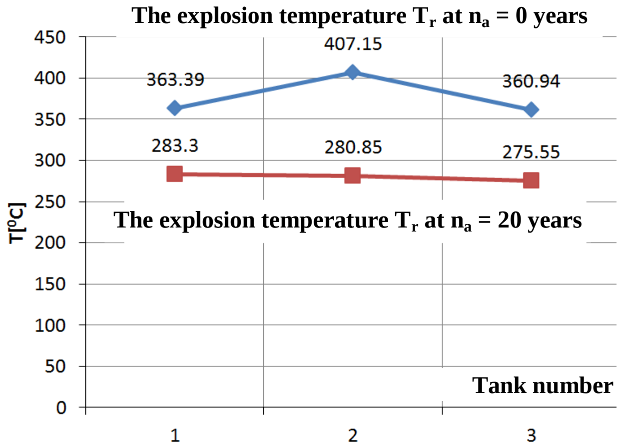

Fig. 19. The graphs of $T_r(n_{tank})$ at n_a = 0 and 20 years

The graphical representations of $T_{max}(n_a, n_{tank})$ and $T_r(n_a, n_{tank})$ are shown in figures 20 and 21.

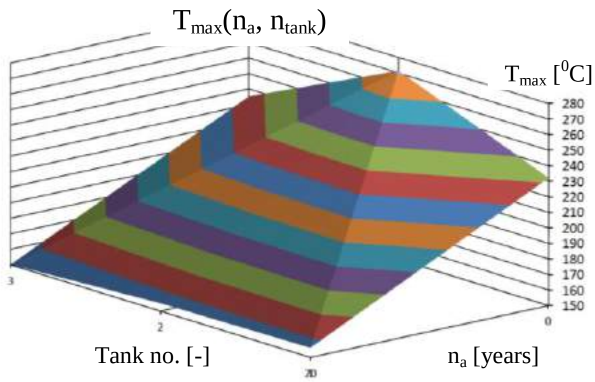

Fig. 20. The 3D graph of $T_{max}(n_a, n_{tank})$

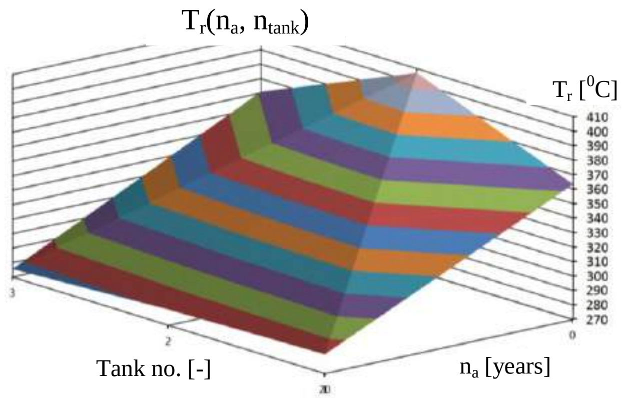

Fig. 21. The 3D graph of $T_r(n_a, n_{tank})$

The graphical representations of $u_{max}(n_{tank})$ and $u_r(n_{tank})$ depending on the number's tank as specified in Table 1, computed for the initial and the final time of exploitation are shown in figures 22 and 23.

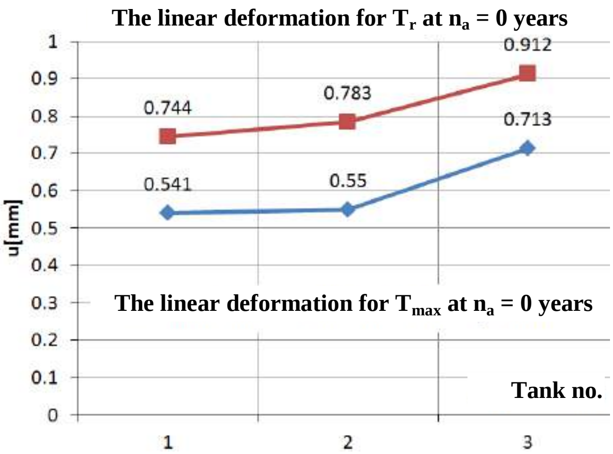

Fig. 22. The graphs of $u(n_a)$ for T_r and T_{max} at n_a = 0 year

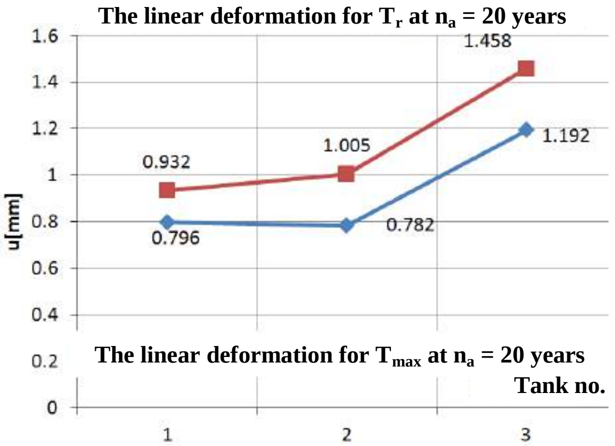

Fig. 23. The graphs of $u(n_a)$ for T_r and T_{max} at n_a = 20 years

The graphical representations of $u_{max}(n_{tank})$ and $u_r(n_{tank})$ depending on the number's tank as specified in Table 1, computed for the initial and the final time of exploitation (and arranged on the same graph for T_{max} and T_r) are shown in figures 24 and 25.

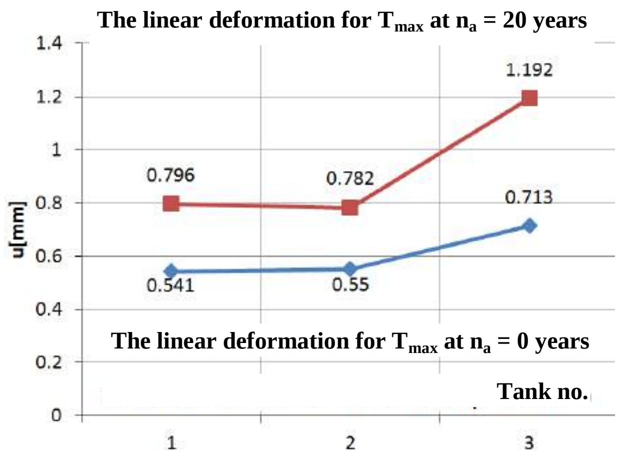

Fig. 24. The graphs of $u(n_a, n_{tank})$ for T_{max}

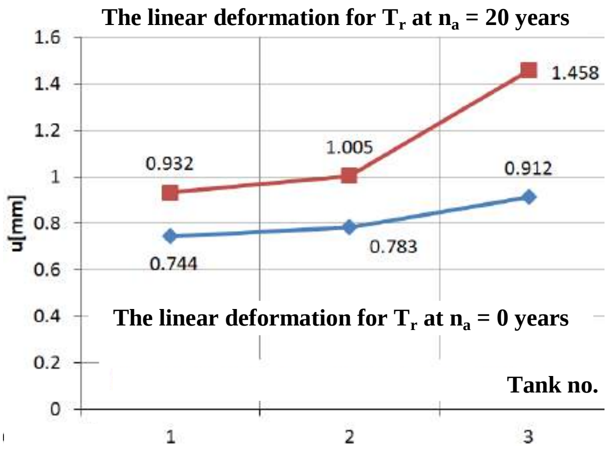

Fig. 25. The graphs of $u(n_a, n_{tank})$ for T_r

The graphical representations of $u_{max}(n_a, n_{tank})$ and $u_r(n_a, n_{tank})$ are shown in figures 26 and 27.

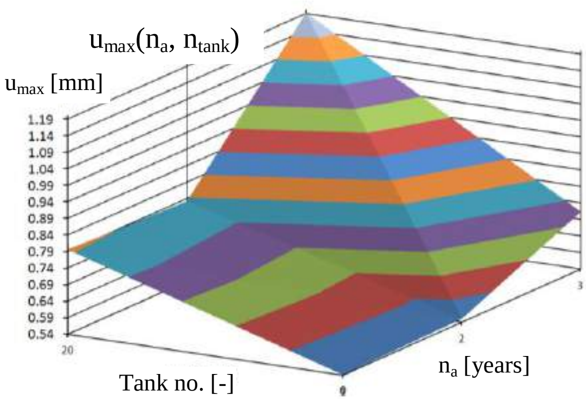

Fig. 26. The 3D graph of $u_{max}(n_a, n_{tank})$

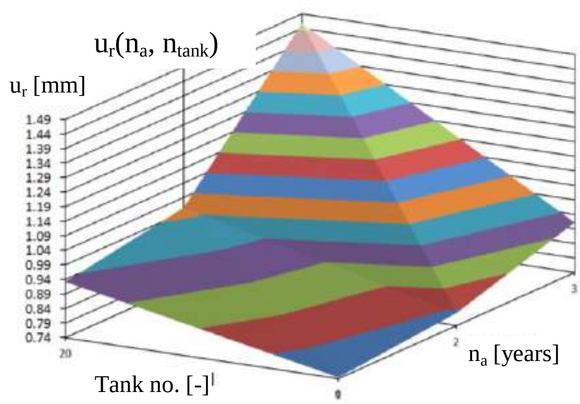

Fig. 27. The 3D graph of $u_r(n_a, n_{tank})$

3. Discussion

The tank with ellipsoidal head covers (at n_a = 0 years) has the highest work temperature T_{max} = 271.55 ^{0}C and the highest explosion temperature T_r = 407.15 ^{0}C, while the tank with low pressure head covers has the lowest work temperature T_{max} = 225.25 ^{0}C and the lowest explosion temperature T_r = 360.94 ^{0}C, (as shown in figure 16).
The tank with torospheric head covers (at n_a = 20 years) has the highest working temperature T_{max} = 156.18 ^{0}C and explosion temperature T_r = 283.3 ^{0}C; while the tank with low pressure head covers has the lowest work temperature T_{max} = 150.2 ^{0}C and explosion temperature T_r = 275.55 ^{0}C, (as shown in figure 17).
The tank with low pressure head covers (at n_a = 0 years, for T_{max} and T_r) has the maximum linear deformation u_{max} = 0.713 mm and u_r = 0.912 mm; while the tank with torospheric head covers has the lowest deformation u_{max} = 0.541 mm and u_r = 0.744 mm, (as shown in figure 22).
The tank with low pressure head covers (at n_a = 20 years, for T_{max} and T_r) has the maximum linear deformation u_{max} = 1.192 mm and u_r = 1.458 mm; while the tank with ellipsoidal head covers has the lowest deformation u_{max} = 0.782 mm and u_r = 1.005 mm.

4. Conclusions

In this study, were analyzed the performances of three different pressurized cylindrical fuel tanks with the same lateral cover, but with various head covers geometries. It was found that the

temperature resistance, the Von Mises stress and deformation are influenced by the tank geometry.
The highest temperature resistance (at n_a = 0 years) was found for the tank with ellipsoidal head covers, while the lowest temperature resistance was found for the tank with low pressure head covers.
The highest temperature resistance (at n_a = 20 years) was found for the tank with torospheric head covers, while the lowest temperature resistance was found for the tank with low pressure head covers.
The lowest linear deformation was found for the tank with torospheric head covers, while the maximum deformation was found for the tank with low pressure head covers.

Financial disclosure: Neither author has a financial or proprietary interest in any material or method mentioned.
Competing interests: The authors declare that they have no significant competing financial, professional or personal interests that might have influenced the performance or presentation of the work described in this manuscript.

References

[1] Ghiţă, C. Mirela, Anton C. Micu, Mihai Ţălu, Ştefan Ţălu and Ema I. Adam. "Computer-Aided Design of a classical cylinder gas tank for the automotive industry." *Annals of Faculty of Engineering Hunedoara - International Journal of Engineering, Hunedoara*, *Romania*, Tome XI, Fascicule 4 (2013): 59-64.
[2] Ghiţă, C. Mirela, Anton C. Micu, Mihai Ţălu and Ştefan Ţălu. "3D modelling of a gas tank with reversed end up covers for automotive industry.", *Annals of Faculty of Engineering Hunedoara - International Journal of Engineering, Hunedoara*, *Romania*, Tome XI, Fascicule 3 (2013): 195-200.
[3] Ghiţă, C. Mirela, Anton C. Micu, Mihai Ţălu and Ştefan Ţălu. "Shape optimization of vehicle's methane gas tank." *Annals of Faculty of Engineering Hunedoara - International Journal of Engineering, Hunedoara, Romania*, Tome X, Fascicule 3 (2012): 259-266.
[4] Ghiţă, C. Mirela, Anton C. Micu, Mihai Ţălu and Ştefan Ţălu. "3D modelling of a shrink fitted concave ended cylindrical tank for automotive industry." *Acta Technica Corviniensis – Bulletin of Engineering, Hunedoara, Romania*, Tome VI, Fascicule 4 (2013): 87-92.
[5] Ghiţă, C. Mirela, Ştefan C. Ghiță, Ştefan Ţălu and Simona Rotaru, "Optimal design of cylindrical rings used for the shrinkage of vehicle tanks for compressed natural gas." *Annals of Faculty of Engineering Hunedoara - International Journal of Engineering, Hunedoara*, Tome XII, Fascicule 3 (2014): 243-250.
[6] Ghiţă, C. Mirela, Anton C. Micu, Mihai Ţălu and Ştefan Ţălu. "Shape optimization of a thoroidal methane gas tank for automotive industry." *Annals of Faculty of Engineering Hunedoara - International Journal of Engineering, Hunedoara, Romania*, Tome X, Fascicule 3 (2012): 295-297.
[7] Ţălu, Ştefan and Mihai Ţălu. "The influence of deviation from circularity on the stress of a pressurized fuel cylindrical tank." *Magazine of Hydraulics, Pneumatics, Tribology, Ecology, Sensorics, Mechatronics (HIDRAULICA)*, no. 4 (December 2017): 34-45.
[8] Bică, Marin, Mihai Ţălu and Ştefan Ţălu. "Optimal shapes of the cylindrical pressurized fuel tanks." *Magazine of Hydraulics, Pneumatics, Tribology, Ecology, Sensorics, Mechatronics (HIDRAULICA)*, no. 4 (December 2017): 6-17.
[9] Ţălu, Mihai. "The influence of the corrosion and temperature on the Von Mises stress in the lateral cover of a pressurized fuel tank." *Magazine of Hydraulics, Pneumatics, Tribology, Ecology, Sensorics, Mechatronics (HIDRAULICA)*, no. 4 (December 2017): 89-97.
[10] Vintilă, Daniela, Mihai Ţălu and Ştefan Ţălu. "The CAD analyses of a torospheric head cover of a pressurized cylindrical fuel tank after the crash test." *Magazine of Hydraulics, Pneumatics, Tribology, Ecology, Sensorics, Mechatronics (HIDRAULICA)*, no. 4 (December 2017): 57-66.
[11] Ţălu, Mihai and Ştefan Ţălu. "Design and optimization of pressurized toroidal LPG fuel tanks with variable section." *Magazine of Hydraulics, Pneumatics, Tribology, Ecology, Sensorics, Mechatronics (HIDRAULICA)*, no. 1 (March 2018): 32-41.
[12] Kișioglu, Yasin. "Burst tests and volume expansions of vehicle toroidal LPG fuel tanks." *Turkish J. Eng. Env.*, vol. 33 (2009): 117-125. DOI: 10.3906/muh-0905-2.
[13] Patel, M. Pankit and Jaypalsinh Rana. "Design & optimization of LNG-CNG cylinder for optimum weight." *IJSRD - International Journal for Scientific Research & Development*, vol. 1, issue 2 (2013): 282-286.
[14] Gopi, Remya and Beena B.R. "Finite Element Analysis OF GFRP LPG Cylinder." *IJEDR - International Journal of Engineering Development and Research*, vol. 3, issue 4 (December 2015): 642-649.

[15] Khobragade, Rashmi and Vinod Hiwase. “Design, and analysis of pressure vessel with hemispherical and flat circular end.” *International Journal of Engineering Science and Computing*, vol. 7, no. 5 (2017): 12458-12469.
[16] Ţălu, Ştefan and Mihai Ţălu. “CAD generating of 3D supershapes in different coordinate systems.“ *Annals of Faculty of Engineering Hunedoara - International Journal of Engineering, Hunedoara, Romania*, Tome VIII, Fascicule 3 (2010): 215-219.
[17] Ţălu, Ştefan and Mihai Ţălu. “A CAD study on generating of 2D supershapes in different coordinate systems.“ *Annals of Faculty of Engineering Hunedoara - International Journal of Engineering, Hunedoara, Romania*, Tome VIII, Fascicule 3 (2010): 201-203.
[18] Ziółkowska, Monika and Dorota Wardzińska. "Corrosiveness of fuels during storage processes", published by IntechOpen. Accessed January 10, 2018. http://dx.doi.org/10.5772/59803.
[19] Mould, Peter, Terry Burton, Rick Daley, Shinichi Itonaga, Toshihiro Kikuchi, Sue Jokela, Michel Luciani, Matt McCosby, Doug Paul, Tetsuo Sakiyama, Gerd Schwerzel, Ray Sheffield, Greg Tarrance and Wilhelm Warnecke. "Evaluation of the corrosion durability of steel systems for automobile fuel tanks." SAE Technical Paper 2005-01-0540, 2005. Accessed January 10, 2018. https://doi.org/10.4271/2005-01-0540.
[20] Ţălu, Ştefan. *Limbajul de programare AutoLISP. Teorie şi aplicaţii. (AutoLISP programming language. Theory and applications)*. Cluj-Napoca, Risoprint Publishing house, 2001.
[21] Ţălu, Ştefan. *Reprezentări grafice asistate de calculator. (Computer assisted graphical representations).* Cluj-Napoca, Osama Publishing house, 2001.
[22] Ţălu,,Ştefan. *Grafică tehnică asistată de calculator. (Computer assisted technical graphics)*. Cluj-Napoca, Victor Melenti Publishing house, 2001.
[23] Ţălu, Ştefan. *AutoCAD 2005*. Cluj-Napoca, Risoprint Publishing house, 2005.
[24] Ţălu, Ştefan and Mihai Ţălu. *AutoCAD 2006. Proiectare tridimensională. (AutoCAD 2006. Three-dimensional designing)*. Cluj-Napoca, MEGA Publishing house, 2007.
[25] Ţălu, Ştefan. *AutoCAD 2017*. Cluj-Napoca, Napoca Star Publishing house, 2017.
[26] Țălu, Mihai. *Calculul pierderilor de presiune distribuite în conducte hidraulice. (Calculation of distributed pressure loss in hydraulic pipelines).* Craiova, Universitaria Publishing house, 2016.
[27] Țălu, Mihai. *Pierderi de presiune hidraulică în conducte tehnice cu secțiune inelară. Calcul numeric și analiză C.F.D. (Hydraulic pressure loss in technical piping with annular section. Numerical calculation and C.F.D.)*, Craiova, Universitaria Publishing house, 2016.
[28] Ţălu, Mihai. *Mecanica fluidelor. Curgeri laminare monodimensionale. (Fluid mechanics. The monodimensional laminar flow).* Craiova, Universitaria Publishing house, 2016.
[29] Ţălu, Ştefan. *Geometrie descriptivă. (Descriptive geometry)*, Cluj-Napoca, Risoprint Publishing house, 2010.
[30] Florescu-Gligore, Adrian, Magdalena Orban and Ştefan Ţălu. *Cotarea în proiectarea constructivă şi tehnologică. (Dimensioning in technological and constructive engineering graphics).* Cluj-Napoca, Lithography of The Technical University of Cluj-Napoca, 1998.
[31] Florescu-Gligore, Adrian, Ştefan Ţălu and Dan Noveanu. *Reprezentarea şi vizualizarea formelor geometrice în desenul industrial. (Representation and visualization of geometric shapes in industrial drawing).* Cluj-Napoca, U. T. Pres Publishing house, 2006.
[32] Ţălu, Ştefan and Cristina Racocea. *Reprezentări axonometrice cu aplicaţii în tehnică. (Axonometric representations with applications in technique).* Cluj-Napoca, MEGA Publishing house, 2007.
[33] Racocea, Cristina and Ştefan Ţălu. *Reprezentarea formelor geometrice tehnice în axonometrie. (The axonometric representation of technical geometric shapes).* Cluj-Napoca, Napoca Star Publishing house, 2011.
[34] Niţulescu, Theodor and Ştefan Ţălu. *Aplicaţii ale geometriei descriptive şi graficii asistate de calculator în desenul industrial. (Applications of descriptive geometry and computer aided design in engineering graphics).* Cluj-Napoca, Risoprint Publishing house, 2001.
[35] Bîrleanu, Corina and Ştefan Ţălu. *Organe de maşini. Proiectare şi reprezentare grafică asistată de calculator. (Machine elements. Designing and computer assisted graphical representations).* Cluj-Napoca, Victor Melenti Publishing house, 2001.
[36] Ţălu, Ştefan. *Micro and nanoscale characterization of three dimensional surfaces. Basics and applications*. Napoca Star Publishing House, Cluj-Napoca, Romania, 2015.
[37] *** Certification tests of LPG and CNG. Accessed January 10, 2018. http://vzlutest.cz/en/certification-tests-of-lpg-and-cng-c3.html.
[38] Nash, H. David. “UK Rules for unfired pressure vessels”. In: “The Companion guide to ASME boiler and pressure vessel code”, 2008. ASME, Chapter 51. ISBN 9780971902717. Accessed January 10, 2018. https://strathprints.strath.ac.uk/6502.
[39] *** Autodesk AutoCAD 2017 software.
[40] *** SolidWorks 2017 software.

Using the Pressure Intensifiers in Hydraulic Units of Heavy Duty Machine Tools

Prof. PhD Eng. **Dan PRODAN**[1], Prof. PhD Eng. **Anca BUCUREȘTEANU**[2]

[1] University POLITEHNICA of Bucharest, prodand2004@yahoo.com

[2] ancabucuresteanu@gmail.com

Abstract: *This paper presents some applications of the pressure intensifiers used in the hydraulic units of the clamping/unclamping systems and unloading systems for the guideways of HBM and GANTRY type heavy duty machine tools. The paper makes a comparison between the systems with and without pressure intensifiers. There are presented mathematical models for the pressure intensifiers and the results obtained after a simulation using specialized programs.*

Keywords: *Pressure intensifiers, machine tools, guideways unloading systems*

1. Introduction

The operating principle of the pressure intensifiers [1, 2, 3] is shown in Figure 1.

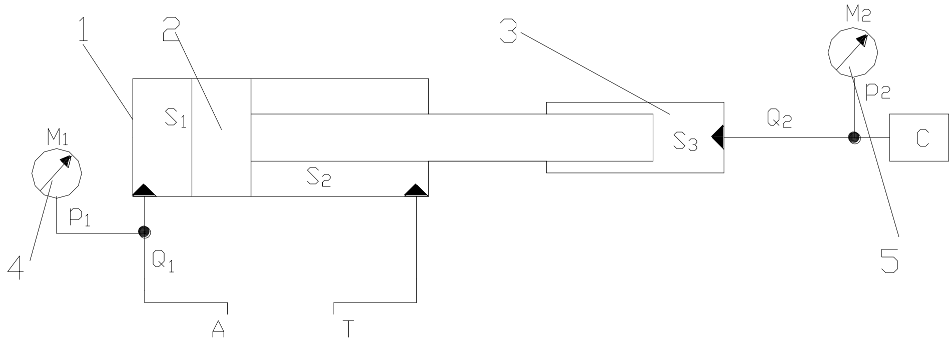

Fig. 1. Operating principle of the pressure intensifiers

If the cylinder 1 is supplied with the flow Q_1 at the pressure p_1 on the path A, the piston 2 moves in the pressure chamber 3 providing the consumer C with the liquid flow Q_2 at the pressure p_2. The pressures are read on the pressure gauges 4 and 5.
The pressure and the flow obtained depending on the surfaces S_1, S_2 and S_3 are the following ones:

$$p_2 = p_1 \frac{S_1}{S_3} \tag{1}$$

$$Q_2 = Q_1 \frac{S_3}{S_1} \tag{2}$$

In the absence of losses, the flow-pressure characteristic in stationary mode for the intensifier of Figure 1 is shown in Figure 2.
The two rectangles in Figure 2 have the same area equal to power P, where:

$$P = p_1 Q_1 = p_2 Q_2 \tag{3}$$

Consumer C can be a cylinder; in this case the flow Q_2 will feed a chamber of limited variable volume or an open circuit such as the systems of liquid jet cutting, in which case the flow Q_2 should be continuous.

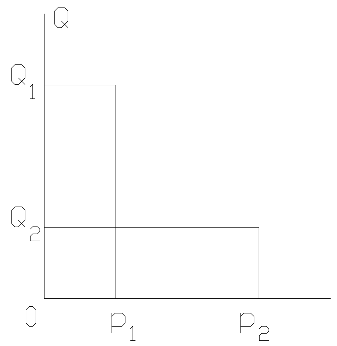

Fig. 2. Flow-pressure characteristic of the pressure intensifier

2. Hydraulic systems for guideways locking/unlocking and unloading

In the case of machine tools, the pressure intensifiers are used for powering the clamping/unclamping systems of the blanks or, in some situations, for powering the guideways unloading systems [1, 4]. In this case, the consumers C can be the single-acting hydraulic cylinders or, in the case of CNC machine tools [1], the double-acting hydraulic cylinders.
Figure 3 shows the actuation schemes for these systems.

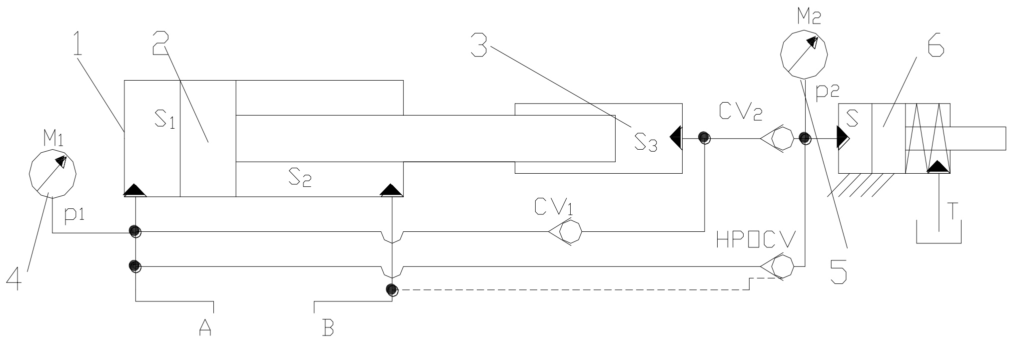

a.

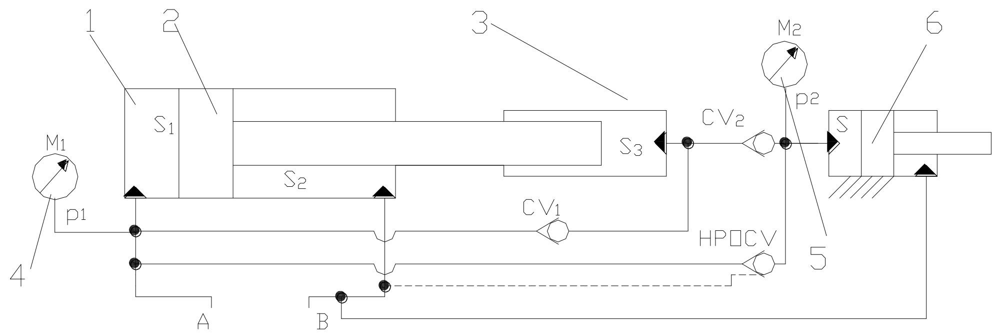

b.

Fig. 3. Using the pressure intensifiers in the hydraulic systems of machine tools

Figure 3 uses the same notations as in the previous figure, plus: 6 - consumer cylinders with useful area *S*, CV_1, CV_2 - one way check valves and HPDCV - Check valve hydraulically operated.
If the liquid supply is made on path A at a pressure lower than the value p_1, the liquid coming from chamber 3, but also directly, through the check valve CV1 and through the check valve hydraulically operated HPDCV, will get on the surface *S* of the consumers. When reaching the pressure p_1, before the cylinders 6 complete their entire travel, the pressure in chamber 3 gets to value p_2, the check valve CV1 closes and thus the locking or unloading of the guideways is

performed. If there are no losses and the oil compressibility ($E_{OIL} \rightarrow \infty$) is not taken into account, even after ceasing the supply with liquid on path A, the pressure p_2 is maintained on the surface S of the consumer thanks to the closing of valves CV_1, CV_2 and HPDCV.
By supplying the chamber B with liquid, the cylinders 6 will be discharged and will return to their initial position due to the spring for the variant shown in Figure 3a and thanks to the pressure (max. p_1) in the case of the consumers in Figure 3b. By supplying on the path B, the piston 2 of the intensifier return to its initial position, moving to the left up to the end of its travel.

3. Mathematical model of the pressure intensifiers in dynamic mode

Starting from the basic diagram of the intensifier shown in Figure 1, in dynamic mode, the following relations [3] can be taken into consideration:

$$M\frac{d^2x}{dt^2} + b\frac{dx}{dt} + c \cdot p_1 S_1 = p_2 S_3 \tag{4}$$

$$Q_1 = S_1\frac{dx}{dt} + ap_1 + \frac{V_{01}+xS_1}{E_O}\frac{dp_1}{dt} \tag{5}$$

$$Q_2 = S_2\frac{dx}{dt} - \frac{V_{02}-xS_2}{E_O}\frac{dp_2}{dt} \tag{6}$$

In the relations above there were also noted: M - mass of the piston, x - instantaneous movement of the piston, t - time, b - linearized coefficient of force losses proportional to the velocity (damping coefficient), c - friction coefficient of the piston operating in the low pressure zone, a - linearized coefficient of flow losses proportional to the pressure, V_{01} and V_{02} - initial volumes of liquid in the two champers, E_0 - elastic modulus of the liquid.
One can notice that the mathematical model is formed of non-linear differential equations. The solution of these equations by classic methods implies their linearization. The mathematical models allow understanding better the operation of the system. At the present moment there are specialized programs that enable the simulation of intensifiers operation without the need to elaborate the mathematical model. We hereby present the results obtained by simulation of a system provided with a pressure intensifier with power ration 3.8, supplied from a constant flow pump 6 l/min and a pressure p_1 = 80 bar. The consumer is similar to the consumer in Figure 3b.
The evolution of pressures p_1 and p_2 in the case of pressure intensifier powering is shown in Figure 4. In approximately 5s the high pressure circuit is supplied at the maximum pressure p_2.
Because the circuits are not sealed, for maintaining the pressure p_2 it is necessary to continue the supply of the low pressure circuit. In the case that the low pressure circuit supply (p_1, Q_1) is stopped, as shown in Figure 5, the high pressure circuit is discharged.

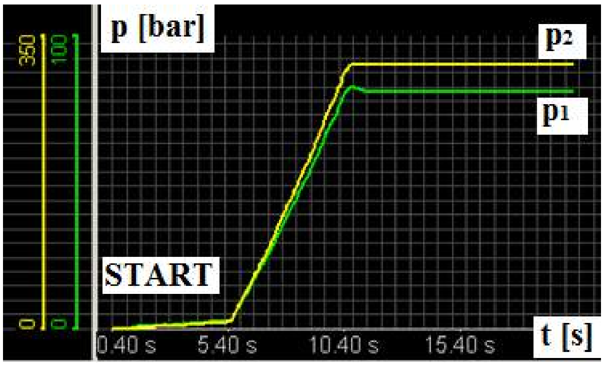

Fig. 4. Evolution of pressures p_1 and p_2

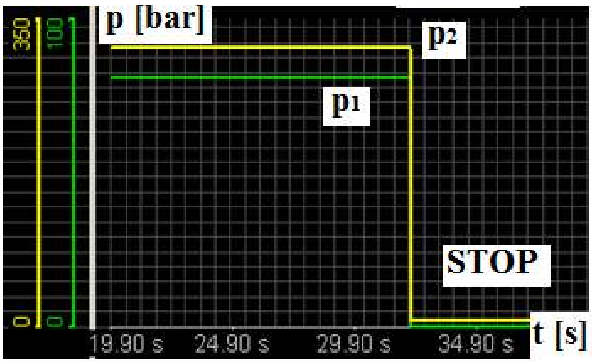

Fig. 5. Discharge of high pressure circuit

In order to avoid such situations but also to prevent the excessive heating of the oil it is recommended to use the pneumatic hydraulic accumulators [5]. Taking into account the pressure limits specific to the accumulators it is recommended to place them in the low pressure circuit.
If such accumulator is used, the evolution of the pressures p_1 and p_2 during the phase of intensifier

powering is shown in Figure 6.
Because the accumulator is charging, one can notice that the time needed to reach the maximum pressure is longer, 10 s approximately. In the case of heavy-duty machine tools, this delay does not affect decisively the auxiliary times. The presence of the accumulator makes possible to maintain the pressure in the high pressure circuit even after the discharge of the low pressure, at the source level, by using the pre-control systems [1].
Figure 7 shows how the pressure p_2 is maintained even if the low pressure circuit is not powered.

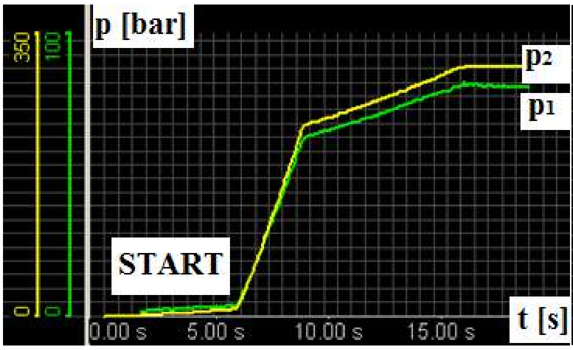

Fig. 6. Evolution of pressures p_1 and p_2 in circuit with accumulator

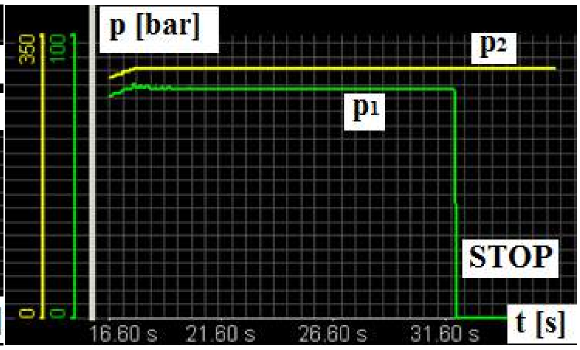

Fig. 7. Keeping the pressure p_2 after discharging the low pressure circuit

The time of pressure p_2 maintaining depends on accumulator size and on the circuit losses as well. If pressure p_2 must be maintained for a longer time, the circuit will be charged again.
For discharging the circuit, it is necessary to discharge the accumulator low pressure circuit too. This situation is simulated in Figure 8.

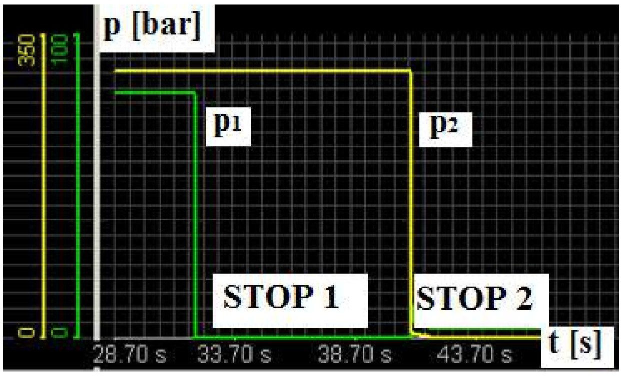

Fig. 8. Discharge of circuit when accumulators are used

In Figure 8, at STOP 1 control, the low pressure circuit is cut off (the pre-control [1] is disconnected); at STOP 2 control, all unit will be discharged, which corresponds to the supply through path B, according to Figure 3a.
The use of simulations in the design phase of hydraulic units allows determining their behavior in dynamic mode.

4. Using the pressure intensifiers in the unloading systems of heavy-duty machine tools guideways

The sliding guideways enable the unloading of large loads, the accurate stopping and locking in a controlled position. The rolling guideways are preferred for the heavy-duty machine tools if long travels must be performed. These guideways are characterized by higher velocities and low resisting forces. The use of combined guideways and unloading systems helps to obtain systems enabling the positioning movements made with high velocity on almost the entire travel, after which a travel with smaller velocity is made on the sliding guideways only, followed by an accurate stop and the eventual axis locking [2, 6].

Figure 9 shows the operating principle of the unloading systems.

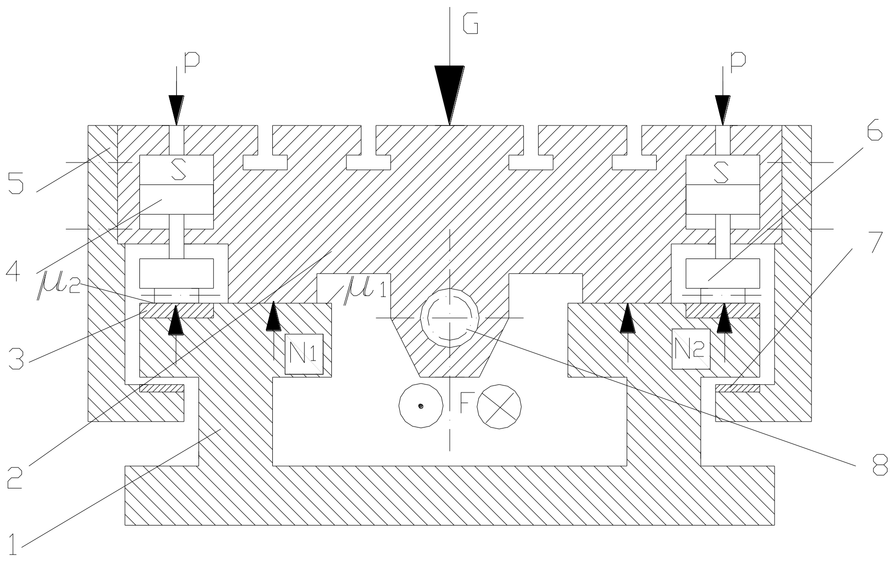

Fig. 9. Hydraulic system for guideways unloading

The saddle 2 with the sliding friction coefficient μ_1 travels on the guideways of the bed 1. Also the harder plates 3 are applied on the bed. Between these plates and the intermediate elements (with rollers) 6 there is the sliding friction coefficient μ_2. In the absence of the supply pressure *p*, the system will operate without unloading. If a pressure *p* is present on the n pistons 4 with the active surfaces *S*, these ones press the elements 6 on the plates 3. The pressure action results in the taking over of a part of the load *G* by the rolling quideways. The guideways will be secured (closed) by means of the closing plates 5. On the lower zone of these ones there is plating made of antifriction material 7. In these two cases the force *F* required at the final component of the feed mechanism 8 will have the expressions:

- Without unloading

$$F = \mu_1 G \tag{7}$$

- With unloading

$$F = \mu_1 N_1 + \mu_2 N_2 \tag{8}$$

In the relation (8) it was noted: N_1 - normal force at the sliding guideways level, N_2 - normal force at the rolling guideways level. These forces have the following expressions:

$$N_1 = G - N_2 \tag{9}$$

$$N_2 = npS \tag{10}$$

The value of pressure *p* is specially established to enable a sufficient unloading at the related kinematic chain but there will be not reached a "total unloading", characterized by the "critical value":

$$p_C = \frac{G}{nS} \tag{11}$$

The dependence of the force (F) developed by the unloading pressure (p) is shown in Figure 10.

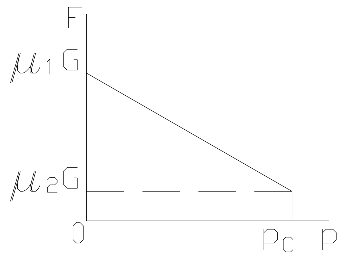

Fig. 10. Dependence of the force required by feed kinematic chain on the unloading pressure

The unloading with a pressure higher than the value p_C leads to the disappearance of the sliding guiding, to unsteadiness and can even overstress the closing elements 3 and 5.
Once determined the value of the operating pressure *p*, this one must be obtained and maintained at the n pistons as long as needed. Usually the pressure is necessary for rapid travels for positioning. These travels are performed in much smaller times that the times required by the machining operations. It is the case of the unloading of X axes guideways in the Gantry type milling machines and the heavy-duty boring and milling machines [1, 6, 7].
The hydraulic units for unloading make pressures of 200 bar usually. Higher values of the pressure entail the use of more expensive components. Figure 11 shows the hydraulic diagram and a part of the hydraulic elements used to unload the guideways of an AFP type machine [1, 6, 7].

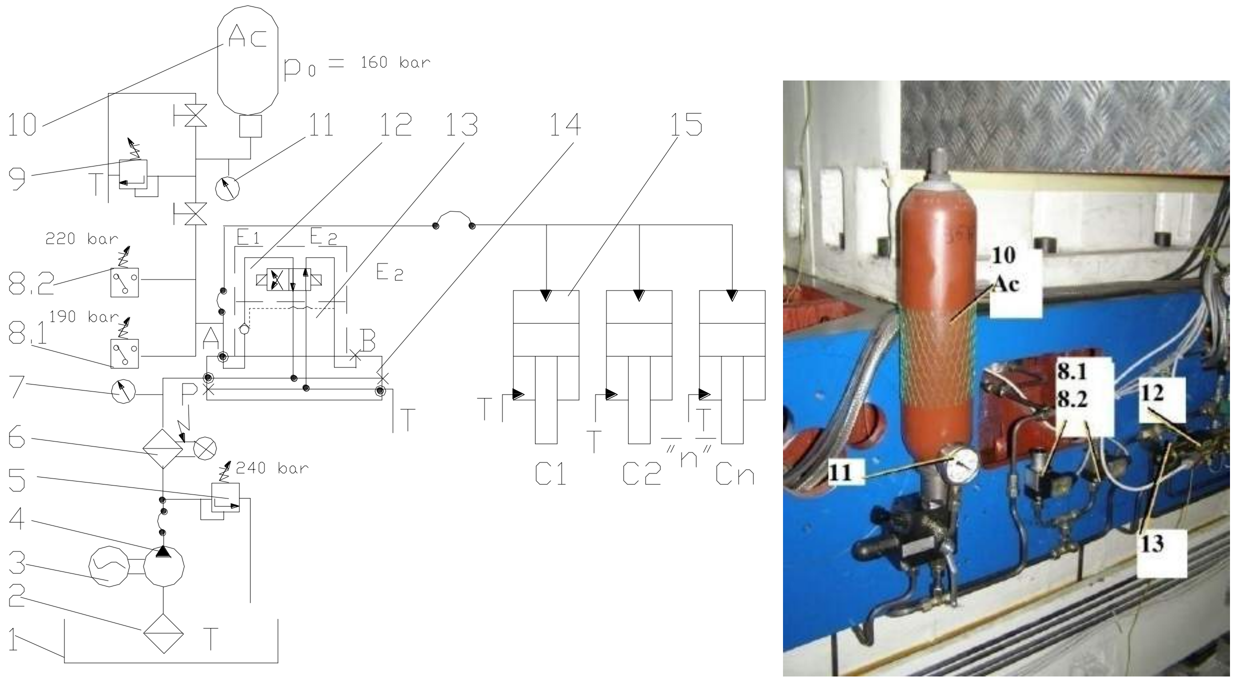

a. b.

Fig. 11. Hydraulic system of guideways unloading on X axis

The pump 4 driven by the electric motor 3 sucks the oil from the tank 1 through the suction filter 2. The operating maximum pressure is adjusted by means of the pressure relief valve 5. Then the oil is filtered by means of the filter with clogging indicator 6. The adjusted pressure is viewed on the pressure gauge 7. Plate 14 is supplied on path P. The electric valve 12 and the check valve hydraulically operated 13 are placed on the plate 14. The actuation of the electromagnet E_2 leads to the loading of the guideways unloading circuit. The pressure at the pressure relief valve 5 is ensured in all n unloading cylinders 15. In this moment the pump can be stopped. The pressure is maintained by means of the accumulator 10 [5] within the values adjusted at the pressure switches 8.1 and 8.2. The switch 8.1 controls the eventual restart of the pump, while the switch 8.2 controls

its stopping. All this time the pressure can be read on the pressure gauge 11. The system discharge is performed by actuating the electromagnet E_1 whether the pump operates or not.
The hydraulic unit includes rather many elements and the power consumed by it is about 3 KW. If a higher pressure is required, it is possible to use hydraulic pressure intensifiers. In this case, the hydraulic diagram includes one or more intensifiers, besides the elements mentioned above. These intensifiers allow operating with a lower pressure of the pump for the same cylinders (in this case under 100 bar). Thus the necessary power of the electric motor decreases (~1.5 KW) and the hydraulic elements of the low pressure circuit are less stressed. The new hydraulic diagram is shown in Figure 12. The notations are the same as the ones used in the previous figure; we mention that the electric valve 12 has another diagram and the item 16 is the pressure intensifier in Figure 12 which serves the consumers C, namely the cylinders 15, in this case.

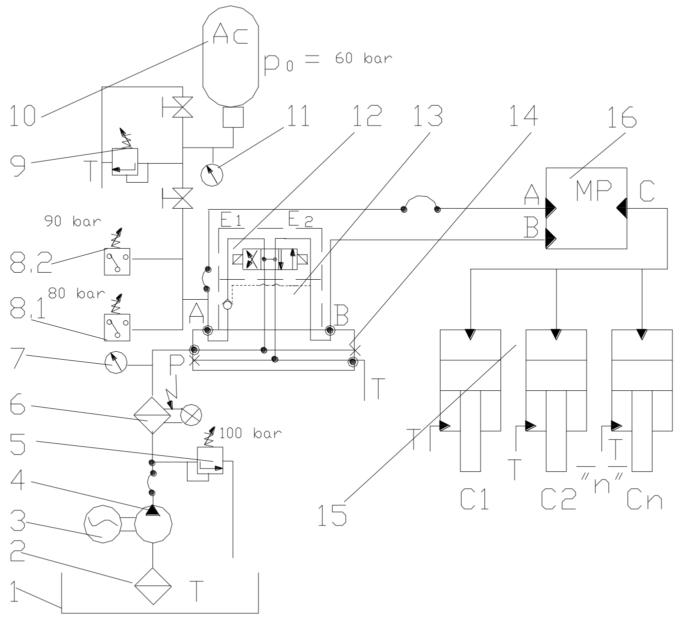

Fig. 12. Hydraulic unit for unloading with pressure intensifier and accumulator

Thanks to the pressure intensifier, the pressure adjusted at the pressure relief valve drops up to 100 bar; in its turn, the accumulator charges at a pressure of 60 bar only. In these conditions the power of motor 3 too decreases by 50%.
In some situations it is possible to use hydro-pneumatic pressure intensifiers. With this type of intensifiers, the pressure p_1 of the primary circuit is obtained from a pneumatic source but usually this one does not exceed the value of 10 bar. The operating principle of these intensifiers is similar [2]. At the same intensification ratio, the maximum pressures obtained are smaller than the pressures obtained by hydraulic intensifiers. We mention some advantages of the hydro-pneumatic intensifiers: small volumes of liquid, compact overall size, no need of pressure hydraulic sources (pumps, devices, tanks etc.).

5. Conclusions

The pressure hydraulic intensifiers are a preferable solution if high clamping/unclamping forces are required and obtained with pressures superior to 300 bar. These intensifiers serve the consumers that need small amounts of liquid. In the case of heavy-duty machine tools, they are recommended for the locking/unlocking systems but also for the unloading systems of the guideways.
As a general rule, the obtained pressures do not exceed 500 bar. These pressures develop only after getting out from the intensifier. Therefore, the devices used in the low pressure floor are not special ones and the hydro-pneumatic accumulators too can be used up to pressures of 250 bar.
For the same consumers and the same pressure (higher than 200 bar), the units that include intensifiers will have electric motors with a smaller power than the units that do not have such

intensifiers. Taking into consideration that the pressure in the low pressure circuit drops even if the tanks volume is diminished, the heating of the unit is reduced if intensifiers are used. The intensifiers entail the increase of the times intended for the performance of the respective functions. Usually, this increase of the auxiliary times in the case of the heavy-duty machine-tools does not interfere with their productivity. For these machines, the auxiliary times, even in the range of minutes, are much smaller than the machining times which are in the range of hours.
The calculation of the systems equipped with intensifiers can be easier if simulations programs are used, making possible the determination of the behavior in static mode and in dynamic mode as well.

References

[1] Prodan, Dan. *Heavy machine tools. Mechanical and Hydraulic Systems / Maşini-unelte grele. Sisteme mecanice si hidraulica*, Printech Publishing House, Bucharest, 2010.
[2] *** Catalogues and leaflets CKD, FESTO, TOX, BOSCH REXROTH, TOX® PRESSOTECHNIK S.A.S., Mini Bosster Hydraulics A/S.
[3] Prodan, Dan. *Machine-Tools. Modelling and Simulation of Hydrostatic Elements and Systems / Maşini-unelte. Modelarea şi simularea elementelor şi sistemelor hidrostatice*, Printech Publishing House, Bucharest, 2006.
[4] Esnault, Francis and Patrick Bénéteau. *Hydrostatics 1. Power Transmission / Hydrostatique 1. Transmission de Puissance*, Ellipses Publishing House, Paris, 1997.
[5] Bucuresteanu, Anca. *Pneumatic Hydraulic Accumulators. Use and Modeling / Acumulatoare pneumohidraulice. Utilizare si modelare*, Printech Publishing House, 2001, Bucharest.
[6] Joshi, Prakash Hiralal. *Machine tools handbook*, McGraw-Hill Publishing House, New Delhi, 2007.
[7] Perovic, Bozna. *Machine tools handbook / Handbuch Werkzeug-Maschinen*, Carl Hanser Verlag, Munchen, 2006.

Improving Roughness Using Toroidal Milling for Complex Surface Processing

PhD. Student Eng. **Andrei OȘAN**[1]

[1] Technical University of Cluj-Napoca - North University Center of Baia Mare, Romania, osan.andrei@yahoo.com

Abstract: *The paper aims to study the processing of complex and convex surfaces using a cutting tool in a milling radius called toroidal end milling in terms of roughness. Roughness presents important influences on machine parts and not only be in operation contact surfaces are either fixed or mobile. This paper includes a series of 11 experiments in which different regimes are tested with the main purpose of finding the optimum regimen for the work to be subjected to the toroidal milling using the roughness value Ra and Rt as the comparison criterion. For roughness determination, the TR200 is used as a measuring tool and data is loaded into a software called Time Surf. At the end of this paper a point of view will be determined regarding the roughness obtained with the toroidal milling.*

Keywords: *Tribology of complex surfaces, roughness, toroidal milling, processing regimes.*

1. Introduction

The roughness defined by SR ISO 4287: 1993[12] represents the set of micro irregularities (relative to an ideal geometric surface) of the surface resulting from a manufacturing process and which are not deviant in shape.
Surface roughness can have a major impact on the proper operation of a product. However, the large number of factors that influence the surface finish of a piece makes it difficult to choose the machining parameters appropriate to it. Selection of the proper strategy for processing and processing parameters such as depth of axial cutting, the radial depth of cut, power per tooth, the cutting speed and the inclination of the tool may lead to an increase in productivity and an increase in surface quality.
In general roughness is defined as the set of surface irregularities whose pitch is relatively small and which includes the irregularities resulting from the manufacturing processes.
According to Vișan A. and Ionescu N. [11], the main causes of influence that determine the roughness of the surfaces are:

- Method and process of surface generation;
- Tool geometry;
- Parameters of the processing regime;
- The properties of the material;
- Processing environment;
- Errors of technical processing systems.

Mike S. Lou et al.[9] states that surface roughness is an important measure of the technological quality of a product and a factor that greatly influences the cost of production. Surface quality is a very important role in the processing performance through a high-quality processed surface that significantly improves wear resistance or corrosion resistance. In addition, surface roughness also affects the surface of friction, light reflection, the ability to retain a lubricant, and electrical or thermal resistance.
Surface roughness is one of the most important parameters to determine the quality of the product. The roughness process is very dynamic, complex and process-dependent. There are two types of factors that influence the finish of the surface and, implicitly, the surface quality of a workpiece. Primary factors are the kinematic geometry of the tool that theoretically affects the surface and can be calculated from processing parameters called controllable factors such as rotation speed, feed rate and cutting depth, and the second category of factors is represented by non-geometric components including tool wear, deformation workpiece material, vibrations, tool deformation, and machine tool axle misalignment errors.

According to Lamikis et al.[8] cutting force is one of the factors that most influence the surface finish of the work surface and the life of the tool in milling complex surfaces. This is due to the fact that the thickness of the non-deformed chip varies with a variation following the cutting force as well as due to the variation of the surface slope in the cutting direction.
Depending on the types of continuous or discontinuous chips, surface finishing will increase directly with increased friction between tool surface and chips formed.
Kalpakjian, S.[7] affirm that in general the use of fluids in surface finishing processes improves the quality of the surface, they reduce the additional friction coefficient by pumping the fluid at high pressures on the surface of the blade considerably reduces adherence between the tool and the chip resulting from the surface velocity.
Decreasing the roughness of a surface will obviously increase manufacturing costs, typically compromising the cost of manufacturing a component and its performance.
According to Alauddin et al. [1] they showed that when the cutting speed is increased, productivity increases, but implicitly, also the quality of the surface. Hasegawa et al.[5] affirm that the surface finishing can be characterized by various parameters such as the average roughness Ra, the maximum height of the profile from its mean line Rp, the square root mean height Rq as well as the maximum height of the profile Rt. The current stage uses the average roughness Ra to characterize the surface quality on a large scale in industry.
Roughness, the important parameter of the surface layer, has a great influence on the wear resistance, fatigue resistance, corrosion resistance and the precision fits. In the case of gadget adjustments, irregularities (asperities) result in a decrease in the real bearing surface compared to the theoretical one considered in the calculations, which produces local increases in the contact pressure, sometimes well above those considered in the dimensioning calculations. They have the effect of accelerating contact surfaces and gaming increase, especially during the first run-up period, especially as the initial (technological) roughness is higher. These effects justify the application of correct roll-out programs after fitting.

2. Roughness parameters and their influence

In order to determine the surface quality with the corner cutter, the main parameters taken into account are the arithmetic deviation of the assessed profile Ra and the total height of the profile Rt..

2.1 Deviation of arithmetic mean of Ra

Also known as AA arithmetic mean or CLA Central Medium Line, is the arithmetic mean of the absolute values of the deviations of the profile effectively measured from the median line of the profile within the basic lengths. The average roughness is the area between the roughness profile and the midline, or the integral of the height of the profile height over the length of the evaluation.
Average roughness is undoubtedly the most commonly used parameter for measuring the surface quality. The oldest analogue roughness measuring instruments only measured Ra by drawing a continuous peak back and forth on a surface and electronic integration (finding the mean). It is easy enough to take the absolute value of a signal and integrate a signal using only the analogous electronics. This is the main reason Ra has such a long history.
In terms of the graph, the average roughness is the area between the roughness profile and its center line divided by the length of the evaluation (normally five sample lengths, each length being equal to one sample cutting).

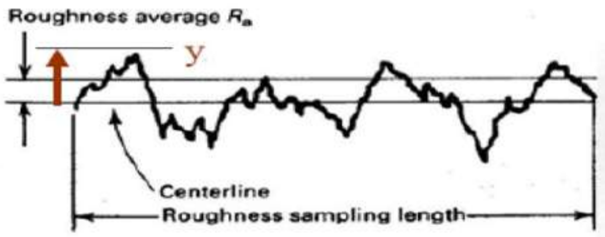

Fig. 1. The graphical representation of the arithmetic mean deviation Ra (Jigar.T [6])

The average roughness value Ra is the arithmetic mean value of the sums of all roughness profile values. According to Dragu D., et al. [9] the deviation of the arithmetic average of the roughness can be calculated with the relation:

$$Ra = \frac{1}{l}\int_{0}^{l} y_R dx_R \tag{1}$$

Where:
l- is the length of the reference line;
yR- the height of the roughness;
dxR- the distance along the „l” dimension.

2.2 Total profile height Rt

It represents the vertical distance between the highest and lowest points of the profile.

$$Rt = Z_{\max} + Y_{\max} \tag{2}$$

Where:
Zmax- maximum height;
Ymax- maximum depth.
This parameter is very sensitive to high peaks or deep scratches; Rt is defined as the vertical distance between the highest peak and the smallest scratch along the length of the profile rating.

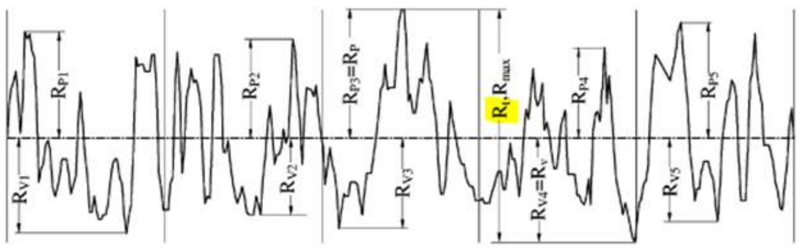

Fig. 2. Graphic representation of the total height Rt (Gadelmawa, E.S., et al., 2002 [3])

2.3 The influence of roughness

Roughness presents important influences on machine parts and not only be in operation contact surfaces, whether stationary or movable. The most important influences are:
The influence of roughness on fatigue resistance. The profile line consisting of peaks and recesses, the latter being stress concentrators. The influence of roughness on fatigue resistance is presented in the calculation for periodic stresses (especially the symmetrical alternating cycle), by the surface condition coefficient.
The influence of roughness on corrosion resistance. According to Gheorghe D. et al.[4], In the working environment of the machine organ, due to the differences in the electro-chemical potential due to the alloy's non-homogeneity, portions of the alloy surface are converted into anodic elements and others into cathode elements. In the presence of an environment that assumes the quality of an electrolyte an anodic dissociation is caused. This is all the more pronounced as the roughness is larger and sharp, due to the micro-currents in the electrolysis process which has a preferential attitude to flow through the peaks. In many situations, even if the surfaces are free but work in a corrosive environment, it is imperative that the surfaces have small roughness to obtain good corrosion resistance.
The influence of roughness on wear resistance. The surfaces of the contacting pieces have asperities, and when pressed by certain forces (F), the contact tips deform elastically, then plastic and when they have a relatively tangential displacement. They break out as wear. In the initial period, the wear period grows very quickly, after which its evolution is much slower. This wear has a much shorter run-out period if the surfaces in contact have a better smoothness.

3. Experimental setup

According to experiments carried out in a previous paper, A.R. Osan, et al.[10] the use of toroidal cutters in complex surface processing can be successfully applied and processing in the climb milling is more efficient than conventional milling.

3.1 Practical experimental part

For practical experiments it has been used numerical control centre of the 3-axis MCV 1016 of the firm S.C. Ramira S.A.

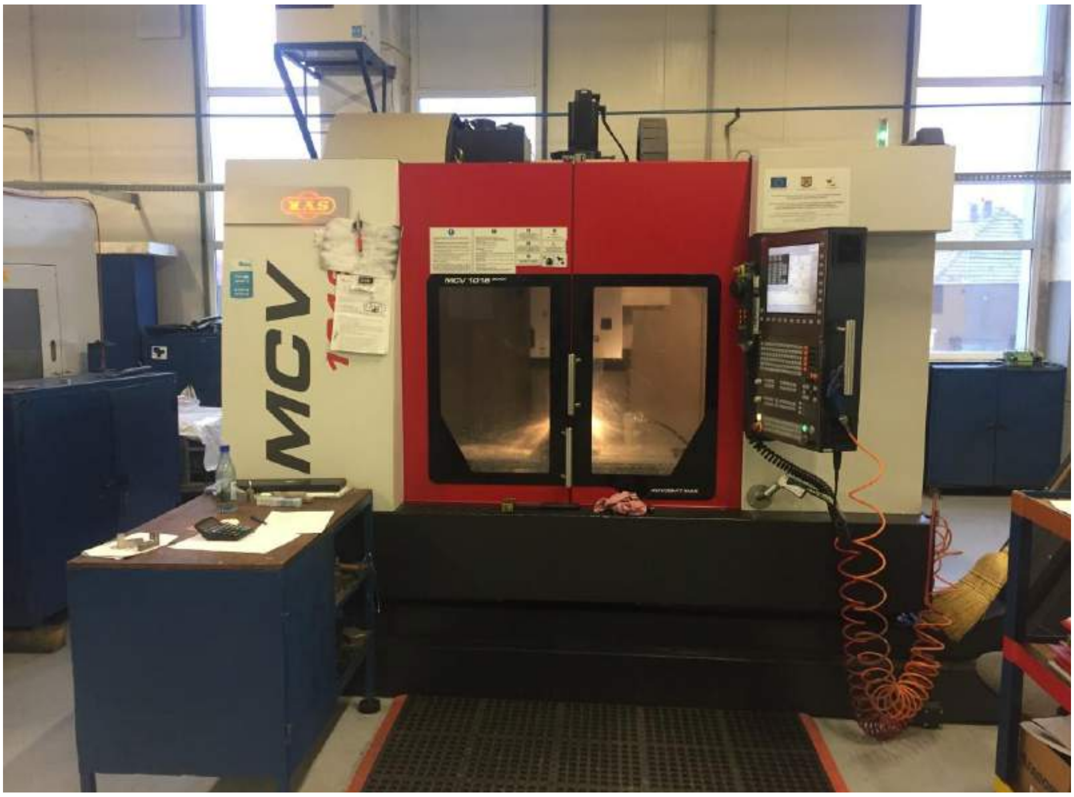

Fig. 3. Vertical machining center in 3 axis MCV 1016

The cutting tool used was a toroidal cutter JHP780160E2R400.0Z4-M64 with a carbide coating of Ø16 with a number of 4 teeth and a radius of R4.

Fig. 4. The toroidal milling cutter

3.2 The workpiece

The material used in the experiment is C45 (1.0503) with the following characteristics: 0.42 ... 0.50% C, 0.5 ... 0.80% Mn, 0.17 ... 0.37% Si, maximum 0.040% P etc. The piece has the shape of a square being machined only one of the ends representing the active part of the piece.

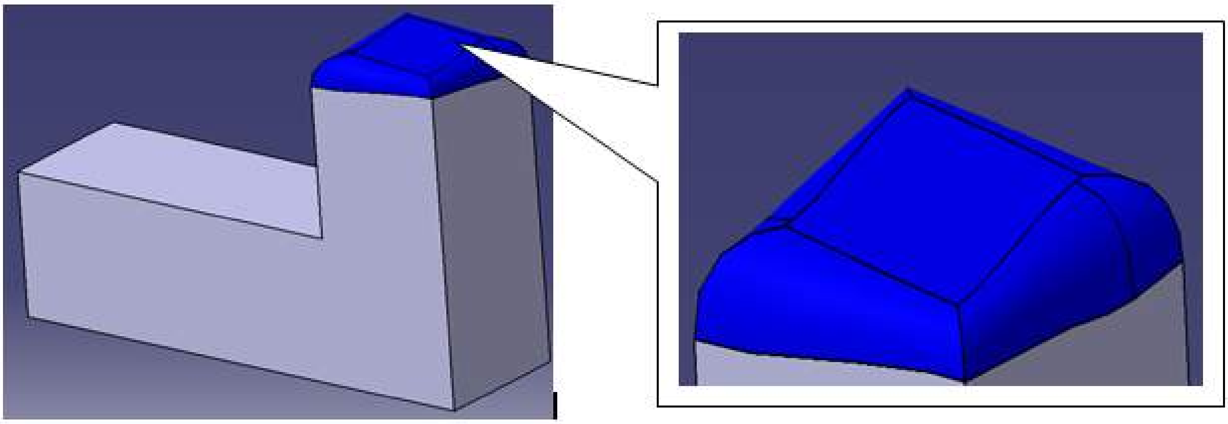

Fig. 5. Surface 3D model

The 11 experiments were performed on the machine MCV 1016 as shown in Figure 3, and a milling cutter used for cutting is one piece with the corner radius r4 and a diameter of ø16 and is provided in Figure 4. For reference number 1, the speed and propulsion proposed by the tool manufacturer were used, with the following increasing exponentially by 10% each, the reference 10 having double cutting parameters from the original ones and the benchmark 11 four times higher. The processing was carried out with a 1 mm machining feed having a 0.2 mm pitch using coolant.

Fig. 6. Workpieces processed

3.3 Machine and verification method

Direct palpation method

This method consists in measuring the surface roughness by palpating the profile with a touch probe (ac) along the measuring direction. The device used is the touch probe roughness with the possibility of amplified profile recording. The profile gauges generally operate on the basis of an electrical principle.

The electronic device is built from the transducer subassembly and the electronic unit. Alternative voltage produced by the oscillator is transmitted to the inductor probe transducer via the symmetrical transformer. When moving the touch probe, which is a diamond or sapphire, with a peak angle of 60 ° and a radius r of between 1 and 10 microns, the surface of the piece due to irregularities will oscillate vertically and with it and the bobbin core thus modifying the relative impedance of it. The impedance variation changes the circuit voltage, amplified, rectified, and indicated by the device.

The method offers a number of advantages such as: universality, rapid profile recording, magnification, and long scanning lengths, and all the information on surface micro-geometry can be reproduced in the modern ones provided with the computer.

The device used to check the roughness is the TIME TR 200, this portable absolute measuring device has the sensitivity required to measure the very fine roughness of the tens and microns.

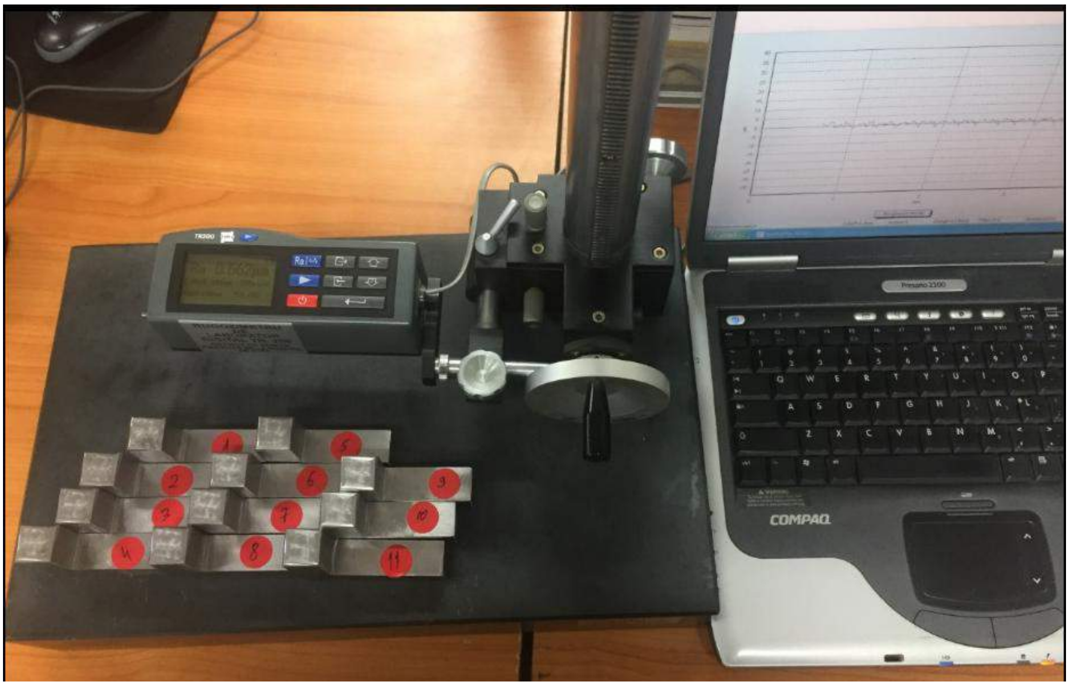

Fig. 7. Roughness measurement with TIM 200 TR

Table 1.1 contains the results of surface roughness measurements, both parallel and perpendicular to the feed direction. It is also noted that the roughness of the surface is analysed both in terms of roughness Ra and Rt, for a complete analysis of the surface processed. All of this was done in order to obtain an overview of the profile of the surface obtained from toroidal milling under different conditions created by the change of the main shaft speed and the cutting advance.

Table 1: Data centralization

Nr. Ctr	Speed (rpm)	Cutting speed (mm/min)	Ra [μm]		Rt [μm]	
			Direction of measurement relative to the feed direction			
			Parallel	Perpendicular	Parallel	Perpendicular
1.	1204	361	0.795	0.986	9.279	10.530
2.	1324	397	0.847	0.962	6.840	8.140
3.	1444	433	0.813	0.955	6.940	8.100
4.	1565	439	0.893	0.937	6.559	8.850
5.	1685	505	0.818	0.850	7.059	8.800
6.	1806	541	0.727	0.838	7.159	8.020
7.	1926	577	0.881	0.965	7.480	8.199
8.	2046	613	0.825	0.897	6.019	9.520
9.	2167	650	0.798	0.942	7.860	8.100
10.	2408	722	0.711	0.798	7.320	7.400
11.	4814	1444	0.450	0.476	3.680	3.900

4. Experimental results

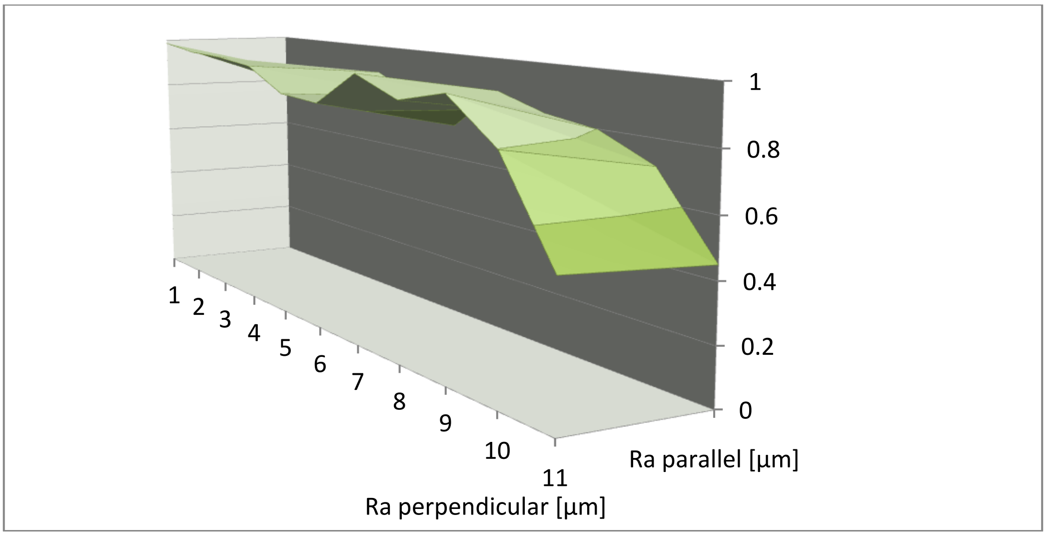

Fig. 8. Graphic representation of the roughness of the 11 landmarks

Based on the analysis of the centralized experimental results in Table 1.1, we noticed that the lowest values for Ra, 0.450 µm in the case of parallel roughness measurement in the direction of the feed and 0.476 µm for the measurements made perpendicular to the feed direction are due to the large processing regimes of 4814 rpm the main shaft speed and the 1444 mm / min feed rate. The maximum values for Ra reached 0.893 µm for the measurements made in the direction of the advance and 0.986 µm for the measurements made perpendicular to the direction of the advance, all of which are caused by the small working regimes.
Analysing the measurements for the vertical distance between the highest and lowest values of the profile (Rt), it can be seen that the minimum value of 3.680 µm is recorded in the case of the roughness measurement in the direction of the advance following the processing of the reference 11 and the maximum value Rt being 10.530 µm after processing with small regimes and measuring in the direction perpendicular to the feed.

5. Conclusions

The reference 11 made at 4814 rpm and the 1444 mm / min feed having the 0.2 step and a 1 mm processing addition is considered to have the best surface quality, the minimum average roughness value (Ra) measured in the direction of the feed is 0,450 µm and the vertical distance between the highest and lowest points of the profile (Rt) has the value of the minimum value of 3,680 µm.
The use of round corner cutters for complex surface processing can result in superior surface quality due to the use of larger machining regimes, increasing productivity at the same time and this can considerably influence the surface tribology that can reduce wear, corrosion or fatigue.

Acknowledgments

The experimental research carried out with the support of the processing department of S.C. Ramira S.A., Baia Mare.

References

[1] Alauddin, M., M.A. El Baradie, and M.S.J. Hashmi. "Prediction of tool life in end milling by response surface methodology." *Journal of Materials Processing Technology* 71, no. 3 (November 1997): 456-465.
[2] Dragu, D., Gh. Bădescu, A. Sturzu, C. Militaru, and I. Popescu. *Toleranţe şi măsurători tehnice*. E.D.P. Bucureşti, 1980.
[3] Gadelmawla, E.S., M.M. Koura, T.M.A. Maksoud, I.M, Elewa, and H.H. Soliman. "Roughness parameters." *Journal of Materials Processing Tehnology* 123, no. 1 (April 2002):133-145.

[4] Gheorghe, D., C. Georgescu, and N. Baroiu. *Toleranțe și control dimensional*. Editura Scorpion, Galați, 2002.
[5] Hasegawa, M., A. Seireg, and R.A. Lindberg. "Surface roughness model for turning." *Tribology International* 9, no. 6 (December 1976): 285–289.
[6] Talati, Jigar. *Surface roughness-Significance and symbol interpretation in drawing*. Hexagon Design Centre, Vadodara.
[7] Kalpakjian, Serope and Steven Schmid. *Manufacturing Process for Engineering Materials*. 3rdEd. Addison Wesley, MenloPark, CA.
[8] Lamikiz, A., L.N. López de Lacalle, J.A. Sánchez, and M.A. Salgado. „Cutting force estimation in sculptured surface milling.” *Int J Mach Tool Manuf* 44(2004):1511–1526.
[9] Lou, Mike, Joseph Chen, and Caleb Li. „Surface Roughness Prediction Technique For CNC End-Milling.” *Journal of Industrial Tehnology* 15, no.1 (January 1999).
[10] Oșan, Andrei, Marius Cosma and Vasile Năsui. “Milling convex surfaces with toroidal cutting edge”. Paper presented at Innovative Ideas in Science, Banja Luka, Bosnia and Herzegovina, 2017.
[11] Vișan, Aurelian and Nicolae Ionescu. *Toleranțe, Precizia formei micorgeometrice a suprafețelor*. Bucharest.
[12] *** SR EN ISO 4287:1993.

Design and Optimization of Pressurized Toroidal LPG Fuel Tanks with Variable Section

Assoc. Prof. PhD. Eng. **Mihai ŢĂLU**[1], Assoc. Prof. PhD. Eng. **Ștefan ŢĂLU**[2,*]

[1] University of Craiova, Faculty of Mechanics, Department of Applied Mechanics and Civil Engineering, Calea București Street, no. 107, 200512 Craiova, Dolj county, Romania. E-mail: mihai_talu@yahoo.com

[2] Technical University of Cluj-Napoca, The Directorate of Research, Development and Innovation Management (DMCDI), Constantin Daicoviciu Street, no. 15, Cluj-Napoca, 400020, Cluj county, Romania. Corresponding author* e-mail: stefan_ta@yahoo.com

Abstract: *This study addresses the design and optimization of the pressurized toroidal LPG fuel tanks with variable section used in automotive industry based on the finite element analysis (FEA) approaches, to model both thermal and mechanical processing conditions. To define specific key performance indicators and to determine the optimal form of toroidal LPG fuel tank with the minimum stress state and linear deformation was applied a mathematical and mechanical foundation for the design and optimization. Computer aided investigations are carried out using 3D models done in the AutoCAD Autodesk 2017 software, which were imported to SolidWorks 2017 software for analysis and can offer an important reference for the design of toroidal LPG fuel tanks.*

Keywords: *Automotive industry, industrial engineering design, optimization methods, pressurized toroidal LPG fuel tank*

1. Introduction

During the past decades, the computer aided engineering design methods to produce pressurized fuel tanks in the automotive industry [1-3] have been developed in a variety of directions to improve vehicle's performance [4-6]. The storage fuel tanks, made from aluminum alloys or various types of steel, are used in the automotive industry for safely storing fuel: compressed natural gas (CNG) or liquefied petroleum gas (LPG) [7-12]. The design, construction, installation, testing and monitoring requirements of the storage fuel tanks (to maintain structural integrity at high pressures) are bounded and regulated by various codes and standards [13-15].

The design procedure of the fuel tanks involves various assumptions, supershapes design variables [16, 17], specific structure parameters [14], design constraints [15], computer tools [18-23], numerical computational methods [24-26], CAD visualization techniques [27-34], test data and experimental data, that permit to obtain an optimal product with a low structural weight and a high structural performance.

The pressurized toroidal LPG fuel tanks have been recognized as a volumetrically efficient storage solution that can reduce final product mass, while improving storage efficiencies [14, 15].

In our study, a finite element analysis of pressurized toroidal LPG fuel tank to meet safety standards and optimization was conducted considering specific geometry and structure parameters.

2. Design methodology

In our study, optimal design of toroidal cross-sectional profiles (considering shape and thickness variation) in order to reduce stress non-uniformity is performed.

2.1 Basic geometry of toroidal surfaces

Let's consider the surface generated by revolving of a closed generating curve C_G along a guiding curve C_{D1}, being tangent in the movement on a second internal curve C_{D2}, as shown in fig. 1a.

The curve C_G (that generates the cross-section) is located in a vertical plane, whereas the reference curves C_{D1} and C_{D2} (that determine the variation in the cross-sectional dimensions) are coplanar and situated in the horizontal plane.

An example of the manufactured product with the apparature monted on the tank that permit an easy access to the filling or drainage connections of fuel tank is shown in fig. 1c.

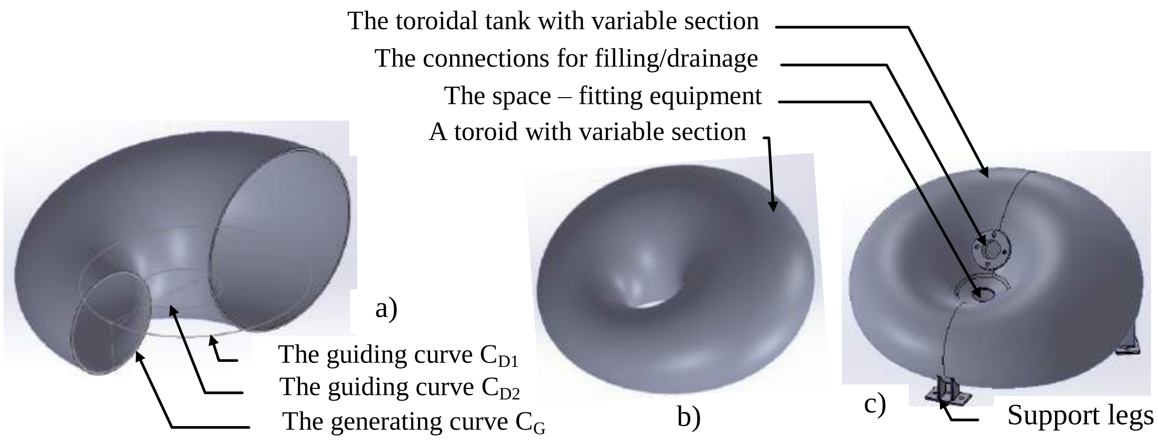

Fig. 1. a) The ½ section of a toroidal tank; b) The model of a toroidal tank; c) The tank constructive solution

The graphical representations of toroidal symmetrical parts in respect with the symmetrical planes is shown in orthogonal views in fig. 2a and 2b, while the axonometric representation is shown in fig. 2c.

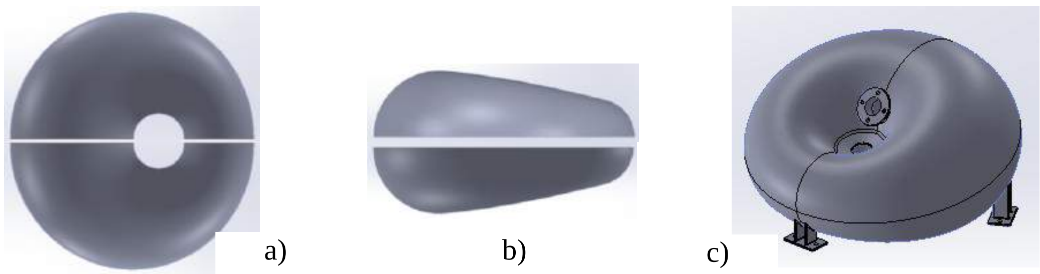

Fig. 2. a) and b) The orthogonal views with the symmetry horizontal plane; c) The axonometric representation of the tank constructive solution

The generating curves and the directories curves are closed curves that do not intersect on themselves, such as: ellipses, circles, triangles, rectangles, etc. Some graphical examples of toroids with variable section are shown in figs. 3 and 4.

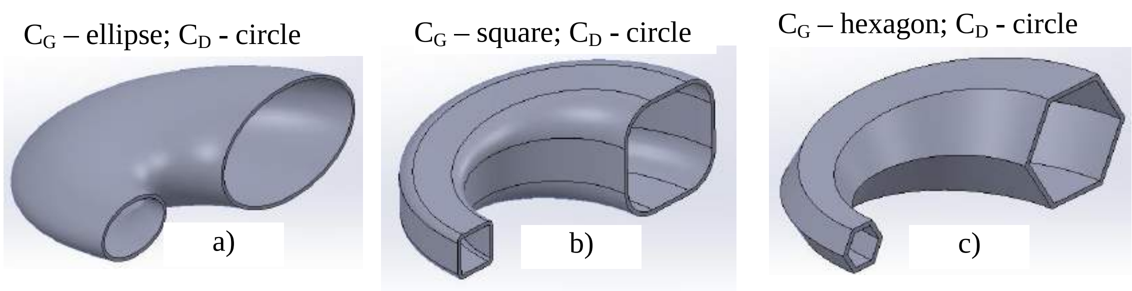

Fig. 3. The axonometric representation of a ½ toroid sectioned generated by: a) C_G – ellipse and C_D – circle; b) C_G – square and C_D – circle; c) C_G – hexagon and C_D – circle

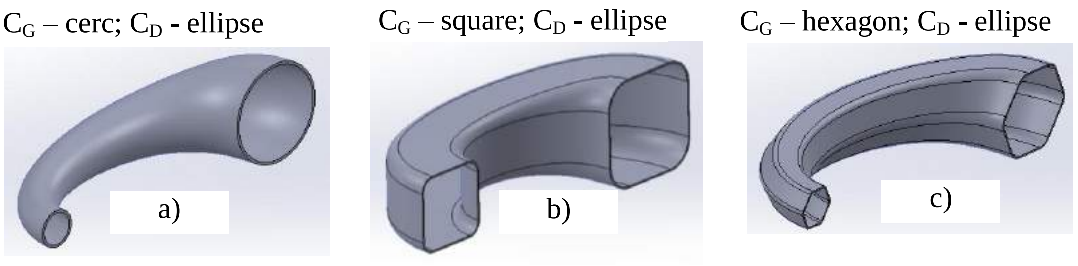

Fig. 4. The axonometric representation of a ½ toroid sectioned generated by: a) C_G – circle and C_D – ellipse; b) C_G – square and C_D – ellipse; c) C_G – hexagon and C_D - ellipse

2.2 The geometrical model selected for numerical analysis

The geometrical model selected for numerical analysis is shown in fig. 5a (C_G – ellipse and C_D – circle), with next numerical values for the diameters of circles: C_{D1} and C_{D2} (C_{D1} = 300 mm and C_{D1} = 130 mm). The eccentricity of the curves: C_{D1} and C_{D2} has the value of e = 25 mm.
The axonometric isometric view of the parameterized geometrical model (non-sectioned and sectioned to ¾ and ½ of the initial model, as a consequence of the tank constructive symmetry) is shown in fig. 5.

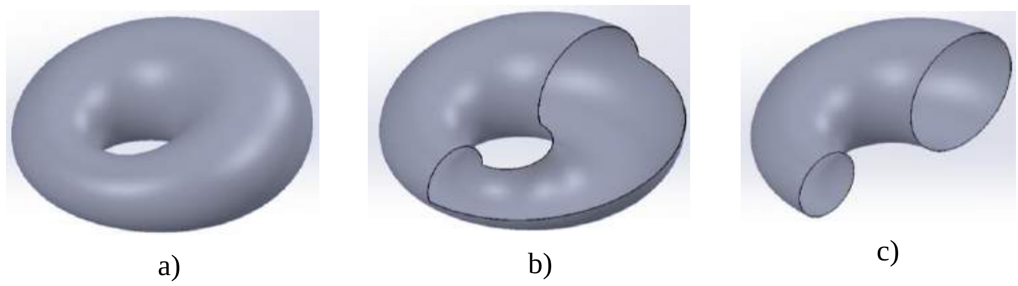

Fig. 5. The geometrical model: a) non-sectioned; b) sectioned at ¾; c) sectioned at ½

The modeling was done in the AutoCAD Autodesk 2017 software [35] and the optimization analysis to ensure quality, performance, and safety was performed with SolidWorks 2017 software [36] with the: Static, Thermal and Design Study modules.
The specified surfaces to which the constraints and restrictions are applied are shown in fig. 6.

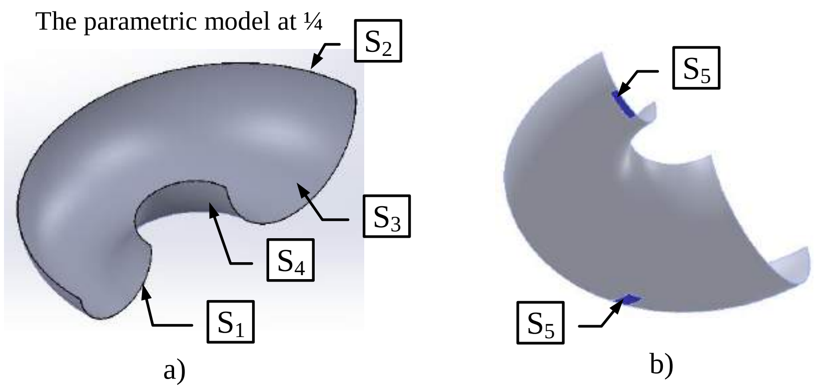

Fig. 6. The geometrical model at ¼ with the specified surfaces

The design data used in this analysis are:
- the maximum static hydraulic pressure: p_{max} = 3 N/mm^2 applied to the surface S_3;
- the working temperature between the limits: T = -30 ^{0}C to T = 60 ^{0}C applied to the surface S_4;
- the symmetry on surfaces: S_1 and S_2;
- the fixed surfaces located on the legs support on S_5 (shown in Fig. 5b);
- the execution material for tank is AISI 4340 laminated steel;
- the exploitation time of tank is: n_a = 20 years;
- the corrosion velocity of material: v_c = 0.09 mm/year.

The optimal design issue here refers to the non-linear constrained optimization and involves minimizing the structural weight W (associated with the cover thickness s = 0.5...3 mm), subjected to the non-linear design constraints (the maximum Von Mises stress must by less than or equal to the admissible traction value of the material, $\sigma_{rez} \leq \sigma_a = 710$ N/mm^2).
Applying the numerical optimization procedure for T = -30 ^{0}C, the following values were obtained: thickness s = 0.9 mm; the maximum Von Mises stress $\sigma_{rez.\ max}$= 703.073 N/mm^2 and the linear deformation u_{max} = 0.533 mm.
The graphs of Von Mises stress and linear deformation distribution computed for T = -30 ^{0}C are shown in fig. 7.

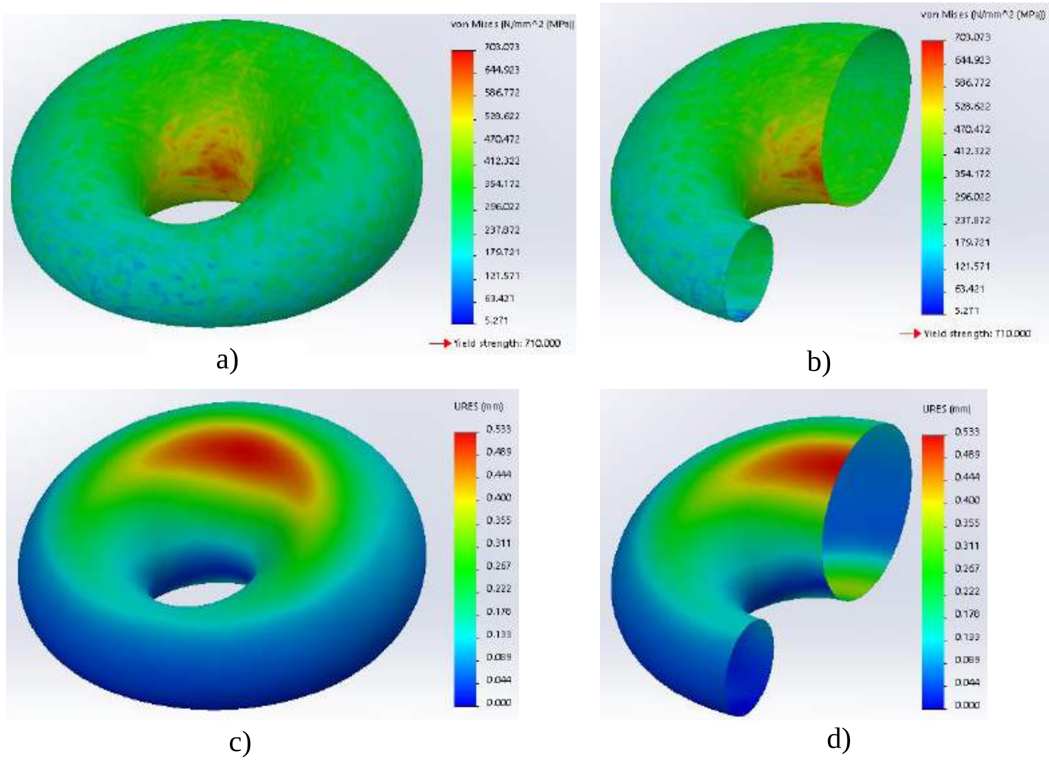

Fig. 7. The graphs of: I) Von Mises stress distribution: a) non-sectioned model and b) sectioned model; II) linear deformation distribution: c) non-sectioned model and d) sectioned model

The optimal thickness is corrected considering the influence of the corrosion phenomenon and the negative tolerance of the metal sheet, using the following formula [10]:

$$s_{real} = s_{opt} + \Delta s_c + \Delta s_T + \Delta s_{am} = s_{opt} + v_c \cdot n_a + abs(A_i) + 0.1 \cdot s \quad (1)$$

where:
- Δs_c, the additional thickness used to compensate the loss of thickness due to the corrosion process;
- Δs_T, the additional thickness used to compensate the loss due to the negative tolerance of the execution of laminate metal sheet;
- v_c, the corrosion velocity of the metal sheet, v_c = 0.08 mm/year;
- n_a, the number of years of exploitation, n_a = 20 years;
- A_i, the negative tolerance of the laminate sheet, A_i = - 0.6 mm;
- $\Delta s_{am} = 0.1 \cdot s$, the additional thickness used to compensate the thinning of wall into the embossing process, Δs_{am} = 0.4 mm.

By substituting the numerical values, the minimum thickness of the laminate sheet has the following value:

$$s_{real\ min} = 0.9 + 0.09 \cdot 20 + abs(-0.6) + 0.1 \cdot 4 = 3.7 \text{ mm} \quad (2)$$

For the execution, we choose a laminate sheet of AISI 4340 steel that has a thickness of $s = 4^{+0.25}_{-0.6}$ mm.

2.3 Three-dimensional stress and strain analysis

In these analyses, the following hypothesis has been applied for the formulation of stresses and strains: a) the 3-D model is subjected to axisymmetric loading and keeps symmetry before and after deformation.
For n_a = 0 years and temperature T = -30 ^{0}C, the numerical value of pressure p = 13.68 N/mm^2 and the corresponding graphs of Von Mises stress distribution and linear deformation distribution are shown in fig. 8.

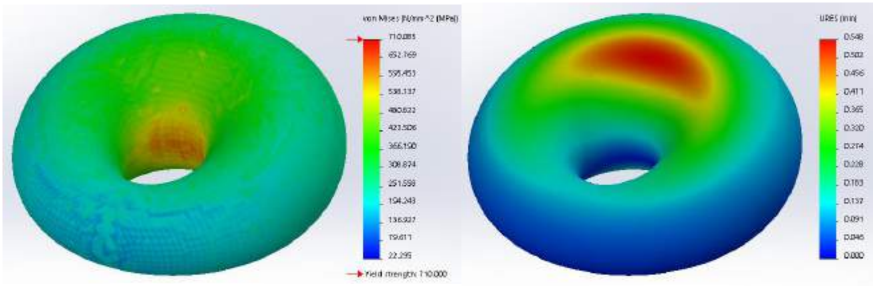

a) b)

Fig. 8. The graphs of: a) Von Mises stress distribution; b) linear deformation distribution; both computed for p_{max}, T = -30 ^{0}C and n_a = 0 years.

The graphs of Von Mises stress distribution and linear deformation distribution (computed for explosion pressure, T = -30 ^{0}C) were shown on the sectioned model at ½ in figures 9b and 9d and in figures 9a and 9c for the entire model. For n_a = 0 years and T = -30 ^{0}C, the computed tank explosion pressure is p = 21.65 N/mm^2 and the maximum linear deformation is u_{max} = 0.855 mm.

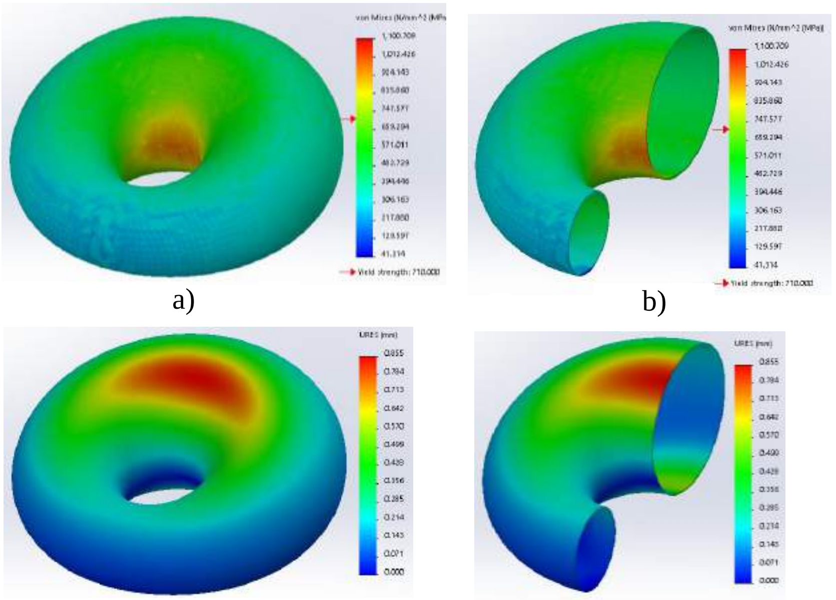

a) b)

c) d)

Fig. 9. The graphs of: I) Von Mises stress distribution: a) non-sectioned model and b) sectioned model; II) linear deformation distribution: c) non-sectioned model and d) sectioned model; both computed for the explosion pressure and T = -30 ^{0}C.

It can be revealed that the explosion pressure is greater by 7.21 times than the maximum test pressure of the fuel tank.
The numerical values of state of stress and linear deformation distribution are given in Table 1.

Table 1: The Von Mises stress and linear deformation of geometrical model

			T [^{0}C]									
No. of years		**s[mm]**	-30 ^{0}C	-20 ^{0}C	-10 ^{0}C	0 ^{0}C	10 ^{0}C	20 ^{0}C	30 ^{0}C	40 ^{0}C	50 ^{0}C	60 ^{0}C
0	σ[MPa]	4	212.57	191.01	174.58	163.27	159.04	156.03	160.08	169.27	183.57	202.99
	u[mm]		0.1073	0.1112	0.1156	0.1204	0.1255	0.1314	0.1376	0.1442	0.1512	0.1587
5	σ[MPa]	3.55	231.19	211.49	194.74	183.86	174.43	168.09	169.58	174.13	193.49	213.83
	u[mm]		0.123	0.127	0.132	0.137	0.143	0.150	0.156	0.163	0.170	0.178
10	σ[MPa]	3.1	235.66	226.12	216.87	207.92	199.31	191.09	192.23	195.78	212.18	233.91
	u[mm]		0.145	0.149	0.154	0.160	0.166	0.172	0.179	0.186	0.193	0.200
15	σ[MPa]	2.65	282.65	264.64	252.84	241.91	231.33	221.67	221.92	234.47	256.54	279.47
	u[mm]		0.177	0.182	0.187	0.192	0.199	0.205	0.211	0.218	0.225	0.232
20	σ[MPa]	1.2	550.48	532.83	515.58	498.78	483.92	478.44	494.58	511.66	529.59	548.27
	u[mm]		0.406	0.412	0.417	0.423	0.429	0.435	0.441	0.447	0.454	0.46
Opti-mal	σ[MPa]	0.9	703.07	685.97	669.18	652.70	636.57	620.82	616.51	636.32	656.87	677.48
	u[mm]		0.533	0.538	0.544	0.549	0.555	0.560	0.566	0.571	0.577	0.583

The graphical representations of Von Mises stress σ(s, T) and the linear deformation, u(s, T) as specified in Table 1, are shown in figures 10 and 11.

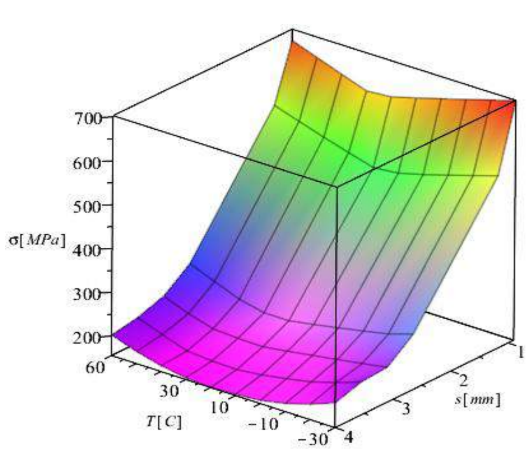

Fig. 10. The graph of Von Mises stress σ(s, T)

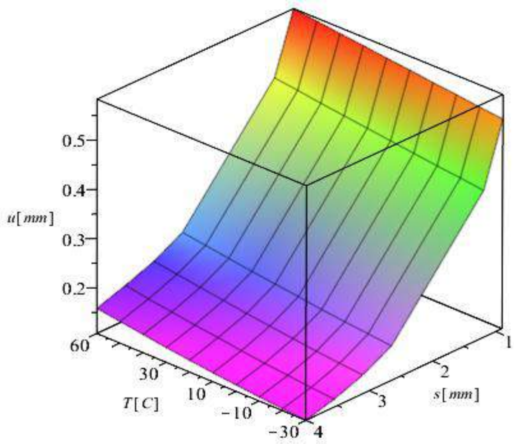

Fig. 11. The graph of linear deformation u(s, T)

The graphs of Von Mises stress (for n_a = 0 years and n_a = 20 years) is shown in fig. 12 and 13 with the corresponding the laws of stress variation computed by polynomial interpolation.

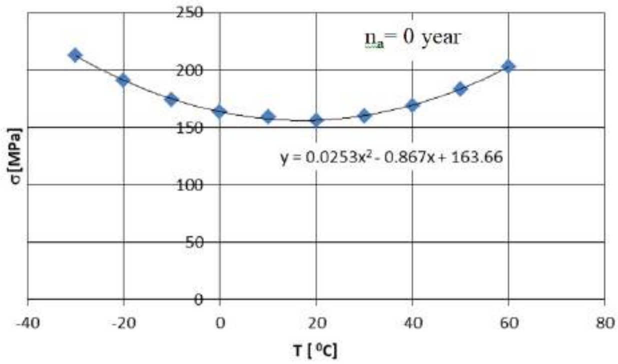

Fig. 12. The graph of Von Mises stress at n_a = 0 years

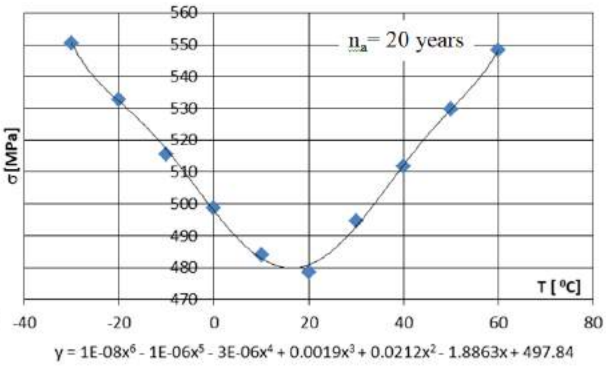

Fig. 13. The graph of Von Mises stress at n_a = 20 years

The laws of stress variation computed by polynomial interpolation are given in Table 2.

Table 2: The laws of stress variation computed by polynomial interpolation

n_a [years]	s[mm]	$\sigma(t)$ [MPa]
0	4	$\sigma(t) = 0.0253 \cdot T^2 - 0.867 \cdot T + 163.88$
5	3.55	$\sigma(t) = 2 \cdot 10^{-7} \cdot T^5 + 6 \cdot 10^{-6} \cdot T^4 - 0.0003 \cdot T^3 + 0.0153 \cdot T^2 - 0.9889 \cdot T + 183.27$
10	3.1	$\sigma(t) = -2 \cdot 10^{-8} \cdot T^5 + 6 \cdot 10^{-6} \cdot T^4 + 0.0002 \cdot T^3 + 0.0013 \cdot T^2 - 0.9278 \cdot T + 207.79$
15	2.65	$\sigma(t) = -2 \cdot 10^{-7} \cdot T^5 + 2 \cdot 10^{-5} \cdot T^4 + 0.0003 \cdot T^3 - 0.0038 \cdot T^2 - 1.1523 \cdot T + 242.06$
20	1.2	$\sigma(t) = -1 \cdot 10^{-6} \cdot T^5 - 3 \cdot 10^{-6} \cdot T^4 + 0.0019 \cdot T^3 + 0.0212 \cdot T^2 - 1.8863 \cdot T + 497.84$

The graphs of linear deformations (for n_a = 0 years and n_a = 20 years) is shown in fig. 14 and 15 with the corresponding the laws of linear deformations variation computed by polynomial interpolation.

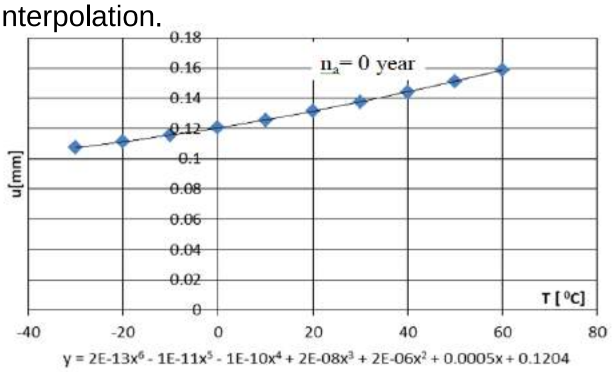

Fig. 14. The graph of linear deformations at n_a = 0 years

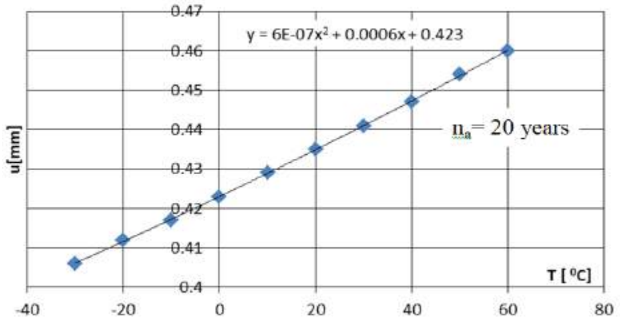

Fig. 15. The graph of linear deformations at n_a = 20 years

The laws of linear deformations variation computed by polynomial interpolation are given in Table 3.

Table 3: The laws of linear deformations variation computed by polynomial interpolation

n_a [years]	s [mm]	$\sigma(t)$ [MPa]
0	4	$\sigma(t) = -1 \cdot 10^{-11} \cdot T^5 - 1 \cdot 10^{-10} \cdot T^4 + 2 \cdot 10^{-8} \cdot T^3 + 2 \cdot 10^{-6} \cdot T^2 + 0.0005 \cdot T + 0.1204$
5	3.55	$\sigma(t) = 1 \cdot 10^{-11} \cdot T^5 + 6 \cdot 10^{-4} \cdot T^4 - 3 \cdot 10^{-8} \cdot T^3 + 3 \cdot 10^{-6} \cdot T^2 - 0.0006 \cdot T + 0.1371$
10	3.1	$\sigma(t) = -3 \cdot 10^{-11} \cdot T^5 + 1 \cdot 10^{-9} \cdot T^4 + 5 \cdot 10^{-9} \cdot T^3 + 1 \cdot 10^{-6} \cdot T^2 + 0.0006 \cdot T + 0.1599$
15	2.65	$\sigma(t) = 9 \cdot 10^{-11} \cdot T^5 - 6 \cdot 10^{-10} \cdot T^4 - 1 \cdot 10^{-7} \cdot T^3 + 3 \cdot 10^{-6} \cdot T^2 + 0.0006 \cdot T + 0.1924$
20	1.2	$\sigma(t) = 6 \cdot 10^{-7} \cdot T^2 + 0.0006 \cdot T + 0.423$

The graphs of Von Mises stress computed for T = -30 ^{0}C for: a) the geometrical model (Fig. 16a); b) and c) on the outer and the inner circumference of geometrical model (fig. 16b and 16c).

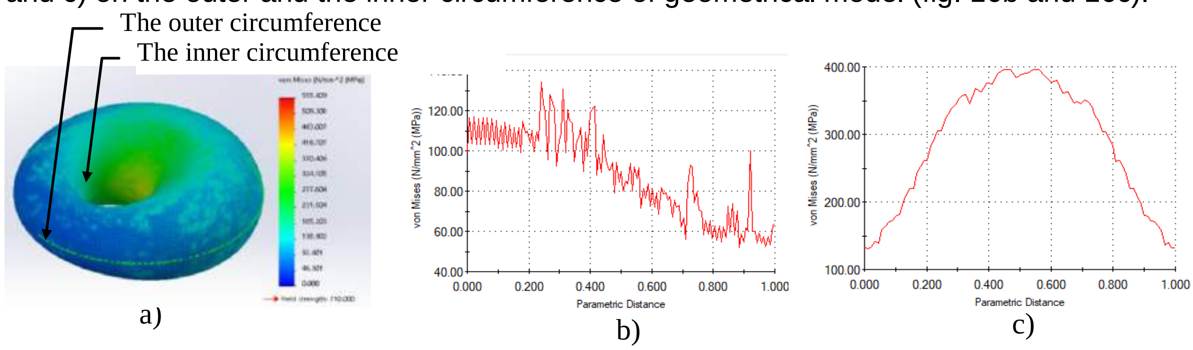

Fig. 16. The graphs of Von Mises stress computed for T = -30 ^{0}C for: a) the geometrical model; b) and c) on the outer and on the inner circumference of geometrical model

The graphs of linear deformations computed for T = 60 ^{0}C for: a) the geometrical model (fig. 17a); b) and c) on the outer and the inner circumference of geometrical model (fig. 17b and 17c).

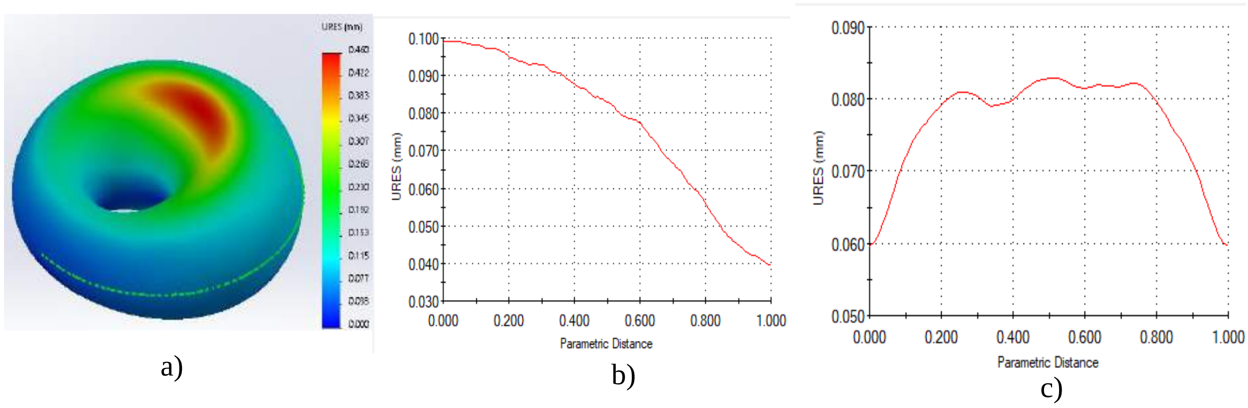

Fig. 17. The graphs of linear deformations computed for T = 60 ^{0}C for: a) the geometrical model; b) and c) on the outer and the inner circumference of geometrical model

The graphs of Von Mises stress computed for T = -30 ^{0}C for: a) the geometrical model (fig. 18a); b) and c) on the minimum circumference of circle and on the maximum circumference of circle (fig. 18b and 18c).

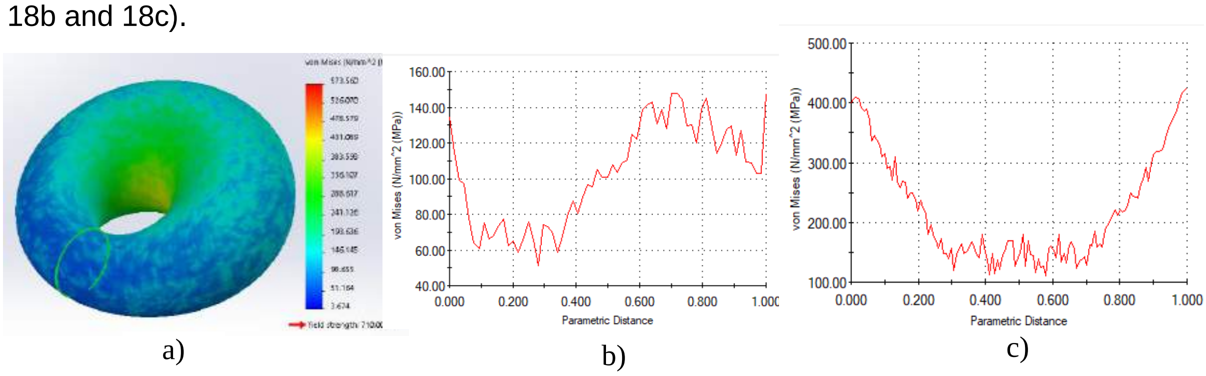

Fig. 18. The graphs of Von Mises stress computed for T = -30 ^{0}C for: a) the geometrical model; b) and c) on the minimum circumference of circle and on the maximum circumference of circle

The graphs of linear deformations computed for T = 60 ^{0}C for: a) the geometrical model (fig. 19a); b) and c) on the minimum circumference of circle and on the maximum circumference of circle (fig. 19b and 19c).

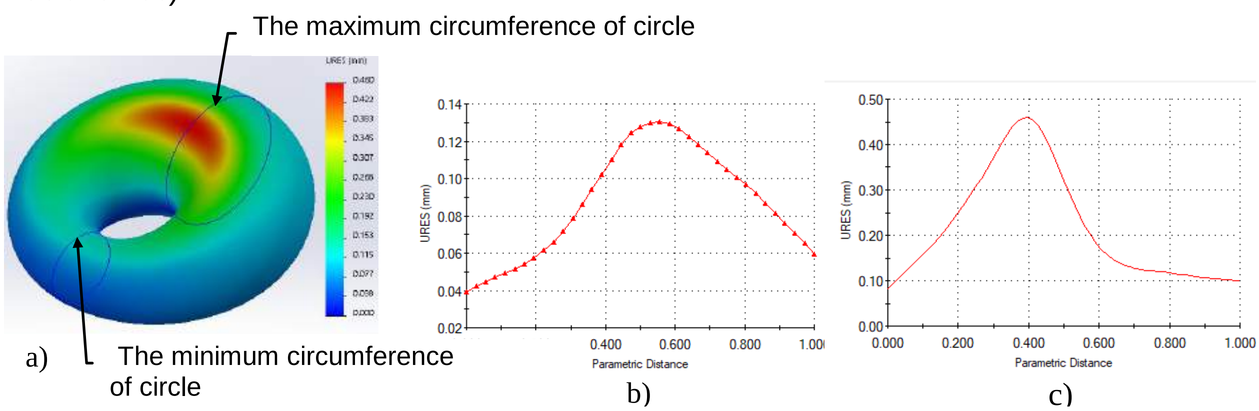

Fig. 19. The graphs of linear deformations computed for T = 60 ^{0}C for: a) the geometrical model; b) and c) on the minimum circumference of circle and on the maximum circumference of circle

3. Discussion

The maximum value of the Von Mises stress (σ = 703.07 MPa) occurs at T = - 30 ^{0}C, while the maximum linear deformation (u_{max} = 0.583 mm) occurs at T = 60 ^{0}C, (as shown in Table 1).

The maximum working pressure at T = -30 ^{0}C is 4.56 times higher than the hydraulic test pressure and the explosion pressure is 1.583 times higher than the maximum working pressure. In the case of linear deformations associated with these two pressures their ratio is u_r / u_{max} = 1.604.
It was revealed that the Von Mises stress and the linear deformations increase simultaneously with the increase of the temperature and the exploitation period, (as shown in fig. 9 and 10).
For n_a = 0 years, the Von Mises stress shows a minimum of σ = 156.03 MPa (at temperature T = 20 ^{0}C), and for n_a = 20 years a minimum of σ = 483.92 MPa (at temperature T = 10 ^{0}C), (as shown in Table 1).

4. Conclusions

In this study, an elaboration of the design and optimization procedure associated with the pressurized toroidal LPG fuel tanks with variable section used in automotive industry based on the FEA approaches were performed. Computer aided investigations were employed to predict the mechanical behavior of toroidal LPG fuel tanks, corresponding to various design scenarios, in order to improve the structural performance for a feasible solution within a prescribed tolerance.
A new possibility to improve the pressurized toroidal LPG fuel tanks performance can be offered by the application of adapted cross-sectional shapes instead of the conventional shapes.
The results revealed that the optimal toroidal geometry provides a lower weight and lower aspect ratio than the circular one, and thus leads to better structural performance and an alternative to spaces having limited height and volume. Determination of the optimal geometric toroidal model with the minimum number of appropriate design variables through the combination of equations and the optimality conditions would also be considered as design objectives in the future study.

Financial disclosure: Neither author has a financial or proprietary interest in any material or method mentioned.
Competing interests: The authors declare that they have no significant competing financial, professional or personal interests that might have influenced the performance or presentation of the work described in this manuscript.

References

[1] Ghiţă, C. Mirela, Anton C. Micu, Mihai Ţălu, Ştefan Ţălu and Ema I. Adam. "Computer-Aided Design of a classical cylinder gas tank for the automotive industry." *Annals of Faculty of Engineering Hunedoara - International Journal of Engineering, Hunedoara*, *Romania*, Tome XI, Fascicule 4 (2013): 59-64.
[2] Ghiţă, C. Mirela, Anton C. Micu, Mihai Ţălu and Ştefan Ţălu. "Shape optimization of vehicle's methane gas tank." *Annals of Faculty of Engineering Hunedoara - International Journal of Engineering, Hunedoara, Romania*, Tome X, Fascicule 3 (2012): 259-266.
[3] Ghiţă, C. Mirela, Ştefan C. Ghiță, Ştefan Ţălu and Simona Rotaru, "Optimal design of cylindrical rings used for the shrinkage of vehicle tanks for compressed natural gas." *Annals of Faculty of Engineering Hunedoara - International Journal of Engineering, Hunedoara*, Tome XII, Fascicule 3 (2014): 243-250.
[4] Ghiţă, C. Mirela, Anton C. Micu, Mihai Ţălu and Ştefan Ţălu. "3D modelling of a shrink fitted concave ended cylindrical tank for automotive industry." *Acta Technica Corviniensis – Bulletin of Engineering, Hunedoara, Romania*, Tome VI, Fascicule 4 (2013): 87-92.
[5] Ghiţă, C. Mirela, Anton C. Micu, Mihai Ţălu and Ştefan Ţălu. "3D modelling of a gas tank with reversed end up covers for automotive industry.", *Annals of Faculty of Engineering Hunedoara - International Journal of Engineering, Hunedoara*, *Romania*, Tome XI, Fascicule 3 (2013): 195-200.
[6] Ghiţă, C. Mirela, Anton C. Micu, Mihai Ţălu and Ştefan Ţălu. "Shape optimization of a thoroidal methane gas tank for automotive industry." *Annals of Faculty of Engineering Hunedoara - International Journal of Engineering, Hunedoara, Romania*, Tome X, Fascicule 3 (2012): 295-297.
[7] Bică, Marin, Mihai Ţălu and Ştefan Ţălu. "Optimal shapes of the cylindrical pressurized fuel tanks." *Magazine of Hydraulics, Pneumatics, Tribology, Ecology, Sensorics, Mechatronics (HIDRAULICA)*, no. 4 (December 2017): 6-17.
[8] Ţălu, Ştefan and Mihai Ţălu. "The influence of deviation from circularity on the stress of a pressurized fuel cylindrical tank." *Magazine of Hydraulics, Pneumatics, Tribology, Ecology, Sensorics, Mechatronics (HIDRAULICA)*, no. 4 (December 2017): 34-45.
[9] Vintilă, Daniela, Mihai Ţălu and Ştefan Ţălu. "The CAD analyses of a torospheric head cover of a pressurized cylindrical fuel tank after the crash test." *Magazine of Hydraulics, Pneumatics, Tribology, Ecology, Sensorics, Mechatronics (HIDRAULICA)*, no. 4 (December 2017): 57-66.

[10] Ţălu, Mihai. "The influence of the corrosion and temperature on the Von Mises stress in the lateral cover of a pressurized fuel tank." *Magazine of Hydraulics, Pneumatics, Tribology, Ecology, Sensorics, Mechatronics (HIDRAULICA)*, no. 4 (December 2017): 89-97.
[11] Ţălu, Mihai and Ştefan Ţălu. "Analysis of temperature resistance of pressurized cylindrical fuel tanks." *Magazine of Hydraulics, Pneumatics, Tribology, Ecology, Sensorics, Mechatronics (HIDRAULICA)*, no. 1 (March 2018): 6-15.
[12] Patel, M. Pankit and Jaypalsinh Rana. “Design & optimization of LNG-CNG cylinder for optimum weight.” *IJSRD - International Journal for Scientific Research & Development*, vol. 1, issue 2 (2013): 282-286.
[13] *** Certification tests of LPG and CNG. Accessed December 10, 2017. http://vzlutest.cz/en/certification-tests-of-lpg-and-cng-c3.html.
[14] Kișioglu, Yasin. “Burst tests and volume expansions of vehicle toroidal LPG fuel tanks.” *Turkish J. Eng. Env.*, vol. 33 (2009): 117-125. DOI: 10.3906/muh-0905-2.
[15] Kartal, Fuat and Yasin Kișioglu. “Fatigue performance evaluations of vehicle toroidal liquefied petroleum gas fuel tanks.” *J. Pressure Vessel Technol*, vol. 139, issue 4 (2017): 041402. DOI: 10.1115/1.4035976.
[16] Ţălu, Ştefan and Mihai Ţălu. “CAD generating of 3D supershapes in different coordinate systems.“ *Annals of Faculty of Engineering Hunedoara - International Journal of Engineering, Hunedoara, Romania*, Tome VIII, Fascicule 3 (2010): 215-219.
[17] Ţălu, Ştefan and Mihai Ţălu. “A CAD study on generating of 2D supershapes in different coordinate systems.“ *Annals of Faculty of Engineering Hunedoara - International Journal of Engineering, Hunedoara, Romania*, Tome VIII, Fascicule 3 (2010): 201-203.
[18] Ţălu, Ştefan. *Limbajul de programare AutoLISP. Teorie şi aplicaţii. (AutoLISP programming language. Theory and applications)*. Cluj-Napoca, Risoprint Publishing house, 2001.
[19] Ţălu, Ştefan. *Grafică tehnică asistată de calculator. (Computer assisted technical graphics)*. Cluj-Napoca, Victor Melenti Publishing house, 2001.
[20] Ţălu, Ştefan. *Reprezentări grafice asistate de calculator. (Computer assisted graphical representations).* Cluj-Napoca, Osama Publishing house, 2001.
[21] Ţălu, Ştefan. *AutoCAD 2005*. Cluj-Napoca, Risoprint Publishing house, 2005.
[22] Ţălu, Ştefan and Mihai Ţălu. *AutoCAD 2006. Proiectare tridimensională. (AutoCAD 2006. Three-dimensional designing)*. Cluj-Napoca, MEGA Publishing house, 2007.
[23] Ţălu, Ştefan. *AutoCAD 2017*. Cluj-Napoca, Napoca Star Publishing house, 2017.
[24] Țălu, Mihai. *Calculul pierderilor de presiune distribuite în conducte hidraulice. (Calculation of distributed pressure loss in hydraulic pipelines).* Craiova, Universitaria Publishing house, 2016.
[25] Ţălu, Mihai. *Mecanica fluidelor. Curgeri laminare monodimensionale. (Fluid mechanics. The monodimensional laminar flow).* Craiova, Universitaria Publishing house, 2016.
[26] Țălu, Mihai. *Pierderi de presiune hidraulică în conducte tehnice cu secțiune inelară. Calcul numeric și analiză C.F.D. (Hydraulic pressure loss in technical piping with annular section. Numerical calculation and C.F.D.)*, Craiova, Universitaria Publishing house, 2016.
[27] Ţălu, Ştefan. *Geometrie descriptivă. (Descriptive geometry)*, Cluj-Napoca, Risoprint Publishing house, 2010.
[28] Florescu-Gligore, Adrian, Magdalena Orban and Ştefan Ţălu. *Cotarea în proiectarea constructivă şi tehnologică. (Dimensioning in technological and constructive engineering graphics).* Cluj-Napoca, Lithography of The Technical University of Cluj-Napoca, 1998.
[29] Florescu-Gligore, Adrian, Ştefan Ţălu and Dan Noveanu. *Reprezentarea şi vizualizarea formelor geometrice în desenul industrial. (Representation and visualization of geometric shapes in industrial drawing).* Cluj-Napoca, U. T. Pres Publishing house, 2006.
[30] Racocea, Cristina and Ştefan Ţălu. *Reprezentarea formelor geometrice tehnice în axonometrie. (The axonometric representation of technical geometric shapes).* Cluj-Napoca, Napoca Star Publishing house, 2011.
[31] Ţălu, Ştefan and Cristina Racocea. *Reprezentări axonometrice cu aplicaţii în tehnică. (Axonometric representations with applications in technique).* Cluj-Napoca, MEGA Publishing house, 2007.
[32] Niţulescu, Theodor and Ştefan Ţălu. *Aplicaţii ale geometriei descriptive şi graficii asistate de calculator în desenul industrial. (Applications of descriptive geometry and computer aided design in engineering graphics).* Cluj-Napoca, Risoprint Publishing house, 2001.
[33] Bîrleanu, Corina and Ştefan Ţălu. *Organe de maşini. Proiectare şi reprezentare grafică asistată de calculator. (Machine elements. Designing and computer assisted graphical representations).* Cluj-Napoca, Victor Melenti Publishing house, 2001.
[34] Ţălu, Ştefan. *Micro and nanoscale characterization of three dimensional surfaces. Basics and applications*. Napoca Star Publishing House, Cluj-Napoca, Romania, 2015.
[35] *** Autodesk AutoCAD 2017 software.
[36] *** SolidWorks 2017 software.

ISSN 1453 – 7303 "HIDRAULICA" (No. 1/2018)
Magazine *of Hydraulics, Pneumatics, Tribology, Ecology, Sensorics, Mechatronics*

Fault Tree Analysis Used in Offshore Industry

Prof. Dr.Eng. **Mariana PANAITESCU[1],** Prof. Dr.Eng. **Fănel-Viorel PANAITESCU[1],**
Assist. Dr. Eng. **Ionuț VOICU[1]**, PhD. Student **Laurențiu-George DUMITRESCU**[2]

[1] Constanta Maritime University; panaitescumariana1@gmail.com, viopanaitescu@yahoo.ro, ctionut2009@yahoo.com

[2] Constanta OILTERMINAL, dumitrescu.laurentiugeorge@yahoo.com

Abstract: *Fault Tree Analysis is one of the engineering tools that provide a systematic and descriptive approach to the identification of systems under risk. Probabilistic Risk Assessment (PRA) is a method to determine the reliability of a system based on the probability of component(s) and/or system(s) failure. Fault Tree Analysis (FTA), which is a part of PRA, provides a method for determining how failures can occur both quantitatively and qualitatively. In this paper we present the FTA for offshore facility: safety flow chart of offshore production facility, fault tree diagrams for different levels (upper level, intermediate state, overpressure, underpressure, excess temperature, ignition, excess fuel). Also, FTA for subsea control systems is presented in this paper. In conclusions, reliability analysis of the surface facilities shows that mechanical components, pumps and compressors, have higher failure rates compared to other mechanical components.*

Keywords: *Fault tree, reliability, analysis, offshore, industry, diagram, facility, probability, risk, assessment, event, symbol*

1. Introduction

Fault tree analysis is one of the engineering tools that provide a systematic and descriptive approach to the identification of systems under risk. It also provides a visual aid in understanding the system's behaviour. Probabilistic Risk Assessment (PRA) is a method to determine the reliability of a system based on the probability of each component and/or system failure. Fault Tree Analysis (FTA), which is a part of PRA, provides a method for determining how failures can occur both quantitatively and qualitatively [1].

2. Fault Tree Diagrams

Fault Tree diagrams provide a means of visualizing all of the possible modes of potential failures, an understanding of the system failure due to component failures and redesign alternatives [2]. These diagrams are formed such that an undesired event appears on top of the diagram, called the top event. The causes that lead to the system failure are broken into hierarchical levels until effects of the basic system components that lead to the top failure can be identified. Branches using event statements and logic gates link the basic events, or fault events, that lead to the top event. The failure rate data must be available for those basic events at the lowest hierarchical level. Once the fault tree is formed, the probability of occurrence of the top event can be found.

- *Fault Tree symbols*

These are used to connect basic events to the top event, during fault tree construction. There are two kinds of fault tree symbols: event symbols (Fig. 1), and gate symbols (Fig. 2) [1], [2].

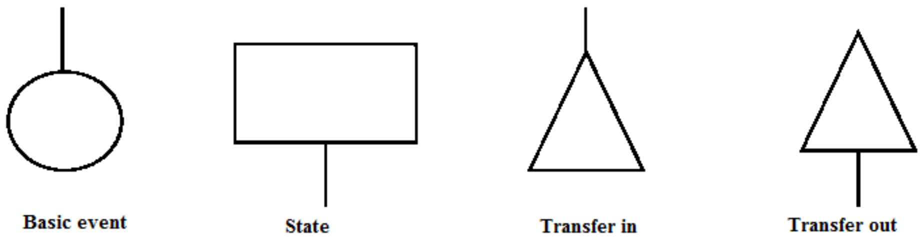

Fig. 1. The events symbols

Fig. 2. Gates symbols

- *Fault Tree Construction*

A fault tree (FT) is constructed such that the undesired event or top event exists at the highest level in the fault tree. Basic events and outputs of gates are connected so that they lead to that top event. Basic events and states are at lower levels.

- *Probability Calculations in Fault Trees*

The calculation of the probability of an undesired event can be done using the Boolean's algebra for the analysed system (with a program in the C^{++}). Using the FTA diagrams, and the results obtained from the calculations, which components and systems are safe was assessed.

2.1 FTA for offshore industry

For this area, first must present offshore production facility for safety flow chart (Fig. 3). In this chart, we can see that safety devices should be used to prevent the propagation of undesirable events. The release of hydrocarbons is the main factor to lead all top events.
The overall objectives of the safety system are: prevent undesirable events that could lead to hydrocarbon leak; shut the process partially or overall to prevent leak of hydrocarbons and fire; accumulate and recover the released hydrocarbons and gases that escape from the process.

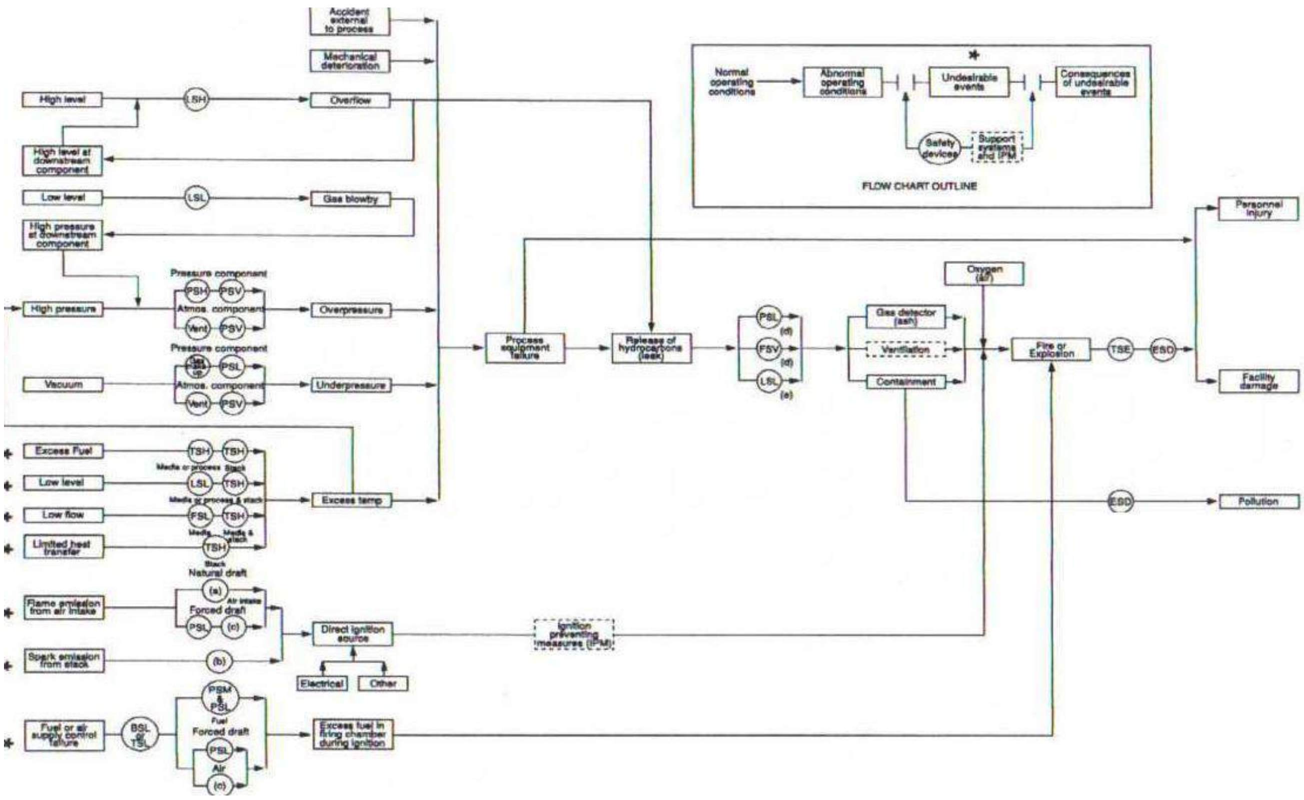

Fig. 3. Safety flow chart

Starting from safety flow chart, we construct: a) *upper level Fault Tree diagram* (Fig. 4), where the top event was personnel injury and/or facility damage; the intermediate state is the state of the safety chart after the release of hydrocarbons and three safety devices (PSL- Pressure Safety Valve, FSV- Flow Safety Valve, LSL- Level Safety Low);

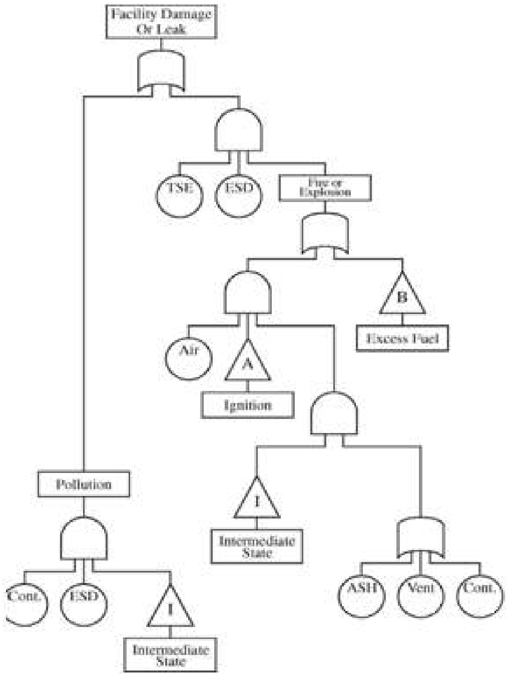

Fig. 4. Upper level Fault Tree diagram

Safety elements (Fig.4) are: temperature safety elements (TSE) (temperature sensors), an emergency shutdown system (ESD) (modeled by valve), containment (a system to collect and direct escaped liquid hydrocarbons to a safe location)[2], gas detector (ASH).
The triangle states are: I- Intermediate State (Fig.5), A-Ignition (Fig.6), B-Excess Fuel (Fig. 7).

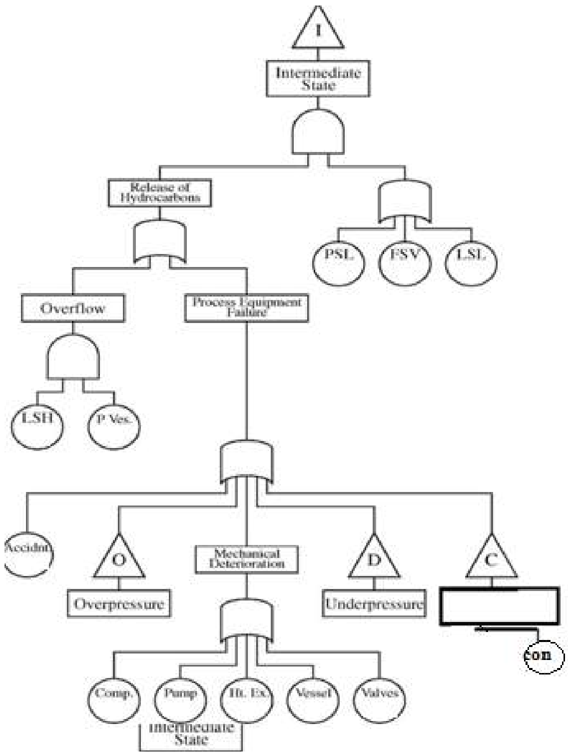

Fig. 5. Fault Tree Diagram of Intermediate State I

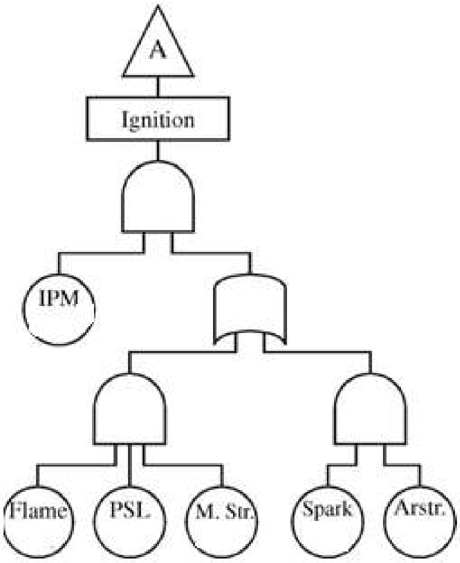

Fig. 6. Fault Tree Diagram of A-Ignition

An ignition source could be: the flame emission from the air intake arises with the failure of the low pressure sensor (PSL), the motor starter interlock failure, or spark emission from the stack arises with stack spark arrestor failure. Flame emission from air intake causes improper fuel usage (a failure of a pump).

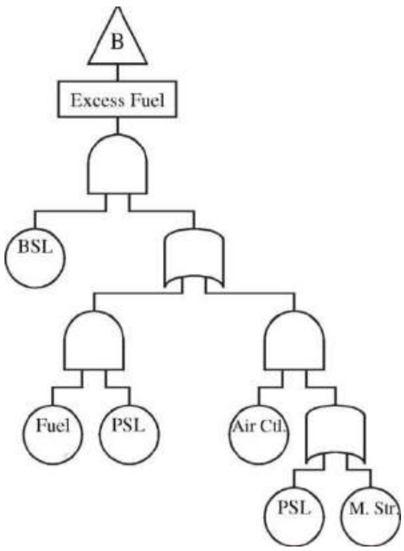

Fig. 7. Fault Tree Diagram of B-Excess Fuel

B represents the excess fuel intermediate state. Excess fuel may occur if the fuel is extraneous in the firing chamber and if the safety device, burner safety low (BSL), fails [2]. Excess fuel in the firing chamber could occur due the failure of the fuel supply control (failure of the pump control unit) and failure of the low pressure sensor, or due air supply control failure with the failure of the motor starter interlock and the low pressure sensor (PSL).

Process equipment failure is due to five factors: accident, O-overpressure (Fig.8), mechanical deterioration of hardware components, D-under pressure (Fig.9), C-excess temperature at component (Fig.10) [3].

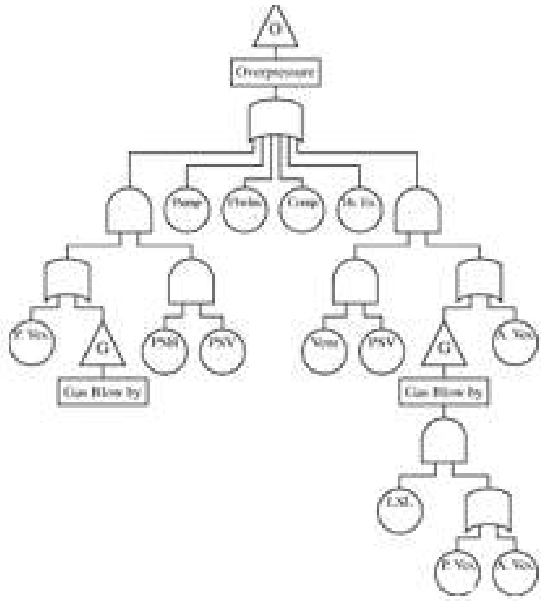

Fig. 8. Fault Tree Diagram of Overpressure

Note: The letters O, D, C-show the triangle states

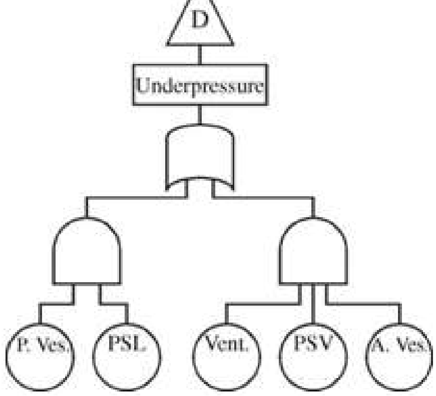

Fig. 9. Fault Tree Diagram of Underpressure

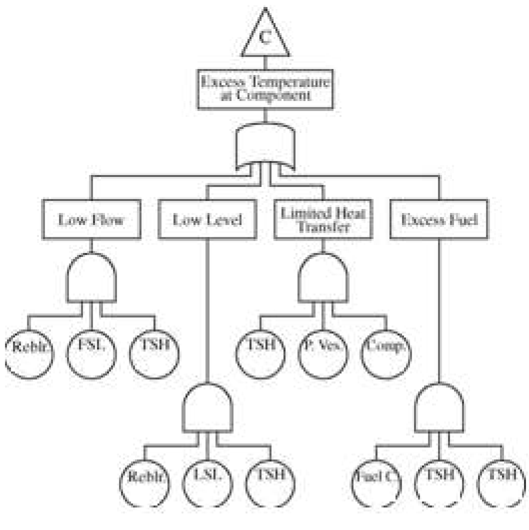

Fig. 10. Fault Tree Diagram of Excess Temperature

The Fault Tree diagrams (Fig.4....Fig. 10) present the causes for personnel injury and/or facility damage due to sensors, control unit failures of various hardware components [4].

2.1 FTA for subsea control systems

FTA for subsea control systems was analyzed using subsea architecture (Fig. 11). Failure modes for the subsea subsystems are: electrical power failure - pod (EFP); hydraulic power failure - connector (HFC); hydraulic power failure - line (HFL); hydraulic power failure - pod (HFP); signal transmission failure - connector (SFC); signal transmission failure - line (SFL); signal transmission failure - pod (SFP); signal transmission failure- surface (SFS). The block diagram of the subsea control subsystems shown in Fig.12.

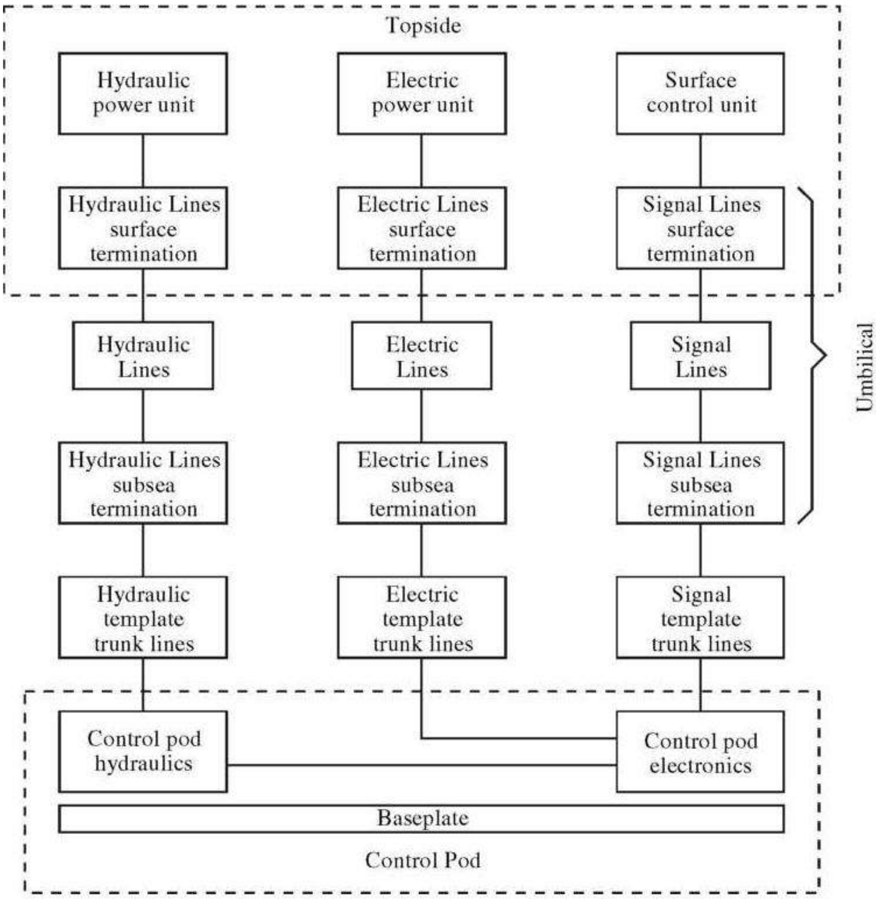

Fig. 11. Subsea architecture [4]

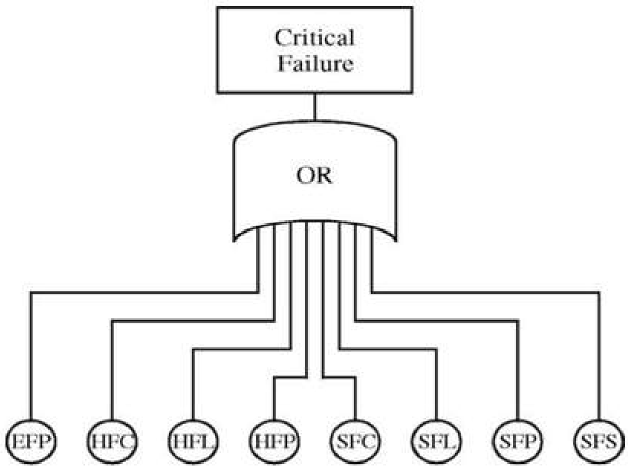

Fig. 12. The block diagram of the subsea control subsystems [5]

Note:
1) SFC- signal transmission failure in the components;
2) three basic events are actually combinations of two or more fundamental events (e.g.: EFP could be either a short circuit at the pod connector or a generic electric failure in the subsea control unit) [3].

The fault tree will consist of only basic events, "OR" gates and derived states, including the top event [5].

3. Conclusions

With this method (FTA) and its tools we can provide all possible modes of potential failures of the components of systems and redesign alternatives. Also, we can identification the risks of systems during operational time.

The use of FTA is a real support for design, construction, inspection and maintenance in offshore industry. The FTA tools are also useful in demonstrating the importance and effects of improving human and organizational aspects.

Acknowledgments

Acknowledgments of Mr. Egemen Kemal Cetinkaia from University of Missouri-Rolla, *Master of Science in Electrical Engineering*, who has provided specialized information from this field in his thesis.

References

[1] Kashubski, Michael. "Offshore Oil and Gas installations Security" *An International Perspective*, Accessed January 20, 2018. http://ref.cern.ch/CERN/CNL/2000/003/scada/.
[2] Çetinkaya, Egemen Kemal. *Reliability analysis of SCADA systems used in the offshore oil and gas industry,* Missouri-Rolla, 2001.
[3] API. *Recommended Practice 14C,* "Recommended Practice for Analysis, Design, Installation, and Testing of Basic Surface Safety Systems for Offshore Production Platforms", sixth edition, March 1998.
[4] Dunn-Norman, S., K.T. Erickson, E.K. Çetinkaya, E.K. Stanek and A. Miller. "SCADA system trends in deepwater developments". Paper presented at Rio Oil & Gas Expo and Conference, October 2000.
[5] Musa, J.D, A. Iannino and K. Okumoto. *Software Reliability: Measurement, predictions, applications,* McGraw-Hill, 1987.

Statistical Analysis of the Pollution of a Hydraulic Oil Based on the Evolution of the Filter Clogging on the Pressure Pipe

PhD. Eng. **Mounir GAHGAH**[1], Pr. **Azzedine BOUZAOUIT**[2]

[1]Department of Mechanical Engineering, Faculty of Technology, Université 20 Aout 1955 de Skikda, Algeria

[2]LRPCSI Laboratory of Research, Faculty of Technology, Université 20 Aout 1955 de Skikda, Algeria
gahgah.mounir@gmail.com / bouzaouit21@gmail.com

Abstract: *We present in this paper the results of an experimental study conducted on the analysis of the influence of clogging of a hydraulic filter, installed on the discharge pipe of a variable displacement pump, the operating pressure is 210 bar. The pump is used to supply hydraulic power to a finisher in the rolling mill at the iron and steel complex in Algeria. In this context, we tested the filter retention efficiency, whose mesh size of the filter element is 15 µm. The influence of the service time and consequently the number of pollutant particles retained per filter on the singular pressure loss ΔP of the filter were characterized. A statistical analysis conducted on the representative sample of ΔP values, followed by adjustment tests has been made. The statistical analysis carried out clearly shows that the evolution of the local pressure losses at the level of the filter follows a Beta law.*
Knowing such a distribution law of a variable is an advantage that will help to establish a predictive maintenance program, with the aim of acting in time, and this to remedy the failures, whose oil pollution is considered the main cause.

Keywords: *Hydraulic fluid, filter, pollution, pressure loss, statistical analysis*

1. Introduction

Hydraulics in general and industrial in particular is unavoidable in several areas such as the industrial sector. Indeed, it has a decisive place in the understanding, analysis and diagnostics of problems related to hydraulic systems. In addition, the control of these systems requires instrumentation that requires the designer and operator to a very advanced knowledge to carry out the hydraulic installations ensuring their operating safety.
The hydraulic fluid is considered the most important element for the proper functioning of a hydraulic mechanism. Hydraulic fluids used in high pressure systems are virtually incompressible, after the hydraulic system is primed with oil, it can instantly transmit power to all parts of the system. However, hydraulic fluids do not have the same properties, so do not have the same efficiency of energy transmission. The correct and proper choice of hydraulic oil depends on the application and operating conditions of the hydraulic system that the objective is to achieve better reliability.
According to studies already carried out, if one analyzes the failures occurring on the hydraulic installations, one notes that a large number of these come from the bad state of the hydraulic fluid, because the oil under pressure, circulating in the installation, loses its physicochemical characteristics [1] and carries all kinds of impurities that can be abrasive or non-abrasive. In any case, it is essential to eliminate them because they will cause breakdowns and abnormal wear of the components leading to leaks quickly. This is the role of filtration.
For the sake of efficiency of the filtration, it is then necessary to ask the question about the best possible location to install a filter as soon as all the other pollution prevention provisions have been taken (removal of pollution due to maintenance, transporting and filtering the air drawn in by the tank and any other external impurity).
For example, on the pump discharge pipe (high pressure), this filtration mode tends to become general but requires filter bodies and filter elements that can withstand the pressure of the circuit. These types of filters are often very expensive but the protection of the components against impurities is guaranteed.
The filtration efficiency is located on average around 10 µm and at times (3-4) µm if it concerns the protection of the servo-valves in particular.

Pressure filters are designed for direct mounting on pressure lines. They are generally mounted upstream of the control and adjustment devices of the hydraulic system. This filtration is effective:

- It protects the hydraulic components.
- Stops debris from pump wear.
- Acts as a safety filter in front of a sensitive component.

Generally, a hydraulic filter is characterized by its size, the mesh size of the filter element (x) in µm, [2] the retention rate (β_x) which is given by the formula (1) and the filter resistance or the permissible local pressure loss (ΔP_{adm}).

$$\beta_x = \frac{N_e(\geq x\ \mu m)}{N_s(\geq x\ \mu m)} \tag{1}$$

With

N_e: The number of particles before the filter of size ≥ x,

N_s: The number of particles after the filter of size ≥ x,

The singular pressure loss, located in a section of the pipe, is caused by a change of direction and intensity of the speed. The fluid flow has become locally (at the hydraulic component) a non-uniform or disturbed flow.

Such non-uniformity of speed can be caused by:

- a branch section of the pipe,
- a change of direction (elbow or distributor),
- a connection or connection (filter, valve),
- a measuring and control device (flow regulator, pressure limiter).

The flowing relation gives the singular pressure loss:

$$\Delta P = \xi \frac{V^2}{2g} \tag{2}$$

With

ξ: Coefficient that characterizes the resistance of the hydraulic component,

V: the flow velocity of the fluid,

g: the acceleration of gravity.

The pressure loss at the filter ΔP, is a kind of specific resistance related to the hydraulic component and its manufacturing technology, it characterizes the singular pressure loss at the filter, so it varies from one filter to one other [3]. It is also related to the quality of the oil passing through it, knowing that a large concentration of polluting solid particles circulating in the oil, which will subsequently be retained by the filter, affects the value of the local pressure loss. That is to say ΔP very sensitive to the increase in the number of solid particles retained [4]. The clogging phenomenon of the filters has become an issue for the maintenance of hydraulic installations. In this context, as we have already mentioned, the pollution of the oil in a hydraulic circuit is responsible for more than 70% of the failures of such a system. This phenomenon is the major concern of maintenance managers and technicians in general and that of precision hydraulic components in particular. As a result, researchers never stop running behind mathematical methods and models to implement it in order to establish a predictive maintenance plan to remedy the filter-clogging phenomenon, namely the evolution of the local pressure loss. To do this, considering ΔP as a variable in time, the knowledge of its law of its distribution is necessary for when can propose a powerful mathematical model describing the pollution process of the hydraulic oil used, it is the objective of this work

2. Methodology of work

The working methodology implemented for the realization of the present study, in order to carry out a statistical analysis on the pressure loss at the filter level is as follows:

The study concerns the monitoring of the evolution of the solid pollutant particles retained at the level of a filter, installed on the discharge line (pressure line) of a hydraulic pump with variable displacement, feeding the hydraulic circuit of the finishing machine located at the steel hot rolling complex in Algeria.

The operating pressure of the installation is 210 bar, the size of the particles to be removed to protect the valves and the rest of the hydraulic components installed is 15µm.
For that, we used an electronic particle counter of the CCS2 type, to allow us to count the polluting particles and to know the real purity class of the oil. It works according to the standards NAS-1638, ISO 4406-99 and ISO 4406-87. Counting is done online (the installation is running), once before the filter to be tested and a second after. On the ends of the filter is connected a differential pressure gauge for reading the pressure difference generated at the filter, the mesh size of the filter element are on average equal to 15 µm, the admissible resistance that the filter can bear is 2 bar. The Figure 1 gives the principle schema.

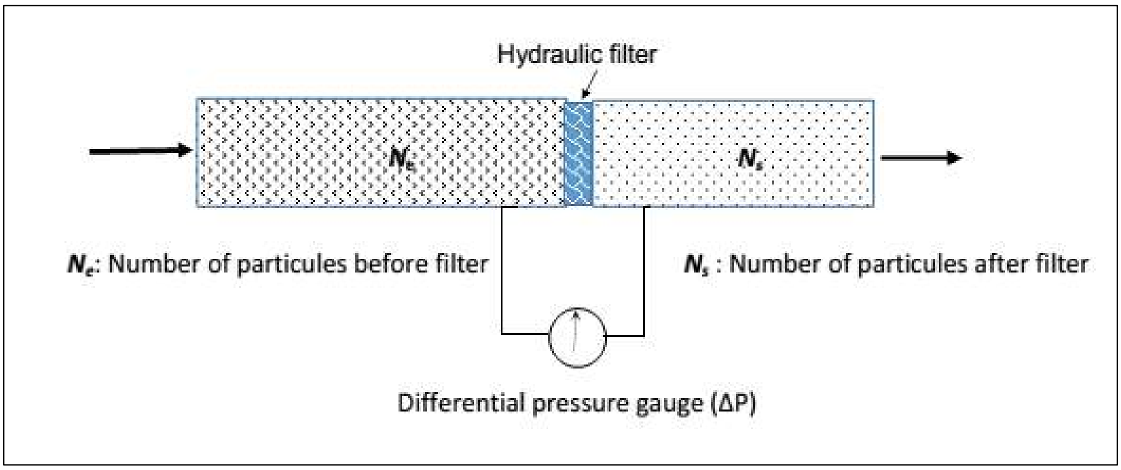

Fig. 1. The principle schema of experimentation

3. Results and discussion

According to the schematic diagram presented by the Figure 1, the measurement of the pressure loss ΔP, as well as the counting of the polluting particles upstream and downstream of the filter, and in order to be able to calculate the cumulative number of particles retained by the filter.
Experimental data are shown in the Table 1.

Table 1: The experimental data of locale pressure loss

No	Time ; (h)	Cumulative number of particules retained	ΔP ; (bar)	No	Time ; (h)	Cumulative number of particules retained	ΔP ; (bar)
1	0	2150	1.15	**16**	164	4480	1.70
2	12	2270	1.15	**17**	172	7125	1.76
3	24	2570	1.18	**18**	180	8200	1.65
4	36	2684	1.27	**19**	188	10588	1.75
5	48	2810	1.15	**20**	200	12780	1.88
6	56	2978	1.20	**21**	208	14025	2.10
7	64	3174	1.32	**22**	220	15848	2.20
8	72	3288	1.38	**23**	228	15900	2.25
9	80	3460	1.40	**24**	236	15820	2.00
10	92	3580	1.36	**25**	260	18700	1.98
11	100	3784	1.45	**26**	284	21800	2.00
12	112	3810	1.42	**27**	292	22540	1.98
13	120	4025	1.48	**28**	312	24400	2.18
14	132	4275	1.56	**29**	320	24670	2.24
15	140	3318	1.62	**30**	325	25460	2.20

3.1 Hypothesis

The assumptions considered for the preparation of the sample data are as follows:
- All the particles retained by the filter will remain stuck on the filter element during the whole analysis period.
- We do not consider the filter after a certain time as a source of pollution, that is to say, we neglect the measurements corresponding to values of (β_x) negative, which mean that the number of particles measured after the filter is greater than the one before the filter.

3.2 Analysis of the filter resistance evolution

The pressure loss ΔP at the filter varies with the service time, from the Figure 2, it is clear that ΔP increases with the increase thereof.

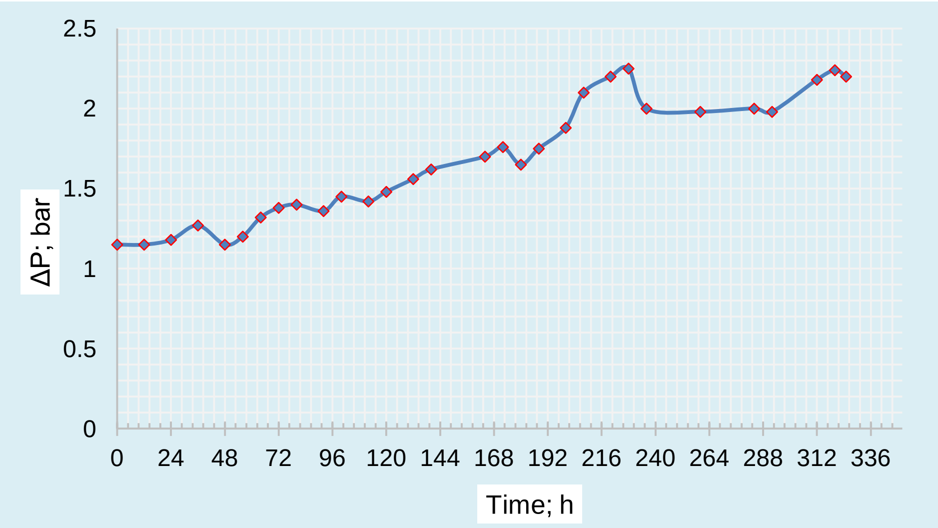

Fig. 2. The evolution of the pressure losses of filter

The only argument of this relation is the increase in the number of polluting particles circulating in the oil that have been stopped by the filter element, causing the reduction of its filtering surface. Therefore, according to the Figure 3, ΔP also increases with the increase of the retained particles number.

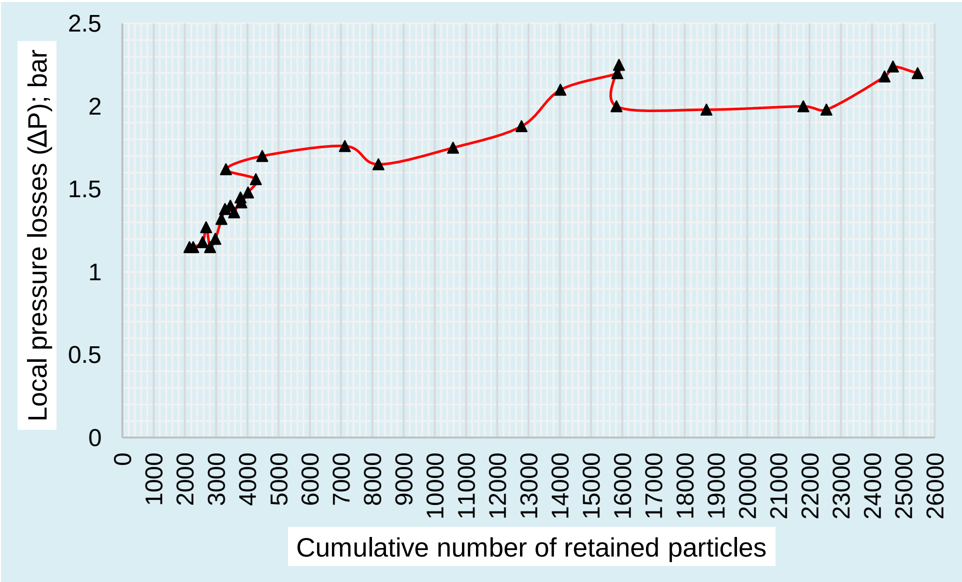

Fig. 3. The local pressure losses with the retained particles number

3.3 Statistical analysis of the pressure losses evolution

A statistical analysis of the representative sample of the ΔP values is considered very important, with the objective of carrying out future work on mathematical modeling and stochastic modeling in particular, in order to predict the evolution phenomenon of ΔP. In this context, MathWave statistical processing and analysis software (EasyFit 5.4) is used.

The density probability function f(x) and the cumulative distribution function F(x) adapted to the variation of the local pressure loss show that ΔP follows a Beta law, whose statistical parameters are: $\propto_1$= 5.2828,$\propto_2$= 5.9935, a= 1.25, b= 2.25, as shown in Figure 4 and Figure 5.

The probability density function:

$$f(x) = \frac{1}{B(\propto_1,\propto_2)} \frac{(x-a)^{\propto_1-1}(b-x)^{\propto_2-1}}{(b-a)^{\propto_1+\propto_2-1}} \quad (3)$$

Where

α1, α2 >0; Continuous shape parameters,

a, b; Continuous boundary parameters, (a<b).

$B(\propto_1,\propto_2)$ is the Beta function;

$$B(\propto_1,\propto_2) = \int_0^1 t^{\propto_1-1}(1-t)^{\propto_2-1}dt \quad (4)$$

The cumulative distribution function:

$$F(x) = I_z(\propto_1,\propto_2) \quad (5)$$

Where

$z \equiv \frac{x-a}{b-a}$,

I_z is the regularized incomplete Beta function, it is given by:

$$I_x(\propto_1,\propto_2) = \frac{B_x(\propto_1,\propto_2)}{\mathrm{B}(\propto_1,\propto_2)} \quad (6)$$

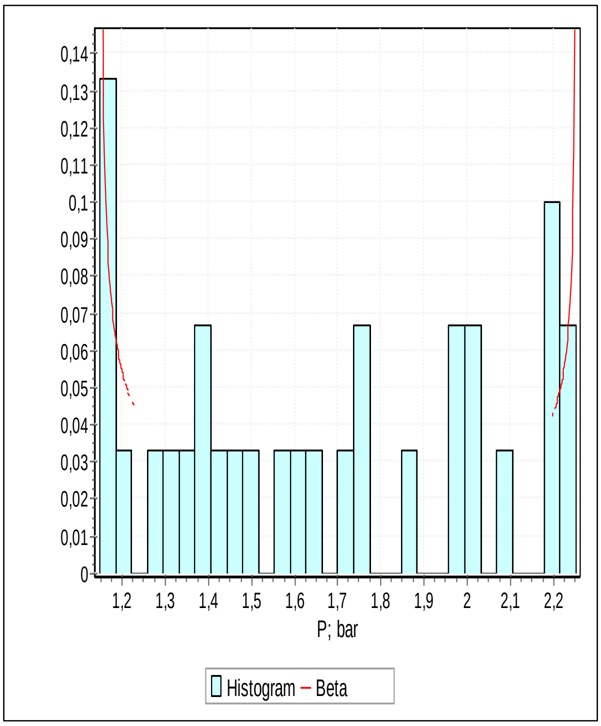

Fig. 4. The probability density function

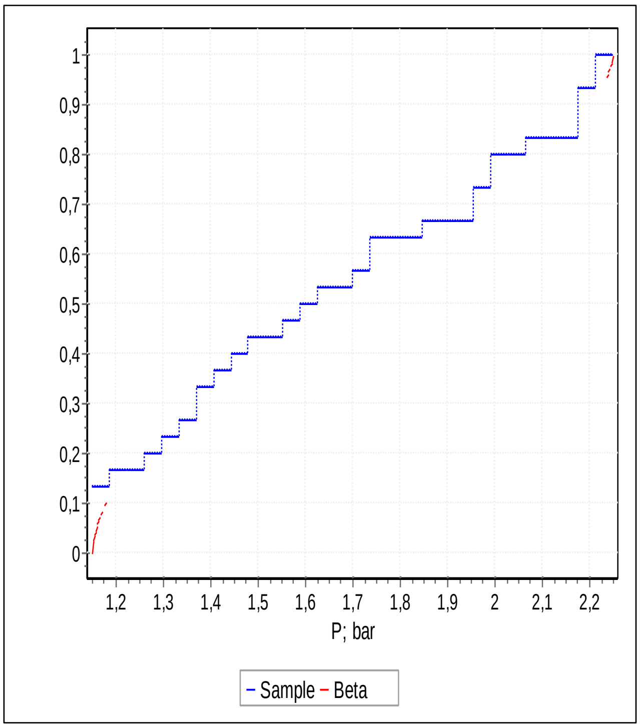

Fig. 5. The cumulative distribution function

The statistical tests of Kolmogorov-Smirnov [5] and Chi-Squared for risk levels of 10%, 5% and even 1% were performed on the ΔP sample, to ensure its adjustment to the Beta law are used. The Table 2 gives the tests results.

Table 2: The statistical test of sample

	The sample statistical test for a Beta law (α_1= 5.2828; α_2= 5.9935; a= 1.15; b= 2.25)					
	Kolmogorov-Smirnov test			**Chi-Squared test**		
Sample	Size = 30			Deg. of freedom = 4		
Statistic	0.1			1.0		
Probability value (P)	0.89608			0.9098		
a (Risk)	0.1	0.05	0.01	0.1	0.05	0.01
Critical value	0.2175	0.2417	0.2898	7.7794	9.4877	13.277
Reject?	NO	NO	NO	NO	NO	NO

It can be seen from the Table 2, that the statistical tests carried out are accepted for the three values of the degree of risk considered.

4. Conclusions

A first part of the present work has been dedicated to general notions on the importance of industrial hydraulics in general, and high-pressure installations in particular. The importance of the essential element in a hydraulic system namely the oil is described. The majority of anomalies disturbing the proper functioning of such a system are directly related to the degradation and contamination of the oil used.
The proper solution for oil contamination is to provide for the installation of filters. Therefore, the choice of location, type, size and even the quality of the filter is very important, in order to preserve the components of the installation, in order to improve the system performance by minimizing the number failures.
In a second part, an analysis of real data resulting from the operation of an industrial system (rolling mill), to describe the evolution of singular pressure losses, with respect to oil pollution was presented. In this context, the clogging of filter on the high-pressure pipe is analysed. The statistical analysis also took a part of our work, in order to rule on a distribution law describing the evolution of the pressure loss around the hydraulic filter, something interesting for the prediction of the possible breakdowns whose oil pollution will be the cause.

References

[1] Gowtham, S. and P. Rajesh Kumar. "Condition Monitoring of I.C Engines by using Oil Analysis." *IJIRST International Journal for Innovative Research in Science & Technology*, Volume 2, Issue 12, (May 2016): 370-375.
[2] http://www.dguv.de/medien/fb-holzundmetall/publikationen-dokumente/infoblaetter/infobl_englisch/082-_filtrationhydraulicfluids.pdf.
[3] Del Fabbro, Laetitia. Modelling of air flours in pleated filters and of their clogging by solid particles. France, CEA SACLAY Inst. de Protection et de Surete Nucleaire, 2002.
[4] Bouzaouit, Azzedine, Aouel Hadjadj, M. Gahgah, and O. Bennis. "Pollution Hydraulic Fluids Analysis by the Differential Pressure Filters Evolution." *U.P.B. Sci. Bull.*, Series D, Vol. 71, Iss.4 (2009): 184-190.
[5] Carricano, Manu, Fanny Poujol, and Laurent Bertrandias. *Analyse de données avec SPSS®*. Pearson France, 2ème édition, 2010.

Numerical Simulation of Thermal Processes Occurring at Testing Hydrostatic Pumps in Cavitation Mode

PhD.Stud. Eng. **Alexandru-Daniel MARINESCU[1],** PhD.Stud. Eng. **Alexandru-Polifron CHIRIȚĂ[1],** PhD. Eng. **Corneliu CRISTESCU[1],** Prof. PhD. Eng. **Carmen-Anca SAFTA[2]**

[1] Hydraulics and Pneumatics Research Institute INOE 2000-IHP, Bucharest, Romania
marinescu.ihp@fluidas.ro; chirita.ihp@fluidas.ro; cristescu.ihp@fluidas.ro

[2] Power Engineering Faculty, University Politehnica of Bucharest, Romania
safta.carmenanca@gmail.com

***Abstract**: This article refers to the use of infrared thermography in the predictive maintenance of hydraulic drive systems. Based on experimental research on the temperature evolution in a hydraulic system which operates in cavitation mode, a numerical simulation model was built. The numerical simulation results are compared with experimental measurements in the points of interest of the hydraulic diagram versus numerical simulation model. The results obtained show that infrared thermal imaging camera procedure can be used in the limit of ± 10% errors as a predictive maintenance method in hydraulic drive systems.*

***Keywords:** Maintenance, hydrostatic pumps, cavitation, infrared thermography, modeling, simulation*

1. Introduction

To maintain in working a long lifetime the hydraulic system at best parameters designed, predictive maintenance is widely used. Predictive maintenance techniques were developed to predict when maintenance should be performed. In 2001, CEN (Comité Européenne de Normalisation – French; European Committee for Standardization) defined the maintenance as "the combination of all technical, administrative, and managerial actions during the life cycle of an item intended to retain it in, or restore it to, a state in which it may perform the required function" [1]. As maintenance defined above, two types of maintenance are developed: preventive maintenance (PM) and corrective maintenance (CM). Preventive maintenance is to control or prevent the deterioration process leading to failure of an engineering object, and corrective maintenance is to restore the engineering object to its operational state through corrective actions after a failure [1]. Through engineering objects one understands products, plants and facilities, infrastructures, assets and systems [1].
A good maintenance experience can compensate the unreliability of an engineering object.
The most common methods of predictive maintenance (as part of PM) are based on: oil analysis, vibration analysis, ultrasonic testing, and infrared thermography. The latter was used by the authors in the experimental research assessing the wear of a gear pump operating in cavitation regime [2].
The non-contact measuring temperature is a common method used in industrial maintenance [3]. The method was developed to avoid more energy consumption and the discontinuing production. Thermography is not a simple measurement method. It was demonstrate that the source of errors in infrared thermography are caused not only because of the incorrect evaluation of some characteristic parameters, such as the emissivity ε coefficient of the analyzed object, the atmospheric temperature T_{atm}, the ambient temperature T_0, the humidity ω, the distance between the termographic infrared camera and the measured object, *d*. The incorrect calibration or evaluation of absorption, reflection and transmission coefficients from the environment and the emergence of the electronic and photonic noise of the system are error sources too [4 ÷ 6]. In most cases, the professional solutions related to measurement errors minimization depends of the thermal imaging camera technical performance and the thermo technical knowledge of the one who uses it.
It is obvious that thermal regime of a hydraulic system is very important in the system design because a critical mode of working as cavitation mode can cause a premature failure of the basic components of the hydraulic system. Usually the hydrostatic pumps are exposed to failures.

Beside the experimental approach developed in INOE 2000-IHP laboratories regarding the infrared thermography maintenance method applied to hydrostatic pumps [2], a theoretical research was developed, too. In this paper a thermal numerical model of the hydraulic system tested in cavitation mode was simulated. The results of numerical simulations are compared in the critical points with the temperatures measured on the hydraulic schematic diagram.

2. Experiments

2.1 Experimental bench

The goal of the experimental study is to measure temperature evolution in time of one hour of a hydraulic drive system which is working in cavitation mode. An experimental bench was designed and physically developed in INOE 2000-IHP Labs, to allow the demonstration of usefulness and efficiency of using the infrared thermography method in the behavioural prediction of hydrostatic drive systems [2]. The hydraulic schematic diagram of the stand is shown in Fig. 1.

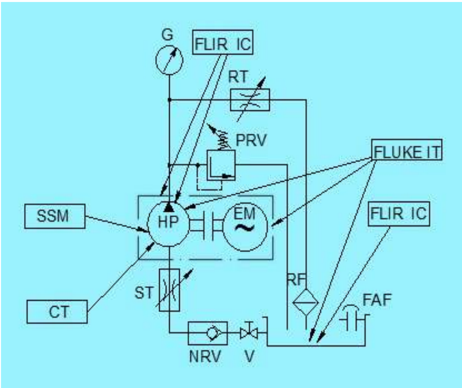

Fig. 1. Hydraulic schematic diagram

Fig. 2. Experimental bench for hydrostatic pump testing [2]

The bench consists of a tank (**T**), with hydraulic oil, provided with a filling and ventilation filter (**FAF**) and a return filter (**RF**). A three-phase electric motor (**EM**) is mounted on the oil tank cover, which, via a coupling (**C**), drives the hydrostatic pump (**HP**) to be tested. The pump (**HP**), sucks the oil from the tank (**T**) via a valve (**V**) and a non-return valve (**NRV**) to keep the oil suction circuit filled of oil, as well as a throttle (**ST**), by which the suction circuit of the pump can be modified (strangled or throttled) in order to modify the suction conditions. The flow section variation through the throttle will lead to an increase of the operating temperature, a phenomenon that will be sensed, measured and recorded by an infrared thermal imaging camera **FLIR**. The hydrostatic pump (**HP**) displaces the oil under the pressure indicated by the pressure gauge (**G**) and is adjusted to the pressure limiting valve (**PRV**) by means of a throttle (**RT**) mounted on the pump discharge, which allows the desired pressure steps to be achieved. The oil will be returned to the tank (**T**) by a return filter (**RF**). In figure 2 is presented the experimental bench.

Fig. 3. Fluke infrared thermometer

Fig. 4. FLIR infrared thermal imaging camera

The experimental bench is used to test a hydrostatic gear pump which is one of the most used types of pump in hydraulic drive systems. The bench was designed so that the pump testing can

operate at different pressure stages controlled by RT throttle and different suction conditions controlled by ST throttle. The experimental studies have been made in cavitation suction mode.
The unwelcome cavitation phenomenon is a complex one: mechanical, thermal, hydrodynamic and chemical. Depending on the flow conditions, the phenomenon of cavitation occurs in the flow of liquids through hydraulic machines and equipment regardless of their application [7, 8]. The cavitation phenomenon occurs when the liquid pressure drops below the liquid vaporization pressure, $p < p_v$. So, if the flow rate is constant but the flow section is narrowing (as on a throttle valve ST) the flow velocities in the flow section are increasing and the pressures are decreasing (Bernoulli equation). Due to the initiation of the vaporization phenomenon, clouds of cavitation bubbles or cavities filled with gas and liquid vapours are formed. Cavitation bubbles are transported by liquid flow in high pressure areas where their implosion occurs. At the time of implosion, the pressures which are developed are several orders of magnitude larger than the average liquid pressure. Once the cavitation phenomenon has developed, the heating process of the liquid is accelerated, the flow hydrodynamic is changed and a biphasic flow (liquid and gas) appears and the efficiency of the system will decrease.
The cavitation phenomenon can be controlled and monitored [9].
In cavitation mode of working on the suction pump in the test bench, environmental temperature, oil temperature, and pump temperature were measured along one hour with a time period of 10 minutes. Pump temperature was measured with three types of temperature devices: a contact thermometer (**CT** type Checktemp 4 by Hanna) directly placed on the pump, a **FLUKE IT,** Fig. 3, infrared thermometer and a **FLIR IC** infrared thermal imaging camera, Fig. 4. Tank and oil temperatures were measured with the same devices FLIR IC and FLUKE IT contactless infrared thermometer. During the experiments the working pressure was read on the manometer (**G**), and the noise in the installation was monitored with the Smart Sensor (**SSM** - Smart Sensor AR 814) soundmeter.

2.2. Experimental results

Temperatures of the pump, tank and oil are measured in working conditions of 75bar pressure step and cavitation. The data are listed in Table 1 where the type of temperature device used is mention too. The temperature at moment zero in the table coincides with the environment temperature.

Table 1: Measured temperatures

Time	T pump FLUKE	T pump FLIR	T tank FLUKE	T tank FLIR	T oil FLUKE	T oil FLIR
0.0	24.0	24.0	24.0	24.4	24.0	24.0
10.0	40.0	41.0	28.0	27.5	28.5	29.5
20.0	51.0	57.2	31.0	31.4	32.0	33.9
30.0	72.0	78.4	42.0	45.5	33.0	49.8
40.0	77.0	84.1	46.0	47.0	65.0	58.9
50.0	83.0	76.0	50.0	51.8	60.0	60.2
60.0	80.0	88.3	50.0	54.0	63.0	60.5

Fig. 5. Thermographic images taken with FLIR Infrared Thermal Imaging Camera

Figure 5 presents the thermographic images, obtained by temperatures measured with the FLIR thermal imaging camera and highlighted in Table 1.

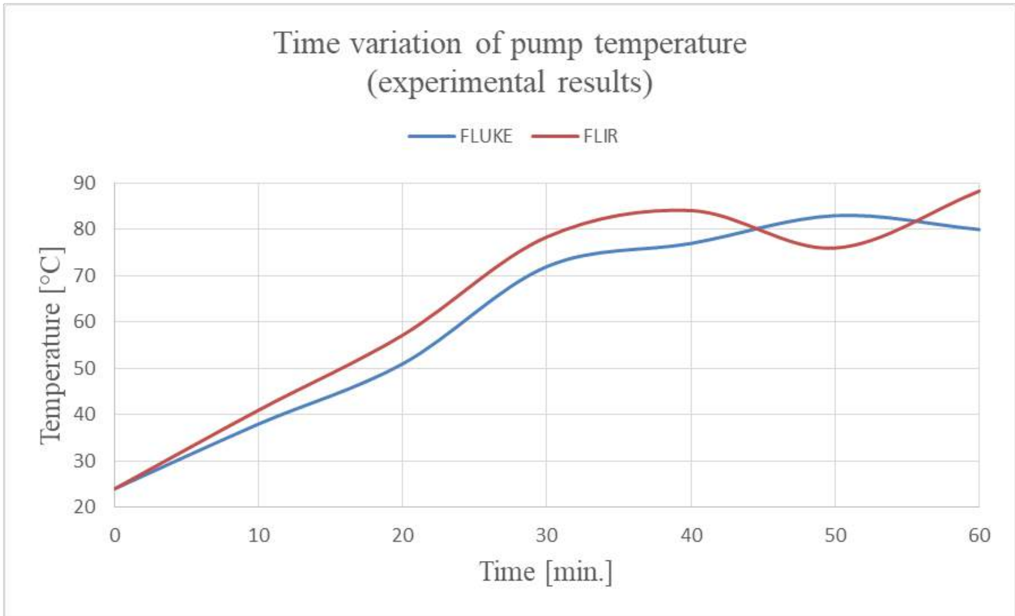

Fig. 6. Trend graph of measured temperatures with Fluke IT and FLIR IC

Based on data from Table 1 the pump temperatures behaviour was plotted in Figure 6, in the case of using the FLUKE IT and FLIR IC devices.

3. Numerical simulation of thermal processes

A theoretical study of the thermal behaviour of the gear pump working in cavitation regime was performed. A numerical simulation network was considered and the points of interest of the hydraulic schematic diagram (Fig. 1) were analyzed in the numerical simulation model, too.

3.1 Developing the Numerical Simulation Network, NSN

Starting from the hydraulic schematic diagram of Figure 1 with the physical parameters of Table 2 there was built the numerical simulation network with the diagram plotted in Figure 7.
Simulation software AMESim from SIEMENS LMS Imagine.Lab was used [10]. The NSN was designed to simulate the thermal processes in the experimental bench of the hydrostatic gear pump working in cavitation mode in the same conditions as experiments.

Table 2: Physical parameters of simulation

NSN Index	Name	Parameters	NSN Index	Name	Parameters
1	Hydraulic oil tank	Capacity - 20 l	**5**	Electric motor	Speed - 1450 rev/min
2.1	Hydraulic hose	Nominal size Ng - 25 mm	**6**	Hydraulic gear pump	Pump disp. - 9 cc/rev
2.2	Hydraulic hose	Nominal size Ng - 10 mm	**7.1**	Volumetric flow rate sensor	
2.3	Hydraulic hose	Nominal size Ng - 10 mm	**7.2**	Pressure sensor	
2.4	Hydraulic hose	Nominal size Ng - 10 mm	**7.3**	Temperature sensor	
2.5	Hydraulic hose	Nominal size Ng - 10 mm	**8**	Hydraulic pressure valve	Cracking pressure - 75 bar
2.6	Hydraulic hose	Nominal size Ng - 10 mm	**9**	HP46 hydraulic oil	Kinematic viscosity - 46 cSt

Table 2: Physical parameters of simulation (continued)

NSN Index	Name	Parameters	NSN Index	Name	Parameters
3.1	Pump inlet throttle		**10**	Earth attraction constant	9.80665 m/s^2
3.2	Pump relief throttle				
4.1	Constant signal source				
4.2	Constant signal source				

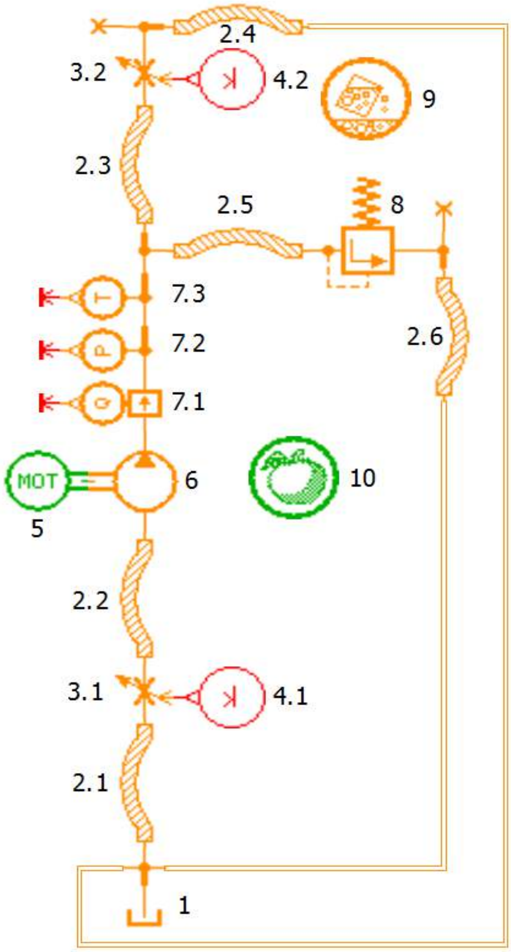

Fig. 7. Numerical simulation network, NSN

The same hydraulic elements used in the hydraulic schematic diagram were modelled with corresponding blocks of the thermal hydraulic library in LMS AMESim ® together with physical parameters of the hydraulic system. The numerical model does not take into account the heat exchange of the hydraulic system with the environment.

3.2 Numerical simulation results

The simulation results are drawn in the following graphs.
Figure 8 shows the pressure variation on the pump intake (green colour) and the output pressure variation of the pump (red colour). The existence of the accentuated vacuum (about 0.4 bar) on the pump input is highlighted which corresponds to cavitation operation mode of the pump at the narrowed flow section controlled with the throttle (**ST**). On the graph one can notice the output pump pressure, which highlights the value set for the safety valve (73 bar), and a slight mitigation in time, caused by heating the oil or lowering the viscosity of the oil.

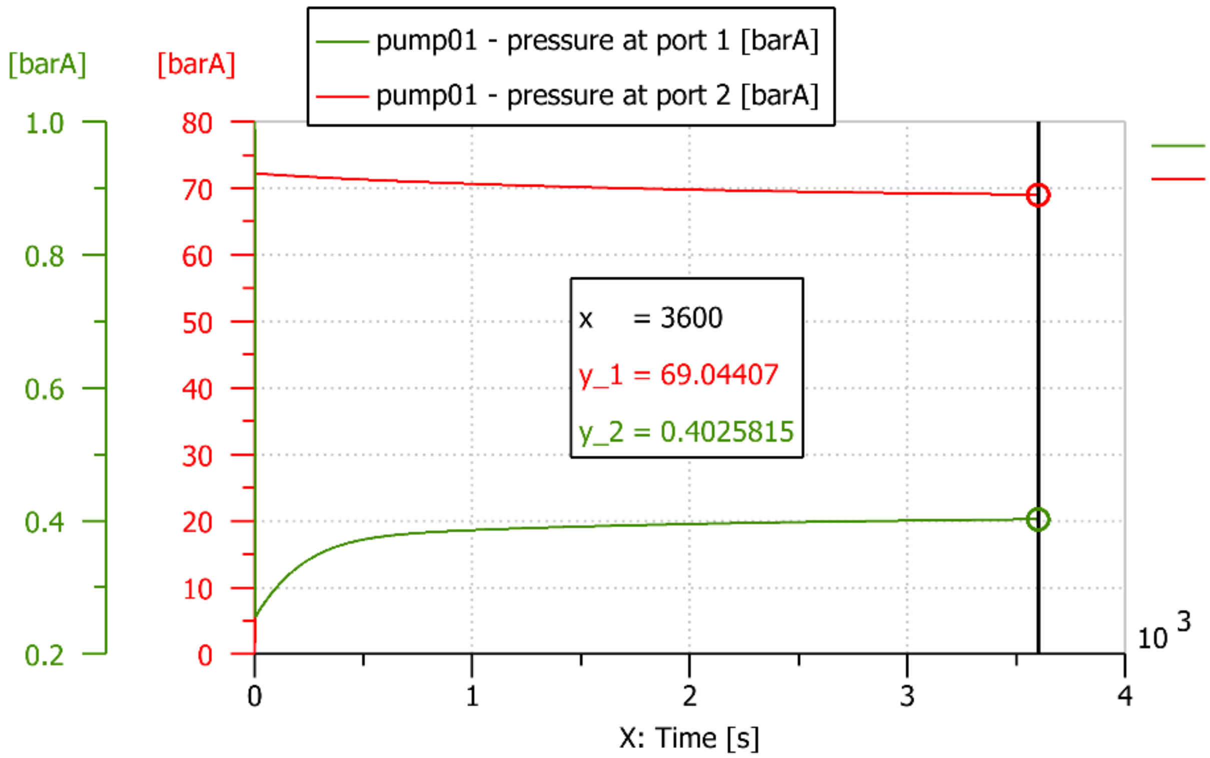

Fig. 8. The pressure developed at the inlet and discharge of the hydraulic pump

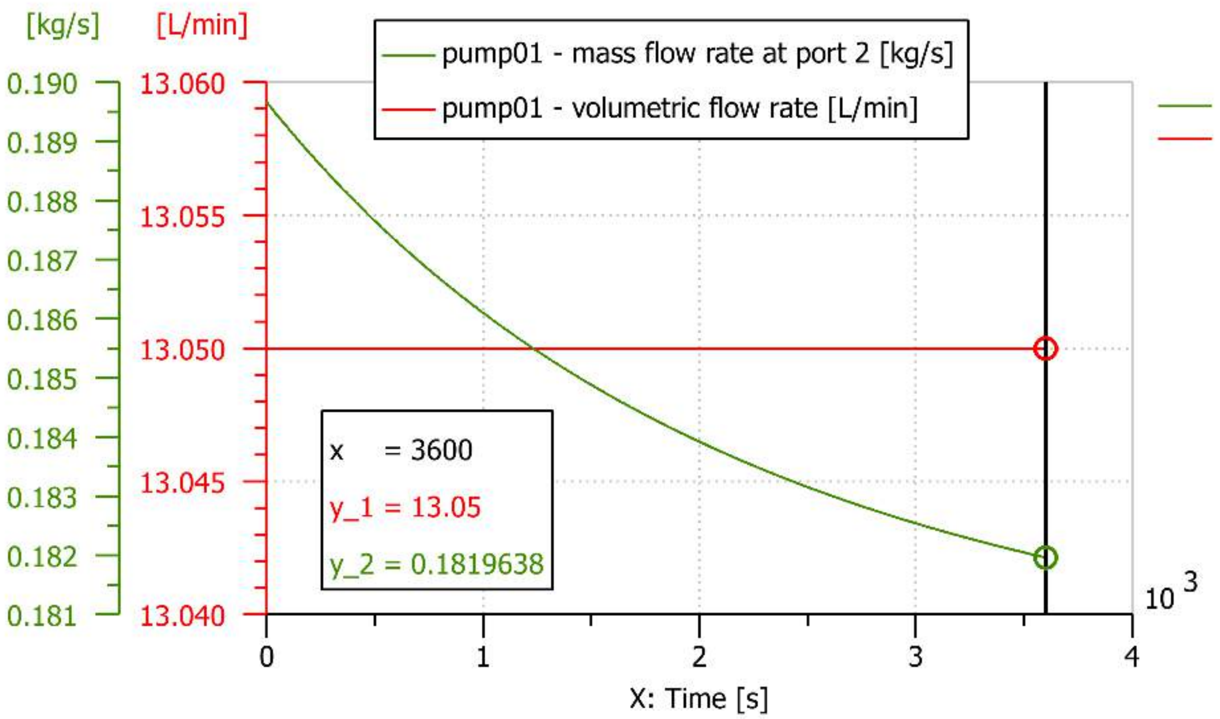

Fig. 9. Volumetric and mass flow of the hydraulic pump

Figure 9 depicts both the pump flow variation (red), and the change in mass flow to the pump (green), which has an interesting dash explainable also by increasing the temperature that makes the density of the oil decrease.

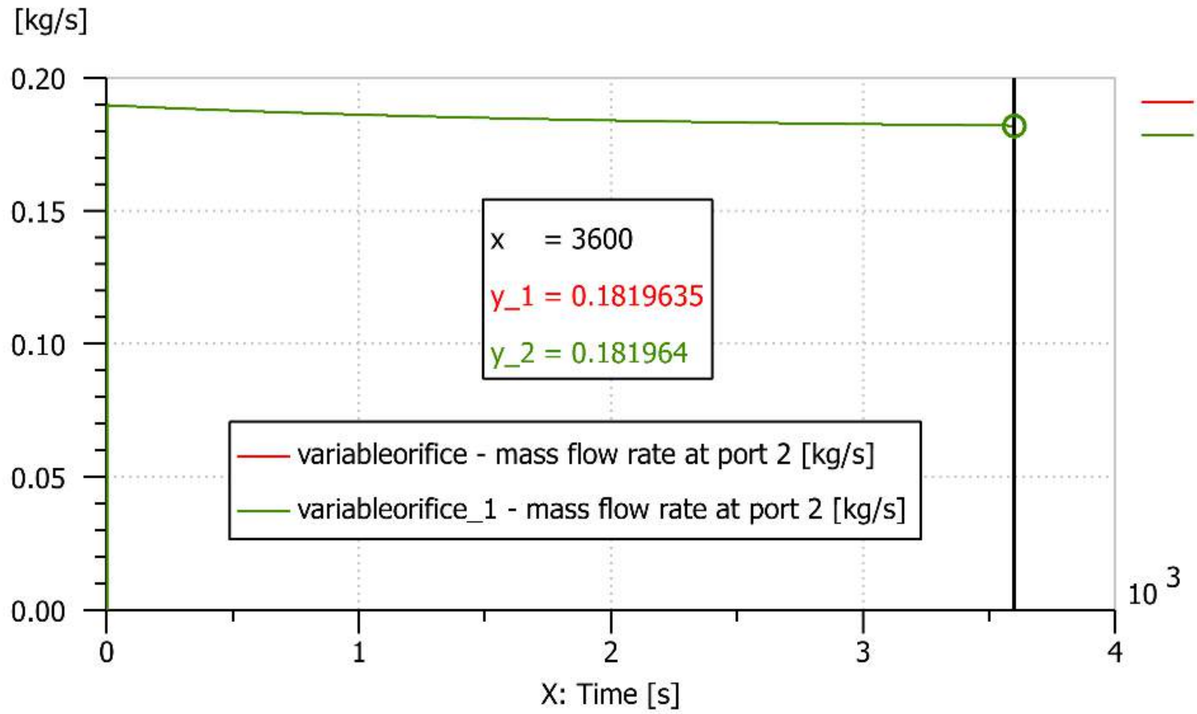

Fig. 10. Mass flow through the hydraulic orifices (throttle)

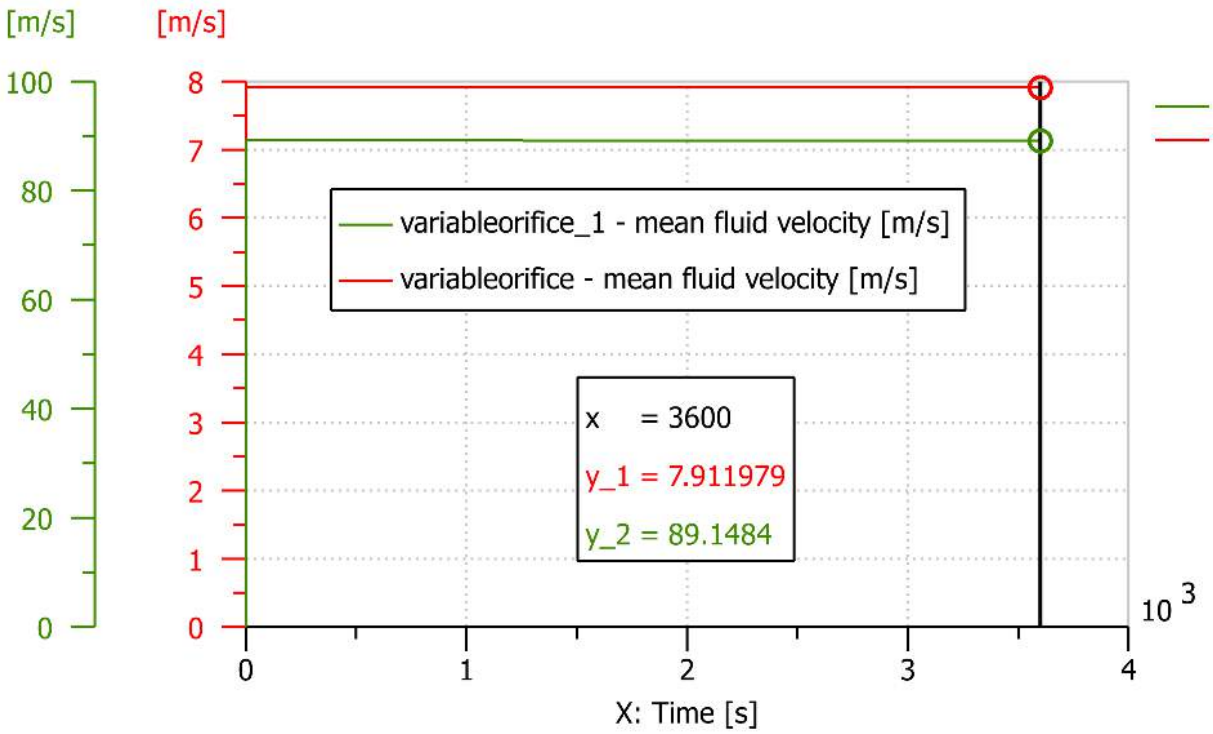

Fig. 11. Velocity of liquid through the hydraulic orifices (throttle)

Figures 10 and 11 show the variation of the mass flows through the throttle holes (almost identical), respectively the variation of the oil flow speeds through the throttle holes on the pump discharge circuit (red 3.1) and respectively on the circuit (green colour 3.2), the latter having lower values because the suction diameter is higher (NRN Index 2.1).

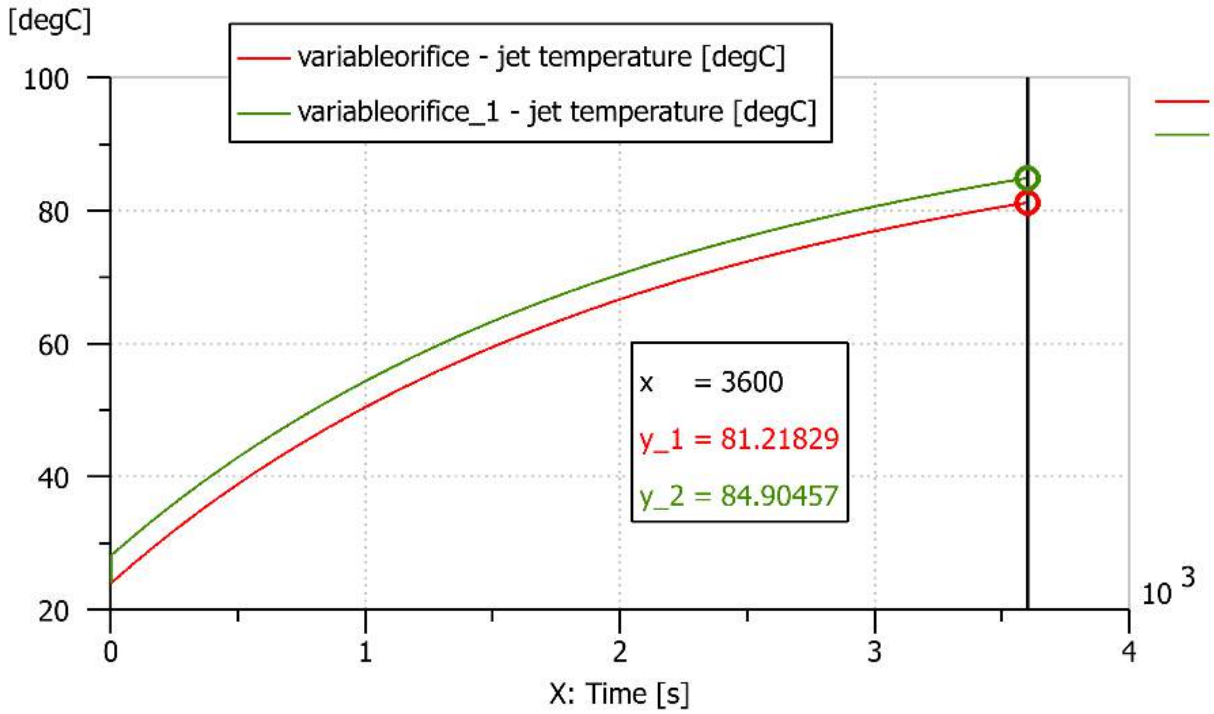

Fig. 12. Liquid stream temperature through the hydraulic orifices (throttle ST and RT)

Figure 12 shows the variation of the oil temperature in throttle holes, with red on the suction circuit, and with green on the discharge circuit, the aspiration being somewhat higher due to the hard cavitation regime.

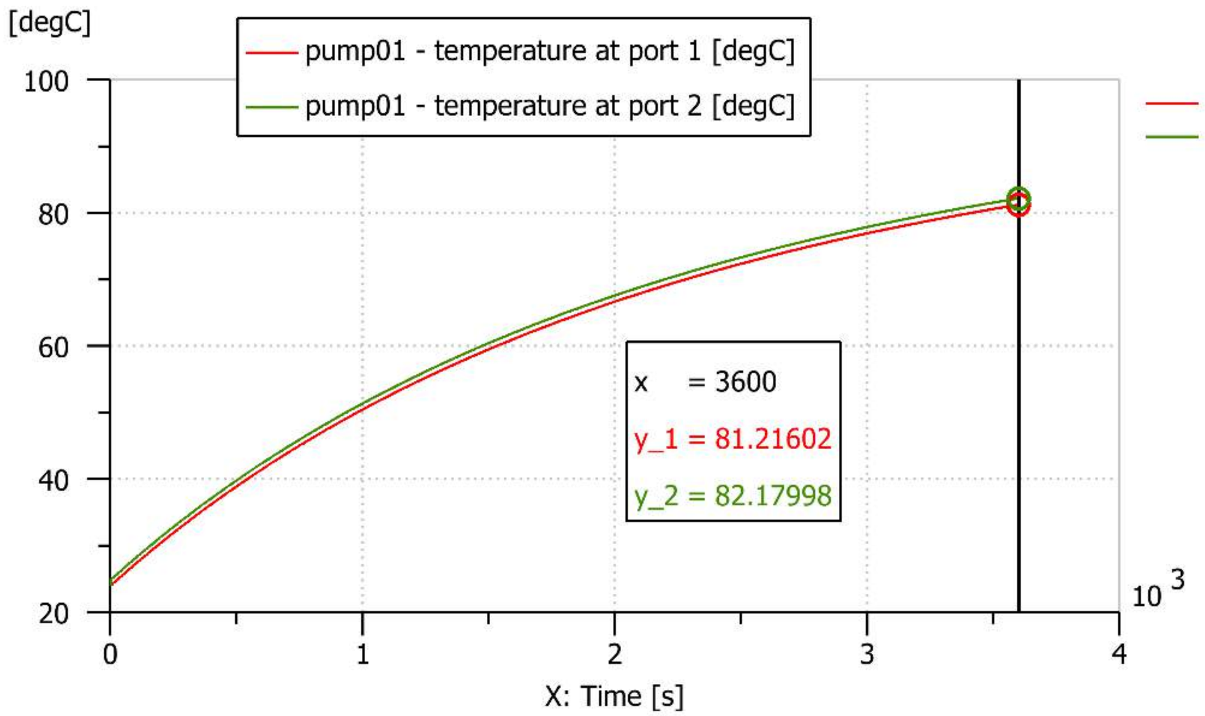

Fig. 13. Fluid temperature in pump inlet and discharge

Figure 13 shows the temperature variation at the pump inlet (green colour) and pump discharge (red colour) which is slightly smaller than the pump temperature because of heat exchange.

3.3 Comparative analysis of experimental and theoretical results

The temperature measurement results from experiments, Table 1, were compared with numerical simulation results. Figure 14 presents on the same graph the measured values with the FLUKE IT (red), FLIR IC (green) thermal imaging cameras and numerical simulation temperature of the pump (blue colour). A good match between experiment and numerical simulation is noticed. The experimental values measured with the FLUKE IT infrared thermometer (red colour) are closer to those obtained by numerical simulation (blue colour). Temperatures measured with FLIR IC infrared camera are not so close to the numerical temperature values. As mentioned in [2], the experimental procedure of using infrared thermography must be improved to minimize the uncertainty of the method.

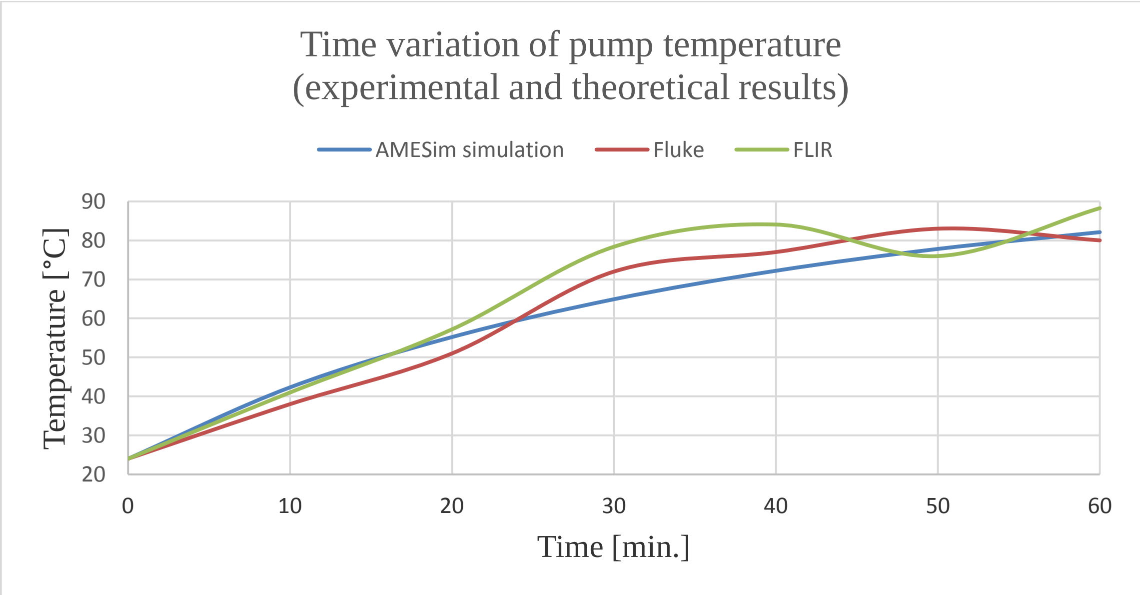

Fig. 14. Hydrostatic pump temperature

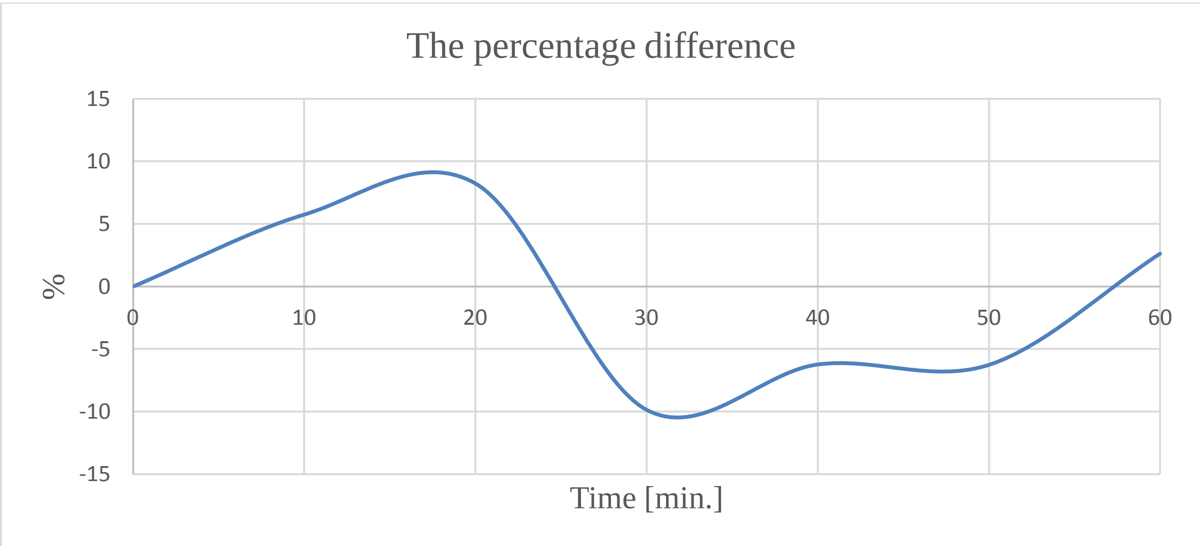

Fig. 15. Percentage difference

To highlight the difference in value between those obtained by measuring with FLUKE IT and those obtained by numerical simulation, in Figure 15 was plotted the percentage of variation differences that are between -10% and 10%, which represents an acceptable error taking into account the complexity of the hydraulic system and the hypothesis of the theoretical study that there is no exchange heat between installation and the environment.

The resumption of the experimental measurements, in a more accurate manner, and a more accurate simulation model will lead to a smaller error between the experiment and theoretical model.

4. Conclusions

The article presents a theoretical study based on experimental measurements of temperatures on a hydrostatic pump bench test performed in INOE 2000-IHP Labs. The goal of the study was to validate a numerical simulation model of the thermal process in a hydraulic gear pump test bench with experimental temperature measurements in the points of interest of the hydraulic system.
In the first part of the article, besides general knowledge regarding preventive and predictive maintenance, it is presents the test bench and some experimental temperature measurements of pump, oil and tank temperatures by using a thermal imaging camera and an infrared thermometer.
The second part of the article presents the theoretical research itself, which consists in the development of a numerical simulation network based on the physical hydraulic diagram and data of the physical model under investigation. Numerical simulation results were plotted and compared with experimental results. A good evolution of temperatures was noticed between the FLUKE IT and numerical simulation results under an error of ± 10%.
This experimental and theoretical approach of a hydraulic system having a gear pump which is working in cavitation mode highlight that the experimental results obtained by using the FLUKE infrared thermometer are closer to the theoretical results obtained by numerical simulation, and so, this device can be a base for development of a predictive maintenance method.

Acknowledgement

Thanks to Hydraulic and Pneumatic Control Systems Labs within Power Engineering Faculty from University Politehnica of Bucharest, for the support in using AMESim, for thermal process simulation.

References

[1] Ben-Daya, Mohammed, Uday Kumar, and D. N. P Murthy. *Introduction to maintenance engineering: modeling, optimization, and management*, John Wiley & Sons, 2016.
[2] Marinescu, Alexandru Daniel, Corneliu Cristescu, Teodor Costinel Popescu and Carmen Anca Safta. "Assessing the Opportunity to Use the Infrared Thermography Method for Predictive Maintenance of Hydrostatic Pumps.” Paper presented at the 8th International Conference of Energy and Environment - CIEM, Bucharest, Romania, October 19 -20, 2017.
[3] Mihai, Al. *Infrared Thermography. Basics*/*Termografia în infraroşu*. *Fundamente*. Bucharest, Technical Publishing House, 2005.
[4] Badea, Adrian, Aureliu Leca, et al. *Processes of heat and mass transfer in industrial installations* /*Procese de transfer de căldură și masă în instalațiile industriale*, Bucharest, Technical Publishing House, 1982.
[5] Childs, P. R N.. *Practical Temperature Measurement,* Butterworth Heinemann, 2001: 238-287.
[6] Minkina, W., and S. Dudzik. *Infrared Thermography. Errors and Uncertainties*. John Wiley & Sons, 2009.
[7] Anton, Ioan. *Cavitation*/*Cavitatia*, vol. II. Timisoara, Publishing House of the Academy, 1985.
[8] Sandor, Ianos Bernad. *Hidrodinamica echipamentelor de reglare pentru actionari hidraulice*. Timisoara, Orizonturi Universitare Publishing House, 2005.
[9] Băran, Gheorghe, Ilie Catană, Ioan Magheți, Carmen-Anca Safta, and Mariana Savu. "Controlling the Cavitation Phenomenon of Evolution on a Butterfly Valve.” Paper presented at the 25th IAHR Symposium on Hydraulic Machinery and Systems, Timisoara, Romania, Sept. 20-24, 2010.
[10] ***IMAGINE S.A. *Advanced Modelling and Simulation Environment*, Release 4.3.0 User Manual, Roanne, 2006.

ISSN 1453 – 7303 **"HIDRAULICA" (No. 1/2018)**
Magazine *of Hydraulics, Pneumatics, Tribology, Ecology, Sensorics, Mechatronics*

Theoretical Aspects regarding the Pressure Safety Valves Operation within a Hydraulic Circuit

Assistant professor PhD. Eng. **Fănel Dorel ȘCHEAUA**[1]

[1] "Dunărea de Jos" University of Galați, fanel.scheaua@ugal.ro

Abstract: *Construction and agricultural machinery and equipment drives are currently accomplished by means of high-performance hydraulic and pneumatic systems through which difficult workloads are easily performed. Such systems have evolved over time, being indispensable from the basic functional machinery aggregate. In research-driven development there is a continuous increase in working power based on the increase of working pressure values inside the hydrostatic circuits used. Primary components represented by pumps, motors, distributors need protection during the circuit operation at medium and high pressure values. This overpressure protection is carried out by means of safety valves or pressure valves that are able to send part of the working fluid flow rate to the plant tank adjusting the pressure to a value at which the plant components are able to operate safely. A pressure valve assembly model is shown in this paper with spherical and tapered locking elements which have the possibility to perform translational movement inside the valve body in this way achieving the valve opening when the pressure values in the circuit exceed a certain set value. A numerical analysis of the working fluid flow through the valve body is made and the results are presented in terms of pressure and velocity of the working fluid, depending on the position of the spherical locking element.*

Keywords*: Pressure valve, hydraulic device, fluid flow, three dimensional model, computational fluid dynamics*

1. Introduction

Today, there are many possibilities for machinery and equipments to achieve multiple workloads with high degrees of difficulty. These skills are possible through the intake of hydrostatic drive systems that fit into these machines. Hydraulics and pneumatics are present in most industrial branches with optimal results that have been continuously improved due to the constant upgrading of materials and components used in work circuits.
In hydraulics the working fluids used are greatly improved in terms of viscosity properties providing the moving parts lubrication which reduce the components wear and extend their service life.
Regarding the hydraulic plant primary components quality, improved designs have been acquired in order to ensure optimal operational results within the working circuit (silent operation in the case of pumps and motors, firm commands in the case of distribution and control elements).
The working pressure values have been steadily increased while reaching higher values of hundreds of bars, which means high values of the hydrostatic forces acting on the installation components used in the equipping of machines and equipment.

2. Constructive and functional details for a safety valve model

The construction model corresponding to a pressure valve device is constituted by a body with inward orifices necessary for the circulation of the working fluid between the active branches of the plant and a valve closing/opening element maintained in the closed state by means of a compression spring which ensures the blocking of the circulation fluid flow to the tank if the pressure value is within the parameters for which the system is operating safely. At the moment when the pressure value rises above the value set on the valve (spring elastic force value), the locking piece is moved from the initial locking position by means of the action of hydrostatic forces, at which point the fluid is able to circulate behind the enclosure being directed to the system tank, reducing the momentary pressure value in the system to the initial value.
Once the pressure value has been lowered, the closure element is again moved to the initial position, ensuring the closure of the fluid drainage orifices, which is maintained until a further increase in the system pressure value when the recovery cycle is achieved.

During the operation of the pressure valve inside the hydraulic circuit the hydrostatic pressure forces are considered (F_h), which acts directly on the blocking element part determining a displacement and the discharge opening surface (*A*), enabling the working fluid circulation to the reservoir.

The mechanical work (L_h) performed to move the closure element of a pressure valve is dependent of force and displacement values of the blocking element, for which a fluid volume (*V*) is circulated, which also enters in calculating the amount of energy required along with the momentary pressure value. [1][2]

$$F_h = p \cdot A \tag{1}$$

$$L_h = p \cdot A \cdot s_a \tag{2}$$

$$V = A \cdot s_a \tag{3}$$

$$E = V \cdot p \tag{4}$$

On the other hand the closing piece movement resistances are given by the compression spring elastic force acting directly on the pressure valve locking element keeping it pressed on the seat practiced in the valve body alignment.

The spring force (F_a) is given by the compression spring constant (c_a) and the amount of displacement (s_a) carried out in the event of spring compression due to the action of the hydrostatic forces acting directly on the closure element: [4]

$$F_a = s_a \cdot c_a \tag{5}$$

$$F_a = \frac{G \cdot d_w^4 \cdot s_a}{8 \cdot D_a \cdot n} \tag{6}$$

$$s_a = \frac{8 \cdot D^3 \cdot F_a \cdot n}{d^4 \cdot G} \tag{7}$$

where:

D_a - spring average diameter;

d_w - spring wire diameter;

G – shear modulus;

n - spiral number.

Possible cases for the functioning of pressure control valves are determined by the values of the involved forces. Thus, when the hydrostatic pressure forces are lower than the spring force value the valve remains closed and when the value of the hydrostatic pressure exceeds the value of the spring elastic force, the valve opens and sends a part of the working fluid to the tank, while the momentary pressure peak value of the system is discharged.

$$\begin{cases} F_h < F_a & -\text{Pressure Valve Closed} \\ F_h > F_a & -\text{Pressure Valve Open} \end{cases}$$

The pressure valves used in hydraulic circuits are driven by means of compression arcs and the value of the spring force can be constant or adjustable. The symbolic mode of these valves is shown in Figure 1.

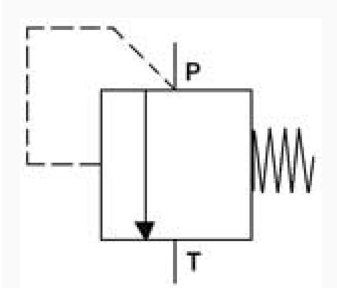

a) pressure valve symbol

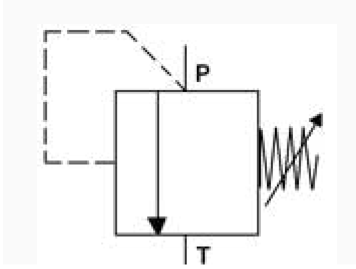

b) adjustable pressure valve

Fig. 1. Pressure valve symbolization

Such pressure valve models are normally closed, being activated only at system high pressure values. If the system does not have such a component mounted, the pressure will greatly increase up to the energy limit of the pumping group and ultimately produce damage to one of the system components (breakdown of the hydraulic ducts, destruction of the distributor, etc).

3. Pressure valve assembly model

An assembly pattern for a pressure safety valve must include the specific elements necessary for operation inside the hydraulic circuit. These components are represented by device body with orifices made for fluid access, the locking spherical or conical piece and the element which achieve and maintain the closed position of the locking piece, which is a compression spring.
A three-dimensional overall model for a pressure valve was made using the Solid Edge V20 program (Figure 2).

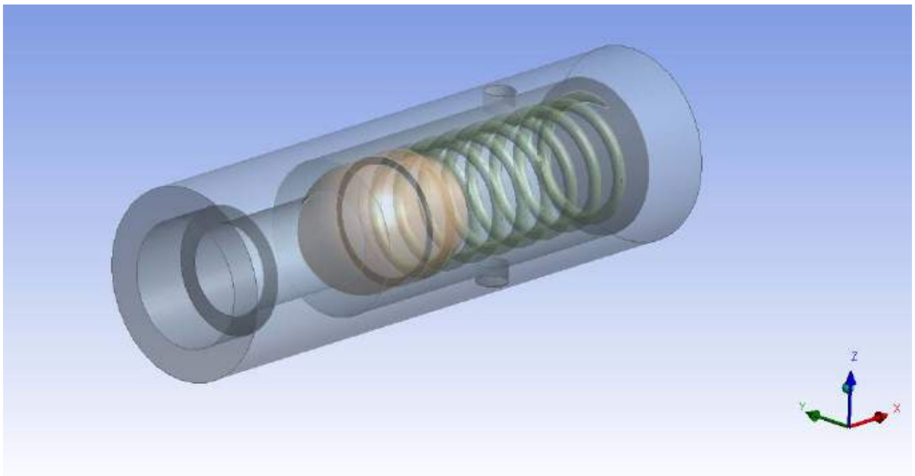

Fig. 2. Pressure valve assembly model

The shown assembly model has the outer dimensions of 30 mm in diameter and 100 mm in height, a main axial orifice for allowing access of working fluid inside the device body of 20 mm diameter, as well as two 5 mm diameter orifices necessary for the working fluid outlet when circulating to the reservoir.
The locking piece is positioned inside the body being connected to the spring that keeps it in contact with the seat (an inner edge of the body). The seating edge of the closure piece has a diameter of 14 mm and the arc contains 8 spirals with a 3 mm diameter.
During operation of the hydraulic system, the pressure valve receives a pressure signal from the circuit branch in which it is mounted. The pressure valve is normally closed and this state depends on the value of the hydrostatic forces acting directly on the spherical part wall, while the possible situations can be presented as follows:

1) Case 1 - when the hydrostatic forces are lower than the elastic spring force the valve remains closed;

2) Case 2 - when the hydrostatic pressure forces exceed the value of the elastic force in the spring the valve opens by moving the spherical piece in the axial direction.

4. Fluid flow analysis on the pressure valve assembly virtual model

Having pressure valve three-dimensional assembly model available, an analysis of the working fluid flow through the valve body is carried out corresponding to the moment in which the spherical piece is displaced on the axial direction, which allows the fluid access in the chamber behind the spherical piece and the circulation to the two outlet circular openings. This displacement corresponds to the moment when the valve is opened by the pressure forces acting directly on the spherical part wall and compression force on the spring.
Flow analysis is performed using the ANSYS CFX program, a fluid analysis dedicated program. The working fluid is a mineral oil with a density of 900 kg/m^3, and a kinematic viscosity of 33.4 cSt at $40^O C$.

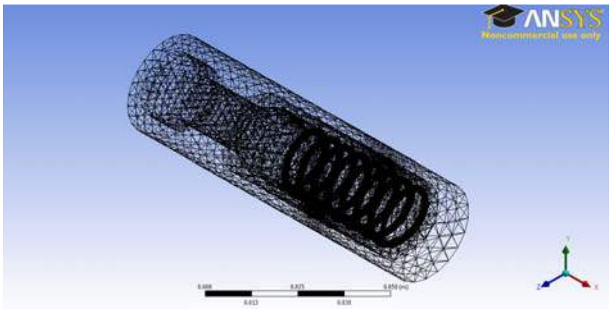

a) mesh network with triangular shaped elements

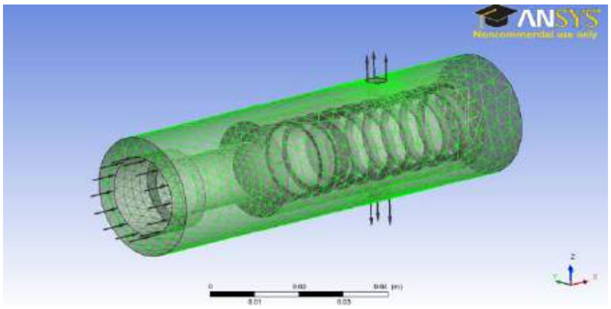

b) pressure valve body– solid domain

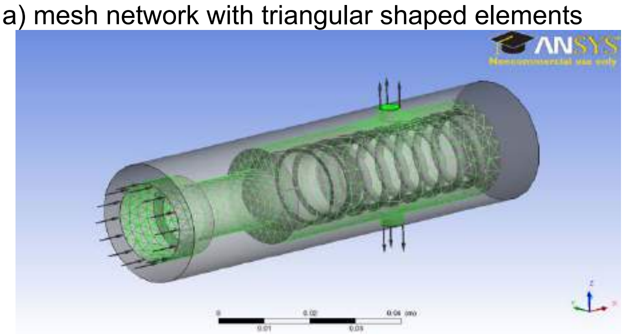

c) fluid domain

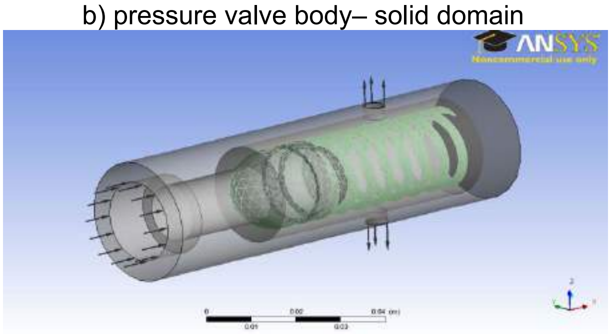

d) blocking element (spherical piece with compression spring) – immersed solid

Fig. 3. Fluid flow analysis domain details

The fluid flow analysis domains represented by the valve body assembly are established, the solid range being steel, valve fluid domain positioned inside the body and the closure element with spring form together a solid domain (steel material) submerged in the volume of the fluid, as shown in Figure 3.
The fluid flow analysis is of transient type which describes better the pressure valve assembly operation on a finite period of 1 second operation time in 0.2 seconds steps. Thus, on the fluid domain having a reference pressure value of 150 bar, the three orifices ports as one inlet (20 mm diameter) and two outlets (diameter 5 mm each) are defined. At the inlet the fluid has the possibility of movement with a velocity of up to 8 m/sec. For the spherical blocking piece has been declared an axial directional movement with a translational velocity of 5 mm/sec.
The results are presented in terms of pressure and velocity of the working fluid calculated at the analyzed fluid region (Figure 4).

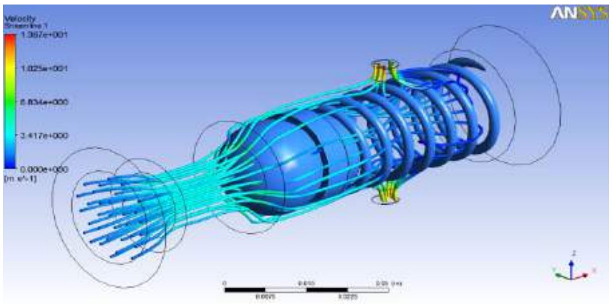

a) path-lines for fluid velocity values

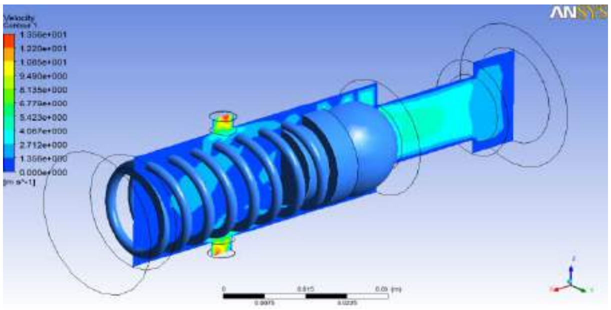

b) fluid velocity values on XZ plane contour

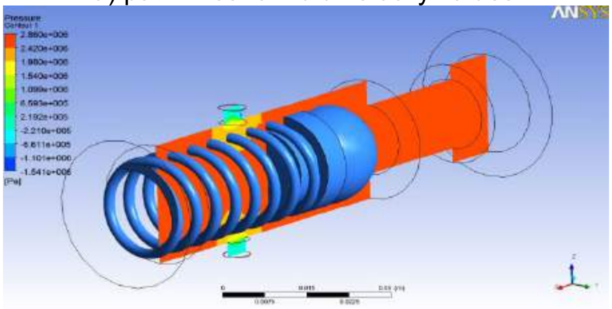

c) static pressure values on XZ plane contour

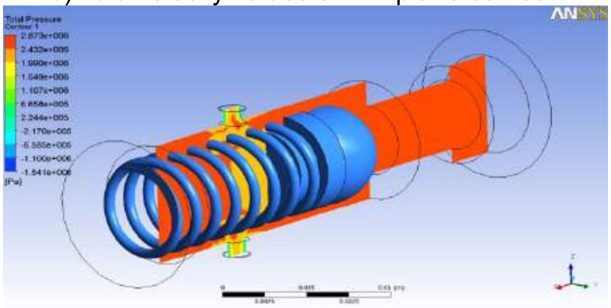

d) total pressure values on XZ plane contour

Fig. 4. Fluid flow analysis results

Based on the results shown in Figure 4, it can be observed the working fluid flow model inside the pressure valve body when axial movement of the locking element is performed. The values for the fluid circulation velocity are appropriate for the analyzed fluid areas, with large values being recorded at the pressure valve exit ports. The static and total pressure values are comparable, with higher general values recorded for the main fluid region and lower values recorded on small regions at the outlet openings.

The fluid flow analysis was performed taking into account the total working time divided by several working steps.

In order to highlight the results for the working fluid circulation velocity and pressure are presented three representative analysis steps that coincide with the start of the locking device movement from the initial position to the maximum stroke.

The results obtained on the analysis work steps reveals the higher pressure values when the locking piece is in the closed position and gradually according with the axial displacement lower values are recorded. Circulation velocity are rising towards the exit ports where the maximum values are recorded as the working fluid flow through reduced outlet orifices in this fluid region.

The diagrams corresponding to the values obtained from the analysis for the three steps are shown in Table 1.

Table 1: Result diagrams for fluid velocity and pressure

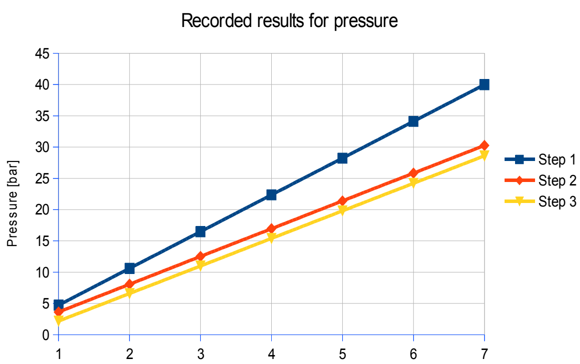

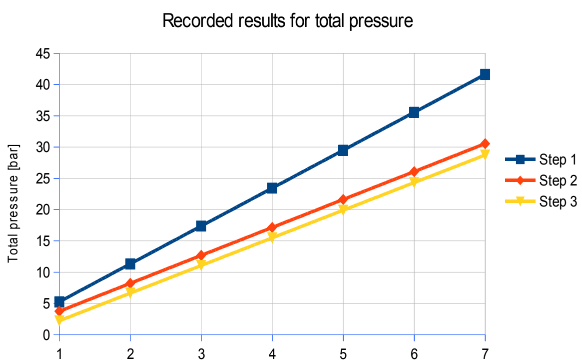

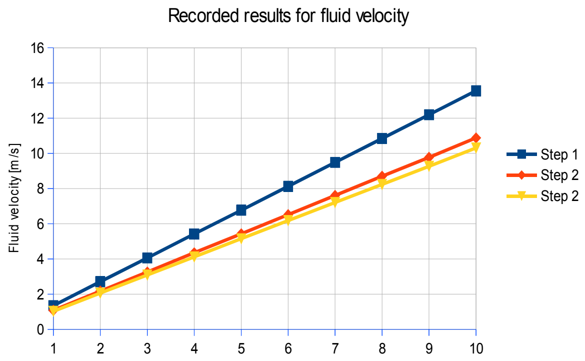

The pressure signal that performs the displacement of the locking piece, initially in a closed position, is taken from the main circuit powered by the plant pump. It is the compression spring constant that determines the adjusted value of the pressure required to open the pressure valve. Also, such pressure valves models benefit from the adjusting system, needed for adjusting the pressure value at which the valve can be opened and for higher circulation fluid flow rates, constructive models with pilot are used.

The pressure valves are used in circuits at pressure values in the range of 315-630 bar and fluid flow rates of 80-330 l/min but piloted constructions are capable to circulate higher flow rates values of up to 650 l/min.

5. Conclusions

A direct-operated pressure valve model has been presented in this paper, highlighting the constructive and functional principle.

The assembly model was analyzed with the Ansys CFX program in order to highlight the fluid flow dynamics through the valve body.

The results are presented in terms of velocity and pressure of the working fluid, taking into account the total movement of the locking piece over the total analysis time.

Specific velocity and pressure values are recorded corresponding to the relative positions between the locking piece and the valve body, depending on the surface area created between the locking member and the valve body as a result of the gradual displacement.

References

[1] Axinti, Adrian Sorin and Fănel Dorel Șcheaua. *Introduction to Industrial Hydraulics/Introducere în hidraulica industrială*. Galati, Galati University Press, 2015, ISBN 978-606-696-032-8.

[2] Axinti, Gavril and Adrian Sorin Axinti. *Fluid Power Systems/Acţionări hidraulice şi pneumatice*, Vol I-V. Chişinău, Tehnica-Info Publishing House, 2008-2012.

[3] Șcheaua, Fănel Dorel. „Functional description of a hydraulic throttle valve operating inside a hydraulic circuit." *Hidraulica - Magazine of Hydraulics, Pneumatics, Tribology, Ecology, Sensorics, Mechatronics*, ISSN 1453 – 7303, no. 1 (March 2016): 47-50.

[4] https://www.hennlich.ro/fileadmin/_migrated/ro_arc_compresiune.pdf.

From Human-Environment Interaction to Environmental Informatics (I): Theoretical and Practical Implications of Knowledge-Based Computing

PhD stud. **Bogdan CIORUȚA**[1], Assoc. Prof. eng. **Mirela COMAN**[2], Stud. **Alin-Andrei CIORUȚA**[3], Stud. **Alexandru LAURAN**[2]

[1]Technical University of Cluj-Napoca - North University Centre of Baia Mare, Office of Information and Communication, 62A Victor Babeș str., 430083, Baia Mare; bogdan.cioruta@staff.utcluj.ro
[2]Technical University of Cluj-Napoca - North University Centre of Baia Mare, Faculty of Engineering, 62A Victor Babeș str., 430083, Baia Mare; comanmirela2000@yahoo.com **|** alexandru.lauran@cunbm.utcluj.ro
[3]Technical University of Cluj-Napoca - North University Centre of Baia Mare, Faculty of Science, 76 Victoriei str., 430122, Baia Mare; aciorutza02@gmail.com

Abstract: *During recent decades the stirring up of the processes of globalization, practically in all spheres of present day civilization, has aggravated the society and brought numerous problems resulting from human-environment interactions. To overcome these problems, it is necessary to develop and adopt new concepts and techniques to manage the changes occurring on the Earth's ecosystem. For this, application of information and communication technology via Environmental Information Systems (EISs) - as integrated part of Environmental Informatics (EI) - is the best option. This paper deals with new and interactive approach to process, analysis and synthesis of environmental systems using various IT applications, so we could underline that environmental science and technology are therefore a vital component of productive knowledge and thus a high priority for the mankind sustainable fraternity with nature.*

Keywords: *Human-Environment interaction, IT&C applications, Environmental Information Systems*

1. Introduction

During recent decades the stirring up of the processes of globalization, practically in all spheres of society (as presented in Fig. 1), has aggravated and brought numerous problems resulting from *Human-Environment Interactions* (HEI). To overcome these problems, it is necessary to develop and adopt new concepts and techniques to study, understand, evaluate and manage the changes occurring on the Earth's ecosystem [1, 2].

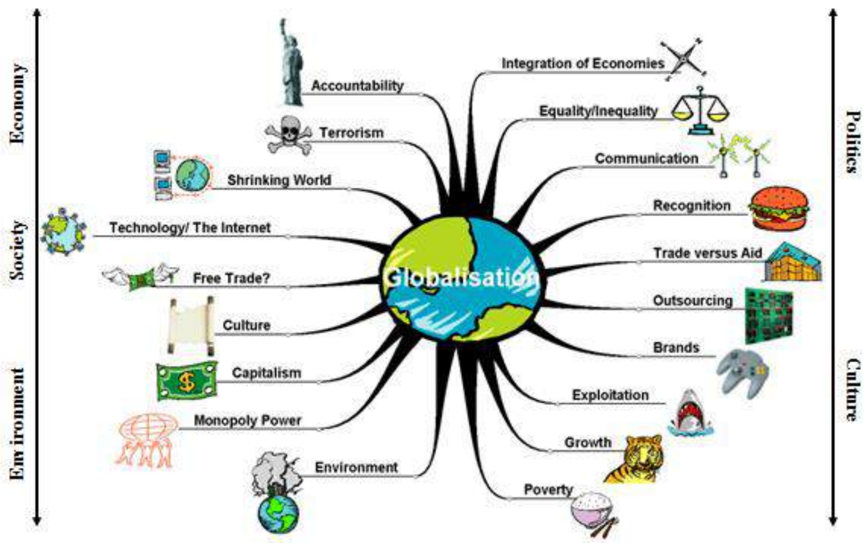

Fig. 1. Contemporary globalization - conceptual determinations [2]

For this, application of information and communication technology (IT&C) via *Environmental Information Systems* (EISs) - as integrated part of *Environmental Informatics* (EI) - is the best option; much more, understanding this complexity through interactive applications will develop new strategies and ideas to manage and protect ecosystem's values [1, 3].

Ever since "the environment" gained its place in the public international and national agenda (environmental legislation, sustainable development or disaster and hazard management), as well as in the globalization context (Fig. 2), it has been bundled with *data*, *information*, *knowledge* and *information systems* [3, 4, 24]; *Environmental Monitoring Systems* (EMSs), *Environmental Monitoring and Analyzing Systems* (EMASs) and especially *Environmental Information Systems* (EISs) [20, 21] are integrated part of *Environmental Informatics* (EI) platform [3, 4, 22-24].

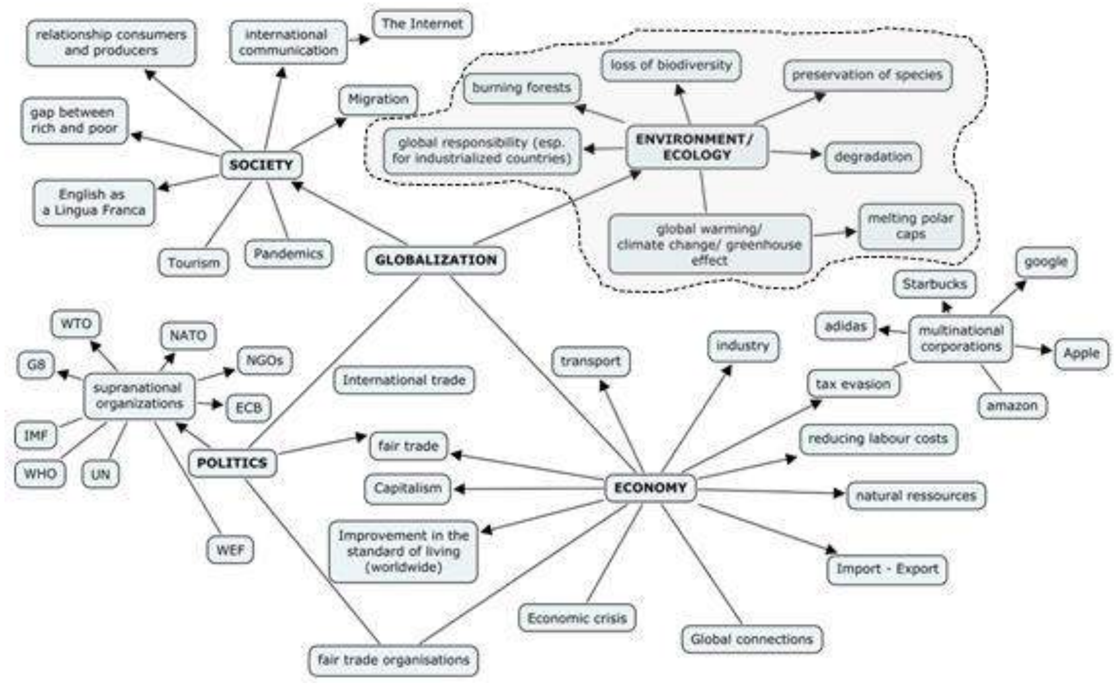

Fig. 2. Contemporary globalization - by reference to Human-Environment Interactions [3]

As we speak the area of Environmental Informatics (EI) is becoming more complex due to the current context and trend of making the EISs available to the public and end-users access (Fig. 3); this phenomena is based on the assumption that public and environmental information end-users awareness, participation and acting is improved by the rate of access to the environmental information to solve the complex problematic covered by the research, engineering and environmental protection fields; in this sense, Environmental Informatics (EI) plays a major role in environmental protection, planning, management and, of course, decision making [4]

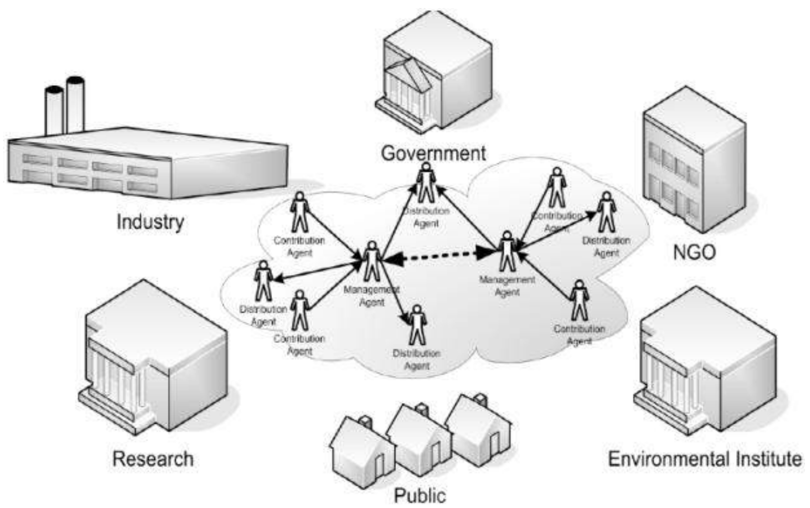

Fig. 3. General perspective according the environmental informatics societies: the main actors interested and involved in Environmental Informatics issues [4, 17]

The communication triangle of *Human-Computer-Environment interaction* (Fig. 4) - presenting the explicit and implicit types of communication - shows that the communication is possible on all levels, between each pair of the involved entities: *human* (users), *computer* (computing devices) and *environment* (context).

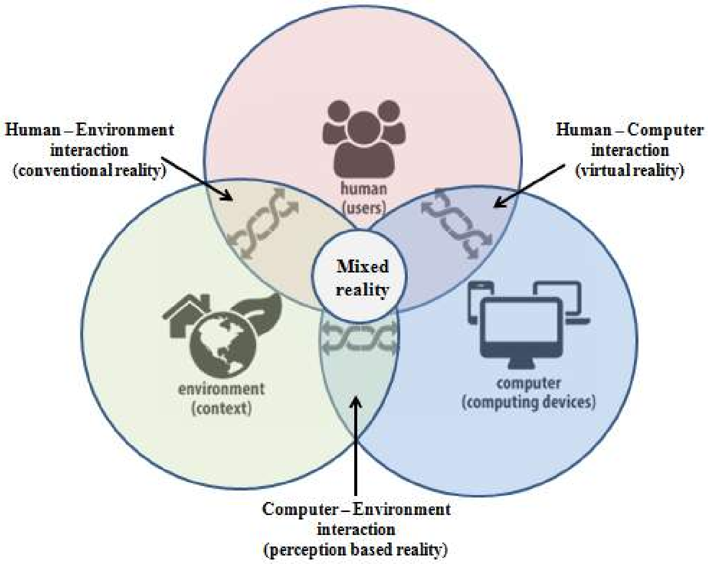

Fig. 4. The communication / existential reality triangle of Human-Computer-Environment interaction

Fields concerned with some aspect of this interaction triangle are, but not limited to, as follows:

- *Intelligent User Interfaces (IUI)* - aim to improve the efficiency, effectiveness, and naturalness of human-machine interaction by representing, reasoning, and acting on models of the user, domain, task, discourse, and media (e.g., graphics, natural language, gesture); as a onsequence, this interdisciplinary area draws upon research in and lies at the intersection of human-computer interaction, ergonomics, cognitive science, and artificial intelligence and its subareas [5];
- *Ubiquitous Computing (UBICOMP)* - is the method of enhancing computer use by making many computers available throughout the physical environment, but making them effectively invisible to the user [6];
- *Pervasive Computing* - can be a portal into an application-data space, by which a user performs a task, not software written to exploit a device's capabilities [7];
- *Physical Computing* - in the broadest sense, means building interactive physical systems by the use of software and hardware that can sense and respond to the analog world;
- *Ambient Intelligence* (AmI) - is about sensitive, adaptive electronic environments that respond to the actions of persons and objects and cater for their needs, this approach includes the entire environment and associates it with human interaction - being the way for us to re-immerse ourselves in life, and not in technology;
- *Everyware* - show us that all information we now look to our phones or web browsers to provide becomes accessible from just about anywhere, at any time and this is delivered in a manner appropriate to our location and context [8];
- *Internet of things (IoT)* - show us that the pervasive presence around us of a variety of things or objects which, through unique addressing schemes, are able to interact with each other and cooperate with their neighbours to reach common goals [9].

This paper suggest new and interactive approach to process, analysis and synthesis of environmental issues using various IT&C applications, so we could underline that environmental science and technology are therefore a vital component of productive knowledge and thus a high priority for the mankind sustainable fraternity with nature. Since years, environmental scientists and computer experts are working on different and innovative computer-based modeling techniques to study the environmental problematic and hazards system and to provide the maximum accuracy in decision making or in elaborating sustainable strategies of community development [3].

Specialists working in the environment protection and engineering or related fields (agriculture, horticulture, forestry, zootechnics, landscape architecture) [10] need a great deal of information and knowledge at each stage of the management and assessment of environmental processes if they want the functioning of society and, implicitly, the economy to be in line with the principles of sustainable development and in favor of a healthy environment; also, for the preparation of a project and its implementation, they must know and understand, after a systematic analysis, the conditions under which these processes are carried out [3, 17].
The analysis carried out should be based on the best available data, methods and techniques and on the acquired knowledge, experience or expertise from other specialists [10]. Traditionally, this information and knowledge is obtained according to the requirements of the moment, through direct access to databases, reports and documents, by transferring information and knowledge among specialists (managers, practitioners, researchers) and by contacts established during the training sessions, workshops, congresses, conferences and symposiums (Fig. 5) [3, 16, 17].

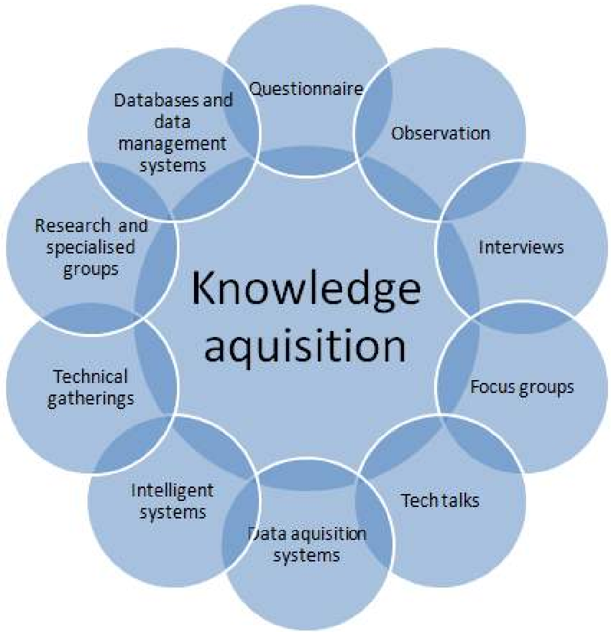

Fig. 5. Different knowledge acquiring techniques specific to environmental management

In order to improve environmental management and assessment capacities, it is necessary for the specialists concerned to be able to manage and implement the concepts of effective and efficient assessment of environmental components and conditions, that can be achieved through environmental information software via EI applications; they also need to have simple and effective access to updated knowledge, in order to be able to take the best decisions, to shape sustainable development strategies, policies and actions for both developed and emerging economies.

2. Regarding ocurrences of environmental information culture

2.1 Documentary information and current society

Lately, as a result of the facilities offered by the new information and communication technologies in all sectors of society and in all aspects of the activities carried out [12, 16], expressions such as the *information society*, *informational era*, *communication society* were imposed, to designate, in fact, a new existential reality - mixed reality (as presented in Fig. 4) [17].
In today's society, defined by this new reality, the success and survival of many businesses, institutions, or people with political or social responsibilities depend on their ability to locate, analyze and use information resources efficiently and intelligently; in fact, the effectiveness to which it refers is intimately linked to the achievement of the proposed goals of documentation, information and knowledge, as well as the existence of concrete situations of making a particular decision, optimizing processes or applying different methodologies [3, 16].

The competence of any kind of individuals is given by the ability to search, retrieve, evaluate, use and understand fully the information resources, regardless of their support and presentation form. In this sense, the new information and communication technologies, which are in the process of developing, through the contribution of knowledge, have led to overcoming and dismantling the separating barriers - the time and space are no longer insurmountable obstacles to communication and relationship - as references to the Super Smart Society, composed by Information, Knowledge and Consciousness Society (Fig. 6) [3, 4, 12-14].

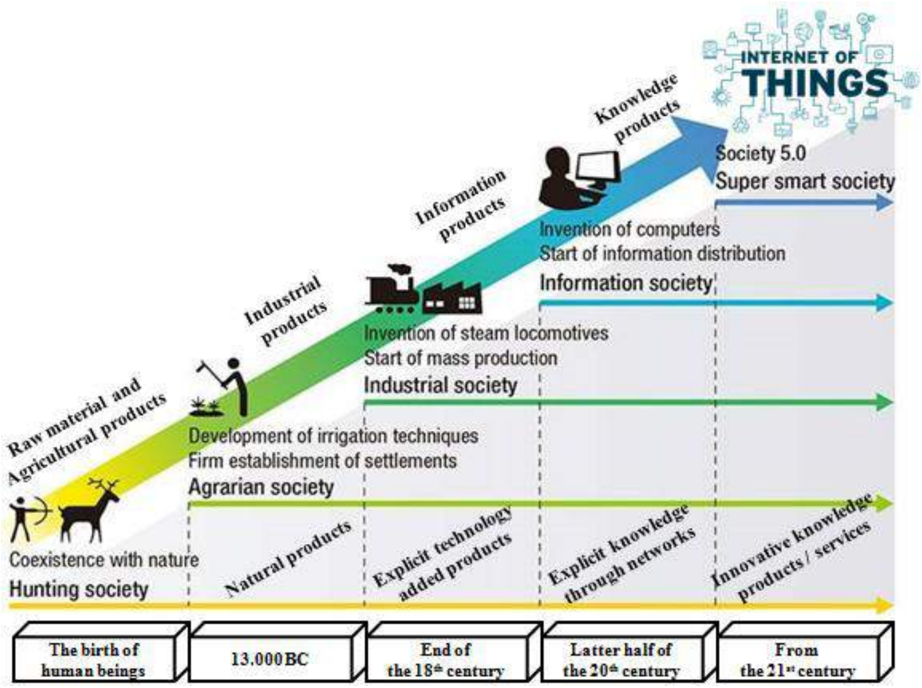

Fig. 6. Evolution of societies from the Hunting Society to Super Smart Society

In line with the extraordinary development of means of access to information, documentary training is at the heart of the global movement of forming an "information culture" irrespective of the field of interest. Documentary training, even the one specific to environmental sciences and individuals closely involved in this vast field, aims at the use and understanding of information and documentation tools and techniques in relation to the principles of sustainable development.
In addition, documentary training was defined as "the acquisition of documentation gathering techniques, integrated into a set of research procedures"; thus, documentary training is regarded as an element of the general research methodology, which includes cognitive and processing and communication activities - dissemination of information elements of interest to the user [12, 15].

2.2 Documentary information as a preoccupation of the university environment

The practice of collecting documents of any kind in collections and further research of their content has existed for a very long time and is regarded as an almost natural appropriation of humanity in its path to the formation of a culture (Fig. 7). The 20th century scientific evolution and the need for information from the 21st century have imposed information and documentation as an independent research area, which has pushed the human will to the frontiers of knowledge as far as possible and has generated an extraordinary documentary mass [12].
New technologies facilitate intimate, direct and immediate proximity to user information without the need for other mediation systems; moreover, because of the particular needs of information needed at a certain point in time, the user has to prove the knowledge of the specific information and documentation methods and techniques, which implies the existence of the formation of an informational culture. The acquisition of knowledge specific to new information and communication technologies expressively grafted on the information culture of each individual is in an effervescent process of development and restructuring as a result of various research environments, one of the most striking, far from being the university [2, 3].

The university environment is the space where the changes generated by New Informatics and Communication Technologies are felt with extraordinary force and represent at the same time the space where the most information needs intersect and the most diversified areas of interest are quantified. The university, equally educated, but also research oriented, is open to all the novelties, ready to assimilate the recent research results, but also to propose and promote new alternatives of knowledge, which is why for such a medium documentary training becomes indispensable [12].

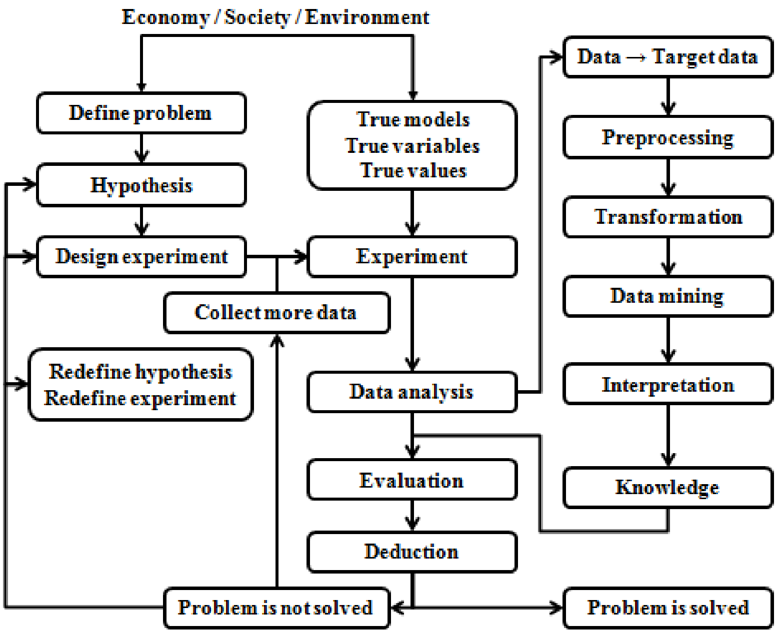

Fig. 7. Specific steps for obtaining environmental information and developing EISs [1, 11]

The educational process specific to the university, for example, is based on three pillars:

- passing the knowledge from the teacher to the student;
- observation and practical-applicative experiments;
- acquiring knowledge by consulting written or electronic documents.

Information and telecommunication technologies have produced unprecedented changes in society in all its aspects, comparable to the transformations produced by the invention and the wide use of printing; tending towards a transformation of the economic life, of the social life and implicitly a cultural transformation, mentality and, last but not least, the everyday life of each individual, the information mediated by the new information technologies penetrated and directs, with or without our will, activities in the universe of each.

The amount of information, the variety of forms of expression, the diversity of tools and information mediation technologies have produced major changes in people's way of communicating, learning, doing business, solving various problems, and reporting to peers and environment. The university environment, through education at all levels, must under these circumstances provide students with information literacy, an informational culture and the skills needed to use information resources, in order to further support the framework of the Society of Consciousness [13, 14].

One of the modern trends in the educational process in general and the environmental protection and engineering in particular is to approach the training of future environmental specialists on the basis of the legal system and policies specific to the field so that future specialists can make decisions and take actions based on their own knowledge and experience [15]. To improve environmental management and assessment capacities, specialists need to be able to manage and implement effective and efficient environmental assessment concepts that can be achieved through environmental information software. Under these conditions, information technology is a fundamental support for all components of fundamental scientific and applied scientific research in the field of environmental protection, being used for numerical simulation of complex interdisciplinary processes, for supervising and conducting experimental processes in laboratory installations, as well as in all applications in the field of environmental information transmission.

3. Environmental Informatics as a result of the info-environment culture

Environmental Informatics is a new research field, which is constantly developing within the wider framework of the confluence of environmental sciences and applied informatics, based on the application of IT&C to environment-specific issues closely studied by specialists [19]. Environmental Informatics applies methods and technologies for the collection, analysis, interpretation, dissemination and use of environmental information. It also includes a broad range of tools that can be used in conjunction to understand environmental issues: *Artificial Intelligence*, *Neural Networks*, *Geographic Information Systems* (Fig. 8), *Global Positioning Systems*, *Remote Sensing*, *Surveillance and Mapping Services*, *data storage* (data banks), *software engineering*, *mobile technology* and *the internet* [3, 16].

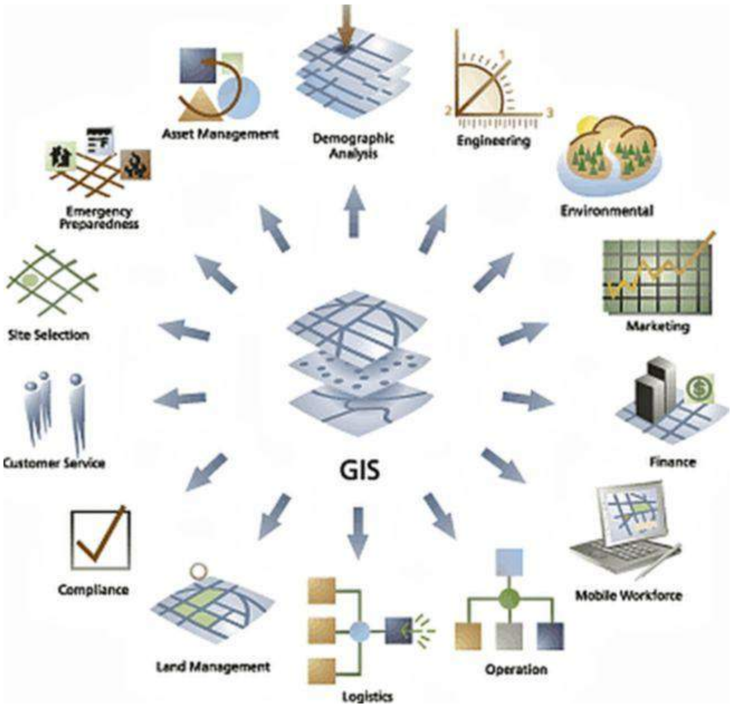

Fig. 8. Geographic Information Systems tools used to understand environmental issues [3, 18]

In Romania, although the activities that want to emphasize the bending towards the subject of environmental informatics are only in the beginning, there is some interest in alignment with the international standards in the field. Thus, a Laboratory of Environmental Informatics was set up at the Faculty of Power Engineering of the Polytechnic University of Bucharest and in the same sense it was acquired the most efficient computing system in Southeastern Europe at that time at West University of Timisoara, where an Institute for Advanced Environmental Research is being created; all this is dedicated to integrating IT&C applications for understanding and possible resolving environmental issues at national level [3]. As far as problems are concerned, they can be at any time or space scale, depending on this, their treatment is based on computational reasoning, mathematical modeling or monitoring, to ensure and allow a better understanding [3].
The main goal of the Institute for Advanced Environmental Research in Timisoara is to create a strategic research infrastructure, of excellence, at international standards that:

- to focus and develop the existing research potential in research centers;
- allow research to be addressed in an inclusive and multidisciplinary manner;
- ensure, through space, adequate endowment and training, international competitiveness and visibility of research results by members of the academic community;
- to contribute to the stimulation of technology transfer based on cooperation between the research institute and the productive enterprises;
- to support and participate in the development of poles of excellence focusing on technological science and environmental research via different IT&C tools (Fig. 9).

It is also intended, as an estimated strategic outcome, to meet the following requirements related to the integration of project research results from major areas of academic activity and scientific research [15, 16]: *environmental science* (geology, geophysics, meteorology etc); *chemistry* (environmental chemistry, biochemistry, biotechnology, enzymology, technological chemistry, analytical chemistry etc); *biology* (ecology, ethology, biomonitoring, ecotoxicology etc); *physics* (environmental physics, biophysics, bioinformatics, solid body physics etc); *mathematics* (mathematical modeling, biostatistics, applied mathematics etc); *computer science* (Fig. 9) (artificial intelligence, parallel and distributed computing, computational mathematics, bioinformatics etc) and *socio-human sciences* (bioeconomy, sustainable spatial planning, ecotourism and marketing, environmental management), which will then provide optimal channels for transfer to the effective beneficiaries - economic and institutional actors (Fig. 4).

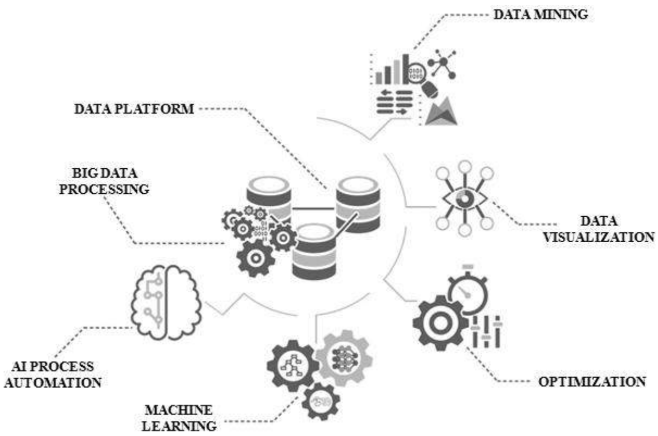

Fig. 9. A broad range of IT&C tools used to understand environmental issues

The research carried out within the Environmental Informatics Laboratory focuses on the implementation of information and communication technology in the field of environmental monitoring and evaluation and the determination of its impact on the health of the population; have as their main objective the application of new, innovative approaches to solving specific problems by focusing on the use of environmental information systems (Fig. 10).

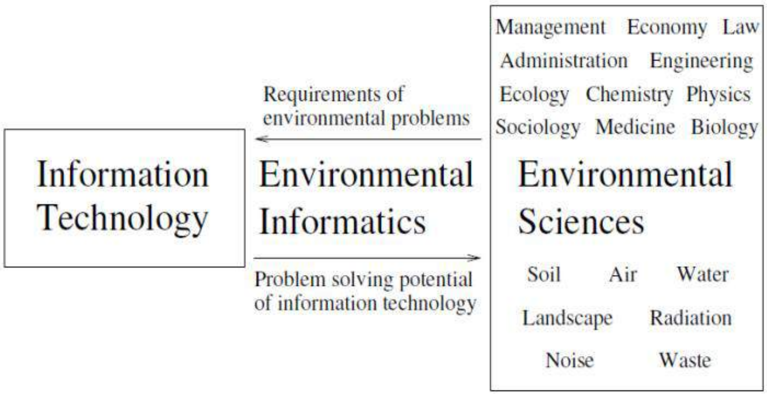

Fig. 10. Environmental Informatics - a bridge-science between IT&C and Environmental sciences [3, 17, 18]

The research team serving the laboratory must be specialized in: *monitoring of environmental factors* - water, air, soil, biodiversity; *use of automatic data acquisition systems* to monitor environmental factors, previously specified; *process management* with the help of industrial computers and programs for this purpose; *implementation of innovative systems* in environmental applications; *development and management of environmental databases*; *use of geographic information systems* for the collection, processing, analysis and visualization of environmental data, information and knowledge; *performing statistical analyzes* and creating databases, and *environmental knowledge management*.

The support of the research activity carried out within the Environmental Informatics Laboratory is the modern endowment with hardware and software, which allows the efficient approach of any research topic. A significant variety of environmental research themes have been addressed so far, most of them being framed and being oriented in several directions, among which we can mention:

- *integrated environmental monitoring* and *pollution control*, which is the basic instrument of environmental decision support systems, both for the recording of environmental changes and especially for understanding and defining the causes of these changes;
- *the use of Geographic Information Systems* (GIS) to monitor environmental factors has become an essential tool in understanding the process of global environmental change;
- *environmental data base management* is defined as one of the fundamental elements that generate and control environmental information flows.

Addressing issues specific to environmental protection, environmental management and research in this area is based, exclusively at least in the last period, on the effective use of environmentall information; this information, collected in different ways and from different sources (Fig. 5), can take the form of biological, physical, chemical, geological, meteorological information. Environmental data, as the first phase of knowledge in the field, describe the status and dynamics of the environment at a given time and for a particular area, and are commonly organized in technical, temporal and space databases or databases covering virtually all environmental domains. By appropriate management, the latter can meet waste, noise and vibration requirements, hazardous substances and products, fauna and flora quality.

Environmental problems which imply one or more decisional steps are more common in engineering and environment protection areas of expertise, and especially common in durable development strategies on a local level [3]. Developing the mathematical apparatus specific to financial and managerial mathematics and more specifically greater use of computers have made scientists take on the decisional problem on a more advanced manner; optimal decision making and optimising took as refference an objective, computational mathematics and technology focused way using this knowledge towards modern techniques regarding inventorying charting and management approaches.

Distribution of information and knowledge over the internet must be in close collaboration with intense preocupation regarding natural resources available for human need satisfaction. Rational allocation of those resources imposes politically influenced decisions but rationally fundamented on scientific needs and opinions and orchestrated by acess towards such scientific knowledge; the decisional support for durable development of communities is given by EISs. With help from Environment Informatics the efficency of identification of new solutions for problem solving regarding environment is greatly enhanced, end users being provided with higher levels of acess to information and so they can develop and maintain an environmental informational culture [3]. We are setting the premises of efficient training in environmental research, based on complete analysis of environment specific issues ,knowing up to date technologies and generating decisions in regards with the personnel needs and specific situations found in field research.

Environment represents the essential foundation of human existence, being the result of human made and natural elements interacting with each other; all of those factor into conditions of existance of society and development prepositions of the before mentioned society. Taking this into consideration, environment protection is a public priority which targets obtaining and mantaining a healthy environment, conservation of resources in concordance with durable development requirements. Fulfilling those objectives neccesitates a raising in levels of education and conciousness among population, in regards to globalisation of information in society which creates a need for producing and for utilisation of information coroborated with knowledge gaining regardless of field of expertise.

Knowledge is meaningful information and information that drives to action, in regards of decision making being influenced by knowledge and sharing of such knowledge among interest groups.

Informational society based on knowledge means more than inevitable progress of technology and IT&C contextualised in the so called new economy based on intellectual dependent activities that characterise an advanced society. Considering this approach, Informational and Knowledge Societies include a series of multilateral developed sub-societies which cover the following dimensions [13, 14]:

- *social* - applies to healthcare and social security, social democracy (e-Health systems, remote workflow systems, remote ensurance systems etc);
- *educational* - develops competences regarding concieving and working in fully informatical workspaces, intelligent management of work-processes (e-learning, virtual libraries etc);
- *ambiental* - with impact on environmental research and protection;
- *cultural* - with impact on developing and maintaining the cultural wealth of a community, and its industrial developments, (online museums and art galleries, digitalisation of coursebooks, international and local cultural wealth digitalisation etc);
- *economic* - develops new approaches to digital economy and knowledge-based economy (e-Commerce, e-Banking, e-Learning, e-Currencies, e-Trading, online payments etc).

First steps into the knowledge society are triggered by a minimal number of technological vectors. We take into consideration the following technological vectors for both the informational and knowledge-based societies [3, 13, 14]: *extended interconnectivity* by geographical extension of bandwith transsmision up to all reachable areas of the globe, taking into it every household, company, and individual; *e-book technologies*; *intelligent agents* which are specialised systems with artificial intelligence implementations embedded in them, used for data mining, intelligent agents will be used for defining most of the technological vectors; *informatised environment* and *nanoelectronics*, which will become the main physical support for processing information.
Analysis methods play a significant role in adding to the environment knowledge base taking into consideration the significant amount of data measurable and measured, amount which is in continuous growth and adaptive to user requests (Fig. 11). Major fields of environmental research which converge towards assuring knowledge neccessary are environmental informatics and statistics. Such fields of research undertake different and multiple variations regarded to informatics providing different systems to analyse specific environmental data.

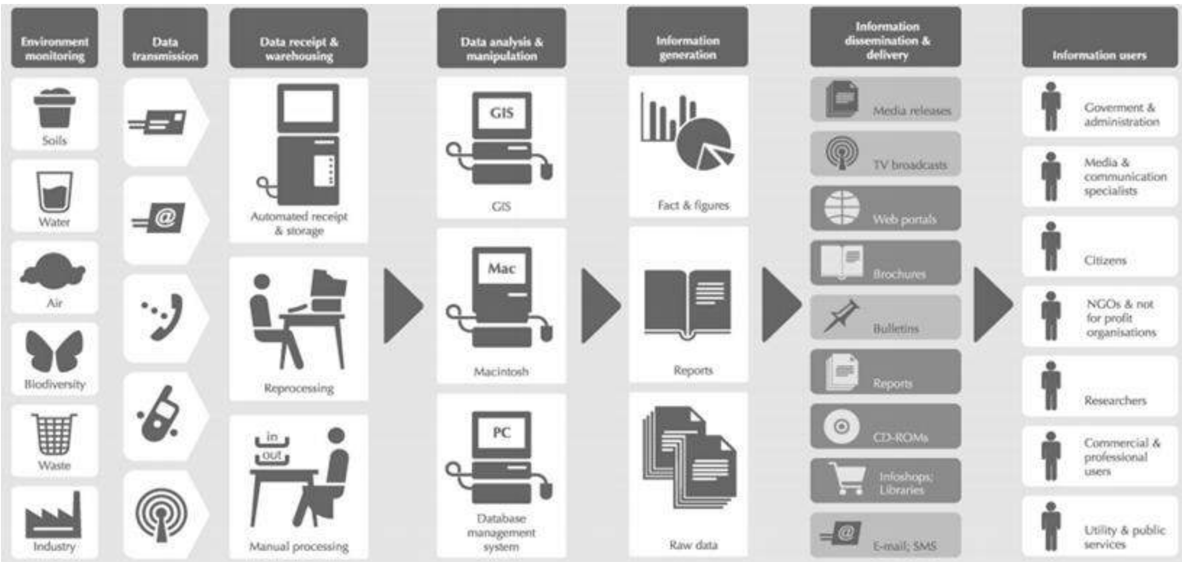

Fig. 11. Schematic diagram for a "complete" Environmental Information System [3, 17, 25]

In contemporary society social, cultural, economic and ecologic dynamics are on of the dominant constants of the 21st century; such transformations of society represent challenges that humankind and its academic structure are called to take on and manage accordingly. The answers to those requirements worked towards changing educational priorities, by going from manually operating the data to automatically operating the data with help from environment softwares.
The use of computers in schools and universities and educational software in the teaching-learning-evaluation process is the solution provided by the informational educational system for the progress of society and environmental protection. The possibilities of processing the collected data from the field and the ones with the help of specific computer environments come together with the traditional teaching and acquiring knowledge system to identify the student motivational resources needed to manage the daily challenges and problems of the environment.

As a result of the "environmental informatics" learning system (Fig. 11) [20-24], which has a solid theoretical base and depending on the version of the environmental software, several research sub-domains are detached, of which we review the following [3]:

- *bioinformatics* - involves the application of IT&C in the field of biology and medicine; is based on specific algorithms, databases, web technologies, artificial intelligence, applications dedicated to the exploitation of biological data, image processing, modeling and simulation of various processes, as well as biostatistics concepts etc.
- *chemioinformatics* - is a mixture of information resources from two different fields of computer science and chemistry, which encompass many of the applications that currently underlie chemical engineering and modern genetics.
- *geoinformatics* - addresses geoscience related issues and related branches of geological engineering, including cartography, geodesy, GIS, photogrammetry, remote sensing etc.
- *hydroinformatics* - has a strong interest in using techniques stemming from artificial intelligence and recognizes the social nature of water management issues.
- *ecoinformatics* - defined as discipline and self-standing science, outlined by the integration of mathematical applications, computer science, statistical and engineering sciences for ecosystem research and management, is an increasingly evolving area.

4. Conclusions

The environment is the essential framework of human existence, being the result of the interaction between natural elements and elements resulting from human activity; all of these influence the existence conditions of society and its development possibilities. As a result, the protection of the environment is a public priority aiming at achieving a healthy environment and the preservation of natural resources, in line with the requirements of sustainable economy and social development. Achieving these goals requires raising the level of education and awareness of the population, as part of the global computerization of today's society. Computer technologies are currently the support of all fundamental and applied scientific research components in the field of environmental protection, being used for numerical simulation of complex interdisciplinary processes, for monitoring and conducting experimental processes in laboratory installations, as well as for all applications in the field of information processing and transmission environmental specific.

It is also of greather importance that the communication and relationship, as well as knowledge and awareness - as contextual references of the Information Society, Knowledge Society and Society of Constitution - are to be supported by the idea and the merits that they can bring the altar of science information systems for the collection, processing and dissemination of environmental information. As an integral part of environmental informatics, the computer systems in question come to outline, in the most direct way possible, to associate and complement the cognitive apparatus of users with new aspects of the environmental information culture that is indispensable for the outcome of the educational act itself.

Nowadays, IT&C systems have a well-defined place in all areas of activity: production, service provision, management, monitoring, research, public involvement in decision-making and in almost all states of the world. Environmental Information Systems become mandatory environmental science tools and can be defined as a collection of packet data and information, described by a number of specific indicators relevant for the study, monitoring and exploration of the environment. Every decade brings new problems, but also new applications in the field of environmental protection, SIM being more involved in the foresight activity, selecting a development alternative, diminishing possible and / or real negative effects.

As a conclusion, it can be said that modern data analysis methods are useful tools in environmental informatics and environmental statistics. Good methods are understandable for the environmental scientists and at the same time reliable, robust and helpful for discovering important relationships in the data. In cooperation between environmental and information scientists, what takes the relationship flourish is the knowledge of both sides about their field and efficient communication concerning the specific needs of a certain problem, and the properties of the methods. Without these ingredients, the results of cooperation projects may not be satisfactory.

References

[1] Cioruța, Bogdan, Mirela Coman, and Andrei-Alin Cioruța. "Studying Environmental Problematics and Hazards with help of Informatics Applications (SEPHIA)". International Conference Scientific Research and Education in the Air Force (AFASES®), Braşov, Romania, May 22-24, 2014: 289-292.
[2] Tănăsescu, Dorina, Felicia Dumitru, and Georgiana Dincă. *The role of the international organisms in the globalization process*, in Cuadra-Montiel, Hector. *Business, management and economics: globalization - approaches to diversity*, InTech open acces books, 2012.
[3] Cioruța, Bogdan. *Contributions on environmental informatics: research and experimental themes* („Contribuții privind informatica mediului: cercetări și teme experimentale") - bachelor degree paper, TUCN-NUCBM, 2012.
[4] Cioruța, Bogdan, and Mirela Coman. "Environmental Informatics - solutions and emerging challenges in environmental protection", *Studia Universitatis AMBIENTUM*, 57, no. 2 (2012): 17-30.
[5] Maybury, Mark. "Intelligent user interfaces: an introduction". Paper presented at the 4th International Conference on Intelligent User Interfaces. 3-4, ACM, New York, 1998.
[6] Weiser, Mark. "Some computer science issues in ubiquitous computing". ACM 36, 75-84, 1993.
[7] Saha, Dippiya, and Amitav Mukherjee. "Pervasive computing: a paradigm for the 21st century". *IEEE Computer*, 36, no. 3 (2003): 25–31.
[8] Greenfield, Adam. *Everyware: The Dawning Age of Ubiquitous Computing*. Berkeley, New Riders, 2006.
[9] Atzori, Luigi, Antonio Iera, and Giacomo Morabito. "The internet of things: A survey". *Computer Networks* 54, no. 15 (2010): 2787-2805.
[10] Coman, Mirela. *General and Applied Ecology* / *Ecologie generală și aplicată*. Cluj-Napoca, Risoprint Press, 2010.
[11] Cioruța, Bogdan, and Mirela Coman. "Studying Environmental Problematics and Hazards by Interactive Applications (SEPHIA)". *Studia Universitatis AMBIENTUM*, 58, no. 1 (2012): 39-46.
[12] Târziman, Elena. *Information and university education* / *Informaţia şi formarea universitară*. Bucureşti, Ed. Tehnică, 2003.
[13] Drăgănescu, Mihai. "Knowledge and knowledge society" / „Cunoaşterea şi societatea cunoaşterii". Presented at Sesiunea de lansare a programului strategic SI-SC, Academia Română, București, 2001.
[14] Drăgănescu, Mihai. "The consciousness - the frontier of science, the frontier of mankind" / „Conştiinţa, frontieră a ştiinţei, frontieră a omenirii". Presented at Academia Română, București, 2000.
[15] Cioruţa, Bogdan, Mirela Coman, and Vlad Mateșan. "Environmental Information Systems: solutions and emerging challenges for modern strategic development of Romanian local communities". Paper presented at the International Conference "Scientific Research and Education in the Air Force" (AFASES®), Braşov, Romania, May 23-25, 2013: 372-375.
[16] Coman, Mirela, and Bogdan Cioruţa. "Environmental Information Systems as a possible solution for strategic development of local and regional communities", Paper presented at the International Conference „Aerul şi Apa – componente ale mediului", Cluj-Napoca, March 22-23, 2013: 516-523.
[17] Cioruţa, Bogdan, Andrei Cioruţa, and Mirela Coman. "Pledoarie pentru necesitatea formării unei culturi informaţionale environmentale". *Journal of Environmental Research and Protection (Ecoterra®)*, no. 30 (2012): 31-39.
[18] Cioruţa, Bogdan, and Mirela Coman. "Evoluţia, definiţia şi rolul Sistemelor Informatice de Mediu în dezvoltarea strategiilor pentru protecţia mediului". *Journal of Environmental Research and Protection (Ecoterra®)*, no. 27 (2011): 11-14.
[19] Cioruţa, Bogdan,and Mirela Coman. "A forey in modern scientific research of the environment. From SIM to environmental informatics*" / "*Incursiune în cercetarea ştiinţifică modernă a mediului înconjurător. De la Sistemele Informatice de Mediu la Informatica Mediului". *Journal of Environmental Research and Protection (Ecoterra®)*, no. 29 (2011): 17-20.
[20] Avouris, N.M., and B. Page. *Environmental Informatics: Methodology and Applications of Environmental Information Processing*. Dordrecht, Kluwer Academic, 1995.
[21] Günter, O.. *Environmental Information Systems*. Berlin, Springer, 1998.
[22] Hilty, L.M., B. Page, F.J. Radermacher, W.F. Riekert. *Environmental Informatics as a new Discipline of Applied Computer Science*. In Avouris, N., and B. Page (Eds.). *Environmental Informatics – Methodology and Applications of Environmental Information Processing*, Dordrecht, 1995.
[23] Page, B.. *Environmental Informatics - Towards a new Discipline in Applied Computer Science for Environmental Protection and Research*. In: Denzer, R., G. Schimak, and D. Russel (Eds.). *Environmental Software Systems. Proceedings of the International Symposium on Environmental Software Systems*, Pennsylvania State University, Malvern, London, 1996.
[24] Page, B., L.M. Hilty. *Trends in Environmental Information Processing*. In Brunnstein, K., and Raubold (Eds.). *Applications and Impacts. IFIP Transactions A-52*, Amsterdam, 1995.
[25] ***, http://documents.rec.org/publications/SnapshotEnvInfSystems.pdf

http://hidraulica.fluidas.ro